Hornsea Project Three
Offshore Wind Farm

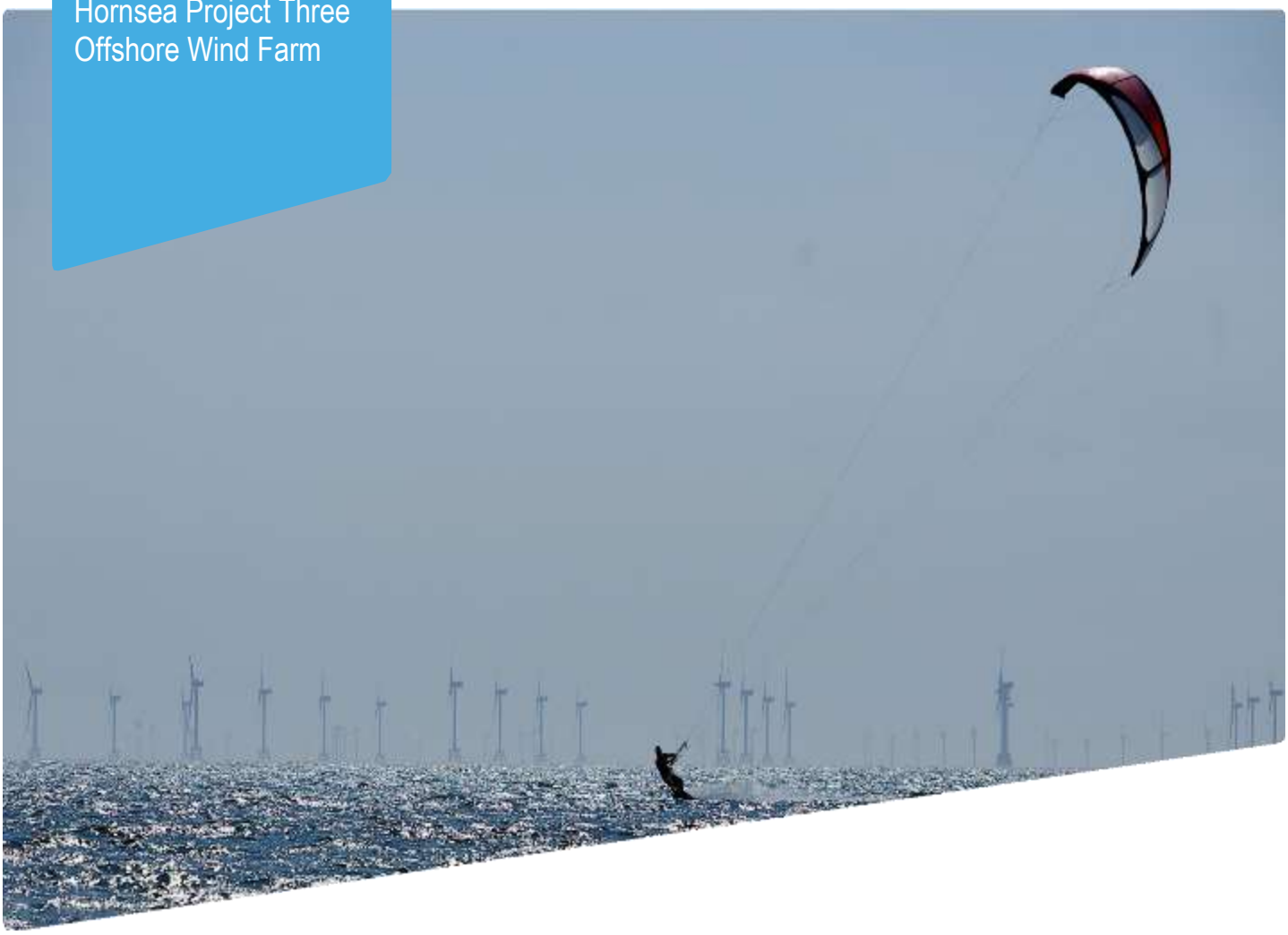

Hornsea Project Three

Offshore Wind Farm

Appendix 42 to Deadline I submission – Paper by Cleasby I.R. et al. (RSPB Research Report no. 63.)

Date: 7th November 2018

Hornsea 3
Offshore Wind Farm

Ørsted

Document Control			
Document Properties			
Organisation	Ørsted Hornsea Project Three		
Author	Cleasby I.R. et al.		
Checked by	n/a		
Approved by	n/a		
Title	Combining habitat modelling and hotspot analysis to reveal the location of high density seabird areas across the UK: Technical Report. RSPB Research Report no. 63.		
PINS Document Number	n/a		
Version History			
Date	Version	Status	Description / Changes
07/11/2018	A	Final	Submission at Deadline I (7th Nov 2018)

Ørsted

5 Howick Place,

London, SW1P 1WG

Front cover picture: Kite surfer near a UK offshore wind farm © Ørsted Hornsea Project Three (UK) Ltd., 2018.

Combining habitat modelling and hotspot analysis to reveal the location of high density seabird areas across the UK

Technical Report

September 2018

A UK-wide report covering

- Processing telemetry data via species distribution models for hotspot analysis
- Review and comparison of different hotspot mapping techniques
- Creation of hotspot maps for four seabird species at multiple spatial scales

Combining habitat modelling and hotspot analysis to reveal the location of high density seabird areas across the UK: Technical Report

RSPB Research Report 63

September 2018

Ian R. Cleasby[1], Ellie Owen[1], Linda J. Wilson[1] & Mark Bolton[2]

[1]RSPB Centre for Conservation Science, RSPB, Etive House, Beechwood Park, Inverness, IV2 3BW, UK
[2]RSPB Centre for Conservation Science, RSPB, The Lodge, Sandy, Bedfordshire, SG19 2DL, UK.

This report should be cited as:

Cleasby IR, Owen E, Wilson LJ, Bolton M (2018) Combining habitat modelling and hotspot analysis to reveal the location of high density seabird areas across the UK: Technical Report. RSPB Research Report no. 63. RSPB Centre for Conservation Science, RSPB, The Lodge, Sandy, Bedfordshire, SG19 2DL.

Cover photo: Andy Dale

Work conducted by RSPB Centre for Conservation Science as part of the 2017/18 project "*Seabird Tracking: from cutting edge science to policy impact*", funded by the RSPB Policy and Advocacy Strategy Board.

Further information
Ian Cleasby, Conservation Scientist, RSPB Centre for Conservation Science, North Scotland Regional Office, Etive House, Beechwood Park, Inverness, IV2 3BW, Ian.Cleasby@rspb.org.uk

ISBN 978-1-905601-59-2

Table of Contents

Non-Technical Summary

From 2010 to 2015, the RSPB and partners undertook a series of large-scale seabird tracking studies across the UK during the late incubation / early chick rearing period of the breeding season using cutting-edge GPS tracking technology. For four of the species tracked, there was sufficient data coverage to map their UK-wide at sea distributions using habitat selection models. These four species were European shag *Phalacrocorax aristotelis*, black-legged kittiwake *Rissa tridactyla*, common guillemot *Uria aalge*, and razorbill *Alca torda*. Habitat selection models were based upon all GPS locations and therefore included coverage of all behaviours (e.g. foraging, commuting, resting etc.). The current report uses the UK distribution maps of these four species to identify important areas of high seabird density at sea, based on hotspot mapping techniques. Two hotspots methods were trialled, maximum curvature and Getis-Ord analysis, both of which have previously been used to identify seabird hotspots for consideration as potential Marine Protected Areas (MPAs). Seabird hotspot maps were generated (i) at the UK-level, based on the distribution of seabirds from breeding colonies throughout the entire UK; (ii) at the level of individual SPAs, based on the distribution of birds originating from breeding colonies within the boundaries of specified Special Protection Areas (SPAs); and (iii) by merging individual SPA-level hotspots onto a single, UK-wide map. At the UK-scale, hotspot locations varied across each of the four species, but for kittiwakes, guillemots and razorbills, the importance of the Scottish coast (particularly the East coast) was apparent. Important hotspots for these species were also found around the Pembrokeshire coast (Wales), Rathlin Island (Northern Ireland) and the Yorkshire coast (England). In shags, hotspots were smaller than observed in the other three species and were typically found in inshore coastal waters centred on the locations of their breeding colonies. Further details on the performance and sensitivity of the different hotspot methods are discussed.

Overall, the report demonstrates how tracking data, distribution modelling and hotspot analysis can be combined to identify important seabird areas at sea. This approach has the advantage that 1) information on species-habitat relationships is incorporated within hotspot analysis; 2) methods for hotspot mapping are transparent and repeatable; 3) mapping can be conducted at a variety of spatial scales; 4) the breeding colony provenance of birds is known. As such, the outputs from this work will assist the conservation of seabirds when at sea by informing the identification of marine protected areas, seabird sensitivity mapping, marine planning, and environmental impact assessments.

Technical Summary

From 2010 to 2015, the RSPB along with other partners undertook a series of large-scale telemetry studies under the auspices of the FAME (Future of the Atlantic Marine Environment) and STAR (Seabird Tracking and Research) projects. These projects used cutting-edge GPS technology to track the movement of birds from multiple species across multiple colonies throughout the UK. Tracking data were then combined with remotely-sensed environmental data to develop predictive species distribution models for four species, (European shags *Phalacrocorax aristotelis*, black-legged kittiwakes *Rissa tridactyla,* common guillemots *Uria aalge,* and razorbills *Alca torda*). Subsequently, work published by the RSPB used these predictive models, applied to birds breeding at individual breeding colonies, to generate UK-wide at sea distribution maps for each species (Wakefield et al. 2017). Species distribution models were based upon birds tracked during the late incubation / early chick rearing period and therefore reflect the distribution of breeding birds during this stage of the annual cycle. In addition, they used all GPS locations and therefore included coverage of all behaviours (e.g. foraging, commuting, resting etc.).

Here, we describe how the species distribution models developed by Wakefield et al. (2017) can, in turn, be used to identify and map seabird hotspots at a variety of spatial scales. In particular, we focus upon the application and performance of two methods previously used to identify potential seabird marine Special Protection Areas (SPAs), maximum curvature and Getis-Ord hotspot analysis. Maximum curvature and Getis-Ord analysis were conducted for each species listed above at both the UK-level (all colonies within the UK) and the SPA-level (all colonies within a defined SPA). The SPA-level hotspots were also merged to create a single UK-wide map and compared to alternative basic mapping approaches in which simple foraging radii are drawn

around colonies based upon measures such as mean or maximum recorded foraging range (Thaxter et al. 2012).

Outputs from Wakefield et al. (2017) took the form of probability density grids describing the expected utilisation distribution (UD) of a given population. UDs are two-dimensional probability distributions that represent the time spent in a specific area and thus the probability of encountering an animal in that location during a future observation period. Combining individual UDs results in a population-level UD that represents the average space use across the population. Population-level UDs can be interpreted as the amount of time the average individual spends at a particular location or as the expected proportion of the population at a location at any given time. Here, population-level UDs derived from species distribution modelling were used as the basis for application of maximum curvature and Getis-Ord analysis.

Maximum curvature boundaries outline the area that best balances the proportion of a population protected against the extent of the protected area. Mathematical models were used to describe how the cumulative density of birds changes as a function of cumulative area and to identify the point of maximum curvature, which is then used as a threshold value of density to determine which areas to include within the boundary.

Getis-Ord analysis quantifies areas in which clusters of density or intensity are statistically distinct from patterns in the surrounding landscape. Getis-Ord scores (Gi*) are calculated on a cell-by-cell basis across the area of interest taking into consideration data values within a user-specified local neighbourhood of a focal cell and comparing these to a global value. Gi* are larger the higher and more clustered values are around a central location, indicating the potential presence of a hotspot. Following previous work, two alternative threshold values were applied to delineate

Getis-Ord hotspots: the top 1% and the top 5% of Gi* scores. In addition, we applied a threshold based on cells in which Gi* scores exceeded a critical significance threshold ($p < 0.01$).

UK-scale hotspot maps for kittiwakes, guillemots and razorbills emphasized the importance of Scottish waters for each of these species. In particular, hotspots covered large areas along the east coast of Scotland. Outside Scotland, other important sites included areas around the Yorkshire Coast, Rathlin Island and the Pembrokeshire coast. In shags, UK-scale hotspot mapping identified a series of smaller hotspots typically centred around the locations of shag colonies, reflecting the limited foraging range and more localised distribution of this species.

Mapping hotspots at the SPA-level allowed us to identify important marine areas for each SPA in which the species in question was a designated feature. This demonstrates how the modular outputs produced by Wakefield et al. (2017) permit hotspot mapping at a variety of spatial scales for bespoke combinations of individual colonies. Merging individual SPA-level outputs onto a single UK map resulted in UK-wide map of hotspots that reflected the distribution of designated colony SPAs and ensured representation of the marine areas used by the populations from these internationally important sites. However, in comparison to a single UK-level hotspot analysis, merging SPA-associated hotspots was less efficient in terms of protecting the largest number of birds in the smallest area. Similarly, drawing foraging radii around SPA colonies (sensu Thaxter et al. 2012) typically encompassed larger areas but was less efficient than the hotspot mapping approaches trialled in terms of protecting the largest number of birds in the smallest possible area, reflecting the methods lack of specificity in targeting highly used areas.

Across species, maximum curvature consistently identified the largest hotspots regardless of the spatial scale of the analysis and typically covered the majority of a species' home range.

Hotspots based on statistically significant Gi* also covered a relatively large area. In contrast, hotspots based on the top 1% of Gi* scores consistently covered the smallest areas and were primarily concentrated in inshore waters close to the locations of breeding colonies.

Both maximum curvature and Getis-Ord analysis were sensitive to how the area over which to perform the analysis (analysis field) was selected. In particular, larger analysis fields gave larger hotspots. This sensitivity was especially acute when defining hotspots as the top 5% or top 1% of Gi* scores as, by definition, this will result in hotspots that cover 5% or 1% of the analysis field respectively. For the final outputs, the analysis field was defined using the 95% home range. The 95% home range is a widely established concept within ecology and also allows for efficient hotspot computation. However, given the importance of analysis field we recommend that the analysis field is clearly reported and should be borne in mind when interpreting results from any such hotspot analysis.

The Getis-Ord Gi* score is calculated as a ratio between the average of a variable within a defined radius around a central location (local neighbourhood), and the average of the variable across the specified analysis field (global value). Therefore, how one defines the local neighbourhood over which local Gi* scores are calculated is also critical. Neighbourhood size was initially defined using either spatial variograms or first-passage-time (FPT) analysis. Both methods identified similar neighbourhood sizes, and the resulting hotspots maps looked similar. However, in certain cases spatial variograms failed to asymptote and could not be used to define neighbourhood size. One reason for the failure of spatial variograms may be due to the patchy or clumped nature of modelled seabird distributions. From an ecological perspective results based on FPT analysis may also be more interpretable as FPT (and hence local neighbourhood size) represents the spatial scale at which individuals forage. Thus, we preferred to use FPT-based

estimates of neighbourhood size when identifying Getis-Ord hotspots and report FPT-based results here.

Both maximum curvature and Getis-Ord analysis have previously been used to identify important seabird marine areas for consideration as potential SPAs. However, the majority of past studies were based on at-sea transect data rather than telemetry data. Here, we demonstrate how telemetry data can be processed via species distribution models for use in hotspot mapping. The technique has the advantage that 1) information on species-habitat relationships is included within the hotspot analysis; 2) hotspot mapping is transparent and repeatable; 3) mapping can be conducted at a variety of spatial scales and 4) the breeding colony provenance of birds is known. As such, we envision that the outputs from this work will assist the conservation of seabirds when at sea by informing the identification of marine protected areas, seabird sensitivity mapping, marine planning, and environmental impact assessments.

1. Introduction

Seabirds are among the world's most endangered avian groups, with nearly half of seabird species known or suspected to be in decline (Croxall et al. 2012). Many of the threats seabirds face come from an anthropogenic source and include interaction with commercial fisheries (Zydelis et al. 2013), marine pollution (Wilcox et al. 2015), invasive species (Jones et al. 2008) and climate change (Doney et al. 2011). Marine Protected Areas (MPAs) represent an important tool for the protection of marine biodiversity, including seabirds (Game at al. 2009, Lascelles et al. 2012). However, designation of MPAs typically lags behind the terrestrial equivalent (Perrow et al. 2015) despite wide-spread recognition that effective seabird conservation requires protecting important at sea areas (Game et al. 2009).

In order to protect biodiversity and ecosystem health the UK is signatory to several international agreements (OSPAR Convention 1992, Convention on Biological Diversity 2004). In particular, the European Union (EU) Birds Directive (Directive 2009/147/EC) requires member states to create a network of sites, termed Special Protection Areas (SPAs), across both the terrestrial and marine environment to protect avian species. In response, the UK along with other EU countries, is part of international efforts to establish a European network of protected sites called Natura 2000. At present, many seabirds are protected within terrestrial SPAs based around the breeding colony (Stroud et al. 2001). In order to identify suitable marine SPAs, the Joint Nature Conservation Committee (JNCC) in collaboration with Scottish Natural Heritage (SNH), Natural England (NE), Natural Resources Wales (NRW) and the Department of the Environment Northern Ireland (DOENI) have undertaken extensive survey and data collection over many years (for details see: http://jncc.defra.gov.uk/page-4184). To help identify marine

SPAs a number of approaches have been adopted through work conducted by the Joint Nature Conservation Committee (JNCC):

1) Marine extensions to existing seabird colony SPAs (e.g. McSorely et al. 2006, Wilson et al. 2009)
2) Identifying inshore areas used by waterbirds outside the breeding season (e.g. O'Brien et al. 2012)
3) Identifying inshore- and offshore areas used by seabirds for foraging and other activities throughout the year (e.g. Kober et al. 2010, 2012).
4) Other types of SPA not covered by the three categories above (e.g. Wilson et al. 2014).

While several of the sites identified have now been formally classified as marine SPAs, the designation process is still ongoing. The focus of the current report is to further inform work under point 3) and aid identification of important at sea areas. Such work will be useful within an MPA context and will also inform future strategic and project level planning of marine activities and developments and help embed the ecosystem approach to decision-making within marine spatial planning. To date, potential offshore SPAs for seabirds in the UK have been identified largely using at sea transect survey data (Kober et al. 2010, 2012). However, information on seabird distributions can also be collected using bird-borne data loggers to track birds while at sea. The exact nature of the data collected differs between transect-based versus tracking approaches and each has its own pros and cons (Camphuysen et al. 2012, Sansom et al. 2018). However, one distinct advantage of tracking data is that the provenance of individuals is known. Such information can be valuable when proposing seabird MPAs or identifying areas at most risk from

human activities as one can prioritize areas of usage associated with protected colonies (Daunt et al. 2006, Wakefield et al. 2011, Camphuysen et al. 2012, Perrow et al. 2015) and apportion the impacts of anthropogenic and natural processes to specific colonies (Zydelis et al. 2011, Montevecchi et al. 2012). In the absence of such data seabird foraging behaviour is often incorporated into Environmental Impact Assessments (EIA) by creating buffers around specific colonies using estimates of foraging range (Eastham 2014). However, such an approach was not intended to be used in isolation (Thaxter et al. 2012) and rests upon the unrealistic assumption that seabirds are uniformly distributed out to some threshold distance from their colonies (Wakefield et al. 2017).

Unfortunately, tracking data is often only available for a subset of seabird colonies, which precludes understanding of broad-scale seabird distributions and hinders efforts to design national MPA networks. One solution is to construct species distribution models (SDM) that describe the distribution of birds at tracked colonies and allow the distribution of birds at untracked colonies to be predicted. Such models are growing in popularity in marine ecology and have previously been used to describe the distribution of cetaceans (Bailey & Thompson 2009, Becker et al. 2012), seals (Jones et al. 2015) and seabirds (Wakefield et al. 2017). Within the UK, predictive SDM has already been used to help identify potential marine SPAs (Wilson et al. 2014) (several of which have now been formally classified, with more pending) and Special Areas of Conservation (SAC, Embling et al. 2013), illustrating the utility of this approach.

Lack of data represents one of the key barriers to MPA designation and hinders effective marine management for seabirds. To help address this, the RSPB and other partners embarked on two large-scale projects (FAME: Future of the Atlantic Marine Environment and STAR: Seabird Tracking and Research) that involved tracking multiple seabird species across multiple colonies.

A key aim of the work was to investigate habitat-use when birds were at sea and identify important marine areas to inform marine management, including MPA designation. RSPB used the tracking data from the FAME-STAR projects, to construct generalized functional response (GFR) models (a type of SDM) to model habitat usage for four UK seabird species (European shags *Phalacrocorax aristotelis*, black-legged kittiwakes *Rissa tridactyla*, common guillemots *Uria aalge*, and razorbills *Alca torda*, Wakefield et al. 2017). As well as describing patterns of habitat usage across tracked colonies, model outputs were used to predict seabird distributions at untracked colonies. Colony-level predictions were then combined and scaled-up to produce UK-level outputs, providing unprecedented new information on the distribution of these species from the local scale (colony-level) through to the national scale (UK-level).

Delineating a potential MPA typically involves mapping the distribution of seabirds and drawing boundaries around important/ high density areas (O'Brien et al. 2012). Thus, the distribution maps produced by Wakefield et al. (2017) represent a valuable tool for MPA management and design. To date, a number of different techniques have been used to delineate important marine sites using distribution maps (Wilson et al. 2009, Garthe et al. 2012, Embling et al. 2013, Perrow et al. 2015). The most common approaches used to delineate the boundaries of marine seabird SPAs in the UK are maximum curvature (O'Brien et al. 2012, Lawson et al. 2016) and Getis-Ord hotspot analysis (Kober et al. 2010, 2012). Maximum curvature provides a mathematical method for identifying the point at which the relationship between the size of a putative protected area and the cumulative number of birds it contains changes the most. As such, it is thought to identify a boundary that balances the proportion of the population protected against the size of the protected area. The Getis-Ord (Gi*, Getis & Ord 1992) statistic is a local indicator of spatial association (LISA, Anselin 1995) used to quantify areas in which clusters of density or

intensity are statistically distinct from patterns in the surrounding landscape (Sokal et al. 1998, Johnston & Ramachandran 2014). Recently, Lascelles et al. (2016) developed an analytical technique to use raw tracking data in order to help define Important Bird Areas (IBA). However, because the IBA approach outlined relies upon tracking data it cannot be used to generate gap-free predictive distributions of seabirds across untracked colonies and hence this approach was not adopted here.

The aim of the current work is to use the predicted seabird distribution maps produced by Wakefield et al. (2017) as the basis for identifying important offshore seabird areas using the established maximum curvature and Getis-Ord methods. For all four species included in Wakefield et al. (2017) (black-legged kittiwakes, common guillemots, razorbills and European shags) we compare and contrast the performance of maximum curvature and Getis-Ord analysis at both the local- and UK-level. At the local-level, we use the outputs of Wakefield et al. (2017) to identify hotspots for birds originating from within the boundaries of existing colony SPAs in which the species in question is identified as an SPA feature. We term these local distributions as SPA-level distributions. Hotspots methods performed on individual Seabird 2000 sites[1] and on birds originating from within a given Site of Special Scientific Interest (SSSI-level) are also available on request. The rationale for focussing upon the SPA-level is that these populations have already been recognised as warranting the highest levels of protection under EU law, therefore to provide effective protection both at their colony and at sea, knowledge of the most important at sea areas used by those colony SPA populations is critical. Without knowing which marine areas are used by those protected colony populations, the default is to assume birds use an area within a buffer around the colony defined by a generic foraging range value (e.g. Eastham 2014). However, a

[1] The seabird colony sites defined and used during the Seabird 2000 census, 1998-2002 (Mitchell et al. 2004)

generic foraging range value does not reflect either the true maximum range or the variation between colonies and individuals, and may either miss important areas or include areas that are used very little (Soanes et al. 2016). In contrast, defining the areas known to heavily utilised by birds on the basis of species distribution modelling may allow us to draw boundaries around important areas of sea smaller than those based on foraging radii and better targeted at high density regions. As not all birds are found within SPAs, by also adopting a UK-level approach, we can include important areas used by birds that do not originate from within an SPA or that arise as at sea aggregations of birds from multiple colonies (both SPA and non-SPA).

2. Methods

Throughout the following report all analyses are based upon the predicted seabird distributions produced by Wakefield et al. (2017), which contains a detailed description of the statistical methodology used to generate such predictions (summarised in Appendix, A1 & A2). Briefly, Wakefield et al. (2017) used telemetry data in order to model habitat use as a function of environmental covariates, intra-specific competition and habitat accessibility for four UK seabird species (species listed above) during the breeding season (May-July, 2010-2014).

2.1. Temporal and behavioural coverage

It is important to note that the Wakefield et al. (2017) distribution maps, and all the work stemming from them described in this report relates only to breeding individuals that were either approaching the end of the incubation period or raising small chicks as these species are most amenable to tracking work during this period (see Table A1 for the dates during which tracking took place). This is also the time when the foraging range of adults is constrained by the need to frequently

return to the colony to adequately provision their small chicks. So while the analysis will identify areas important during this critical time, it may not reflect areas used during other parts of the breeding season or over-winter when birds may roam more widely. The models produced by Wakefield et al. (2017) were based all GPS locations recorded while birds were at sea and therefore include periods of foraging behaviour, but will also include periods of rafting and commuting and any other at sea behaviours.

2.2. Calculating Utilisation Distributions

Model coefficients from the best fitting habitat usage models were used to predict usage for each breeding colony (based on Seabird 2000 sites (Mitchell et al. 2004)) for each species. Raw model predictions provide an estimate of the intensity of tracking locations across an area. Results were then converted to an expected probability density grid, often termed a Utilisation Distribution (UD, (Fieberg & Kochanny 2005)) by normalizing the intensity of locations (i.e. rescaling them so that they sum to one). UDs are two-dimensional probability distributions that represent the time spent in a specific area and thus the probability of encountering an animal in that location during a future observation period (Hooten et al. 2017). UDs also provide a formal way to quantify home ranges (Kie et al. 2010). In practice, home range is derived as a particular probability contour of the UD that represents the proportion of time spent by an animal within the contour (Demsar et al. 2015). For example, the 50% UD is often used to identify the area of core usage and identifies the smallest polygon in which an individual would be predicted to spend 50% of it time. Similarly, the 95% UD contour is a common measure of home range and identifies the smallest polygon in which an individual would be predicted to spend 95% of it time. Combining individual UDs results in a population-level UD that represents the average space use across the sampled population (in the case of Wakefield et al. (2017) the sampled population is breeding adults during late incubation/

early chick rearing), provided a representative sample of individuals has been tracked (Gutowsky et al. 2015). Thus, population-level UDs can be interpreted as the amount of time the average individual spends at a particular location or as the expected proportion/ percentage of the population at a location at any given time. For instance, at any given time we would expect to find 95% of a defined population within the population-level 95% UD. When multiplied by population size estimates, UDs can also be used to depict relative or absolute expected density of birds. Wakefield et al. (2017) displays a national-level (UK and Ireland combined) UD for each species. However, because the original outputs from Wakefield et al. (2017) are predictions for individual colonies they can be combined in a variety of different ways depending on the scale of interest. For instance, we could focus on the distribution of birds originating from one colony, two neighbouring colonies or from all colonies within a defined region.

More formally, to use the outputs of Wakefield et al. (2017) to create distribution maps we first define a set of individual colonies, set *x,* whose UD outputs we wish to combine. For example, set *x* would consist of all colonies located within the UK if the goal was to map the distribution of birds originating from within the UK. More generally, set *x* could comprise a list of any colony/ies of interest. To convert the UD probability distribution into an estimate of relative density of birds per grid cell for a given colony, we applied a conversion factor to the UDs for each Seabird 2000 site based on the number of Apparently Occupied Nests (AON) or individuals recorded during the Seabird 2000 census. For kittiwakes and shags, UDs for each Seabird 2000 site within set *x* were multiplied by two times the number of AONs to give us the number of breeding individuals. For guillemots and razorbills the Seabird 2000 census counted number of individuals rather than pairs, hence there was no need to multiply counts by two and the number of individuals recorded could be used directly. We did not use the traditional conversion factor of 0.67 to determine the number

of pairs for guillemots and razorbills due to concerns about its accuracy across different populations (Harris et al. 2015). Because all analyses deal with relative density and we report the percentage of the population found within defined hotspots rather than absolute numbers, the choice of multiplication factor does not change our results. However, if one was interested in specifying the predicted number of birds within an area the choice of multiplication factor becomes more important.

Currently, the outputs from Wakefield et al. (2017) do not account for differences in time spent at sea among different colonies. Assuming all colonies spend equal amounts of time at sea essentially applies an equal weighting to all colonies. For tracked colonies the proportion of time at sea varied between colonies (and between individuals), but was not associated with either colony size or colony Latitude (Appendix, A3). Therefore, as the vast majority of colonies were not tracked, and we found no significant predictors of proportion of time spent at sea at tracked colonies, we assumed that all colonies spent the same amount of time at sea. Maps of relative density for each Seabird 2000 site within set *x* were then overlaid on a single map and the total density for each grid cell was summed, giving the total density of birds expected in a given cell (see Appendix, A4). This was then normalized so that all grid cells summed to one, resulting in a UD that described the distribution of birds from colonies within set *x*.

A similar approach was used to map the UD and relative density of birds originating from within designated colony SPAs. In this case, the set of colonies *x* over which operations were performed included only (sub) colonies whose location fell within the boundaries of a given colony SPA. An example for one SPA colony is provided in Fig. 1; the process can also be repeated for all colony SPAs and the outputs merged to provide a UK-scale distribution map based only on SPA colonies rather than all Seabird 2000 sites. The boundaries of UK colony SPAs were

contained in shapefiles downloaded from the JNCC website (http://jncc.defra.gov.uk/page-1409, last updated: 04/12/2017). When calculating SPA-level UDs we restricted our focus to those SPAs in which the species in question was listed as a designated feature (note this does not include species only listed as part of a seabird assemblage). A list of which species were designated as features in which UK SPA was taken from the JNCC website (http://jncc.defra.gov.uk/page-1461, date accessed: 01/07/2018, last updated: 01/06/2018). Note that the designation process is ongoing and our SPA-level analysis reported here will not reflect any sites designated since 1 June 2018. Similarly, as the current analysis is based on Seabird 2000 data, it will not reflect the new census data currently being collected as part of the ongoing current seabird census effort (http://jncc.defra.gov.uk/page-7413). However, the R code developed as part of the analysis can allow all the analyses to be updated as required, resources permitting.

Fig. 1. An example of calculating distribution maps at the SPA-level. (a) A density map (birds per km^2) for kittiwakes originating from within the Flamborough and Bempton Cliffs SPA. Estimates of density based only on birds from within the SPA. (b) Utilisation distribution for birds originating from the Flamborough and Bempton Cliffs SPA based upon density estimates in 2a.

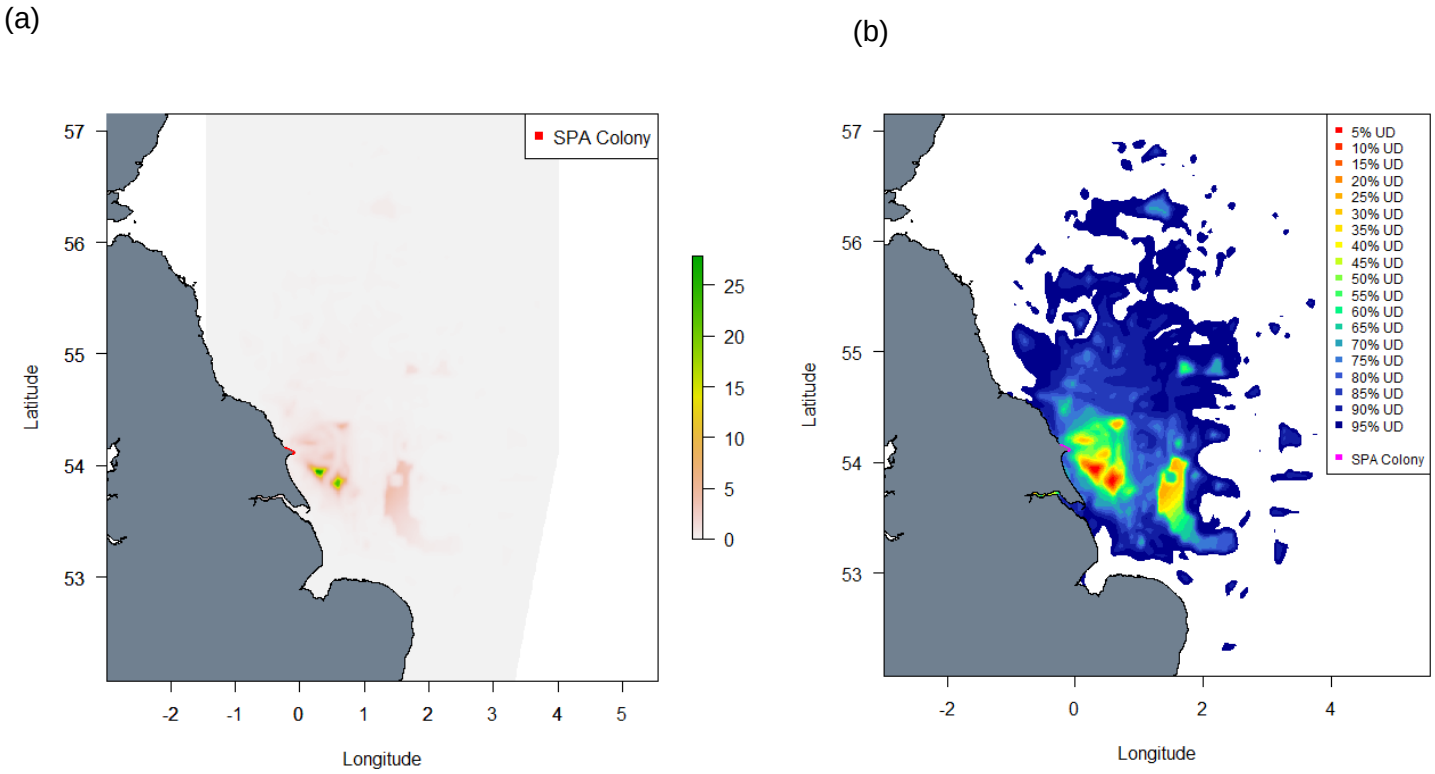

2.3. Delineating hotspot boundaries via maximum curvature

To identify hotspot boundaries we used the maximum curvature method outlined by O'Brien et al. (2012), an approach previously used to identify potential seabird SPAs. Maximum curvature was estimated for each species based on UDs constructed as described above. For kittiwakes, guillemots and razorbills UDs were calculated at a 1 km^2 resolution, whereas for shags resolution was 0.5 km^2. When performing maximum curvature at the UK-level we based results on birds

originating from both the UK and the Republic of Ireland as birds from Irish colonies visit the UK EEZ and may aggregate with British birds. At the SPA-level, the UDs used to calculate maximum curvature were based only on the distribution of birds originating from colonies within the boundaries of a specified SPA. Therefore, SPA-level analysis did not incorporate information on the distribution of birds from out-with a given SPA. Maximum curvature analysis was run independently for each SPA in turn. However, to display identified maximum curvature areas on the UK-scale the maximum curvature boundaries from individual SPAs were overlaid and merged.

To perform maximum curvature anlaysis, UD grid cells x_i were ordered by decreasing probability density and we calculated cumulative probability density, $\rho_{i,}$ against cumulative area, A_i. A was then re-scaled to lie between 0 and 1 to ensure it was on the same scale as ρ. Graphing the curve of the relationship between ρ_i and A_i indicates how predicted usage increases with area (Fig. 2). Maximum curvature works by identifying the point, $k_{max,}$ at which the relationship between A_i and ρ_i changes the most. Beyond k_{max} disproportionately larger areas would be required to encompass further increases in bird numbers. By determining the cumulative area at this point, A_max, the set of grid cells at which $A_\mathrm{i} < A_\mathrm{max}$ can be identified. The maximum curvature boundary is then defined as the polygon bounding these grid cells.

Fig. 2. Example of identifying point of maximum curvature. (a) Plot of ρ against A, black line gives the raw data and the dashed, red line represents the curve fitted to the data by Loess smoothing. The blue line indicates A_{max}, the cumulative area at the point of maximum curvature. Cells to the left of this line are selected for inclusion within a maximum curvature boundary and those to the right are excluded. (b) Plot displays the curvature of the lines from plot 3a, the clear peak in curvature allows k_{max} and hence A_{max} to be determined.

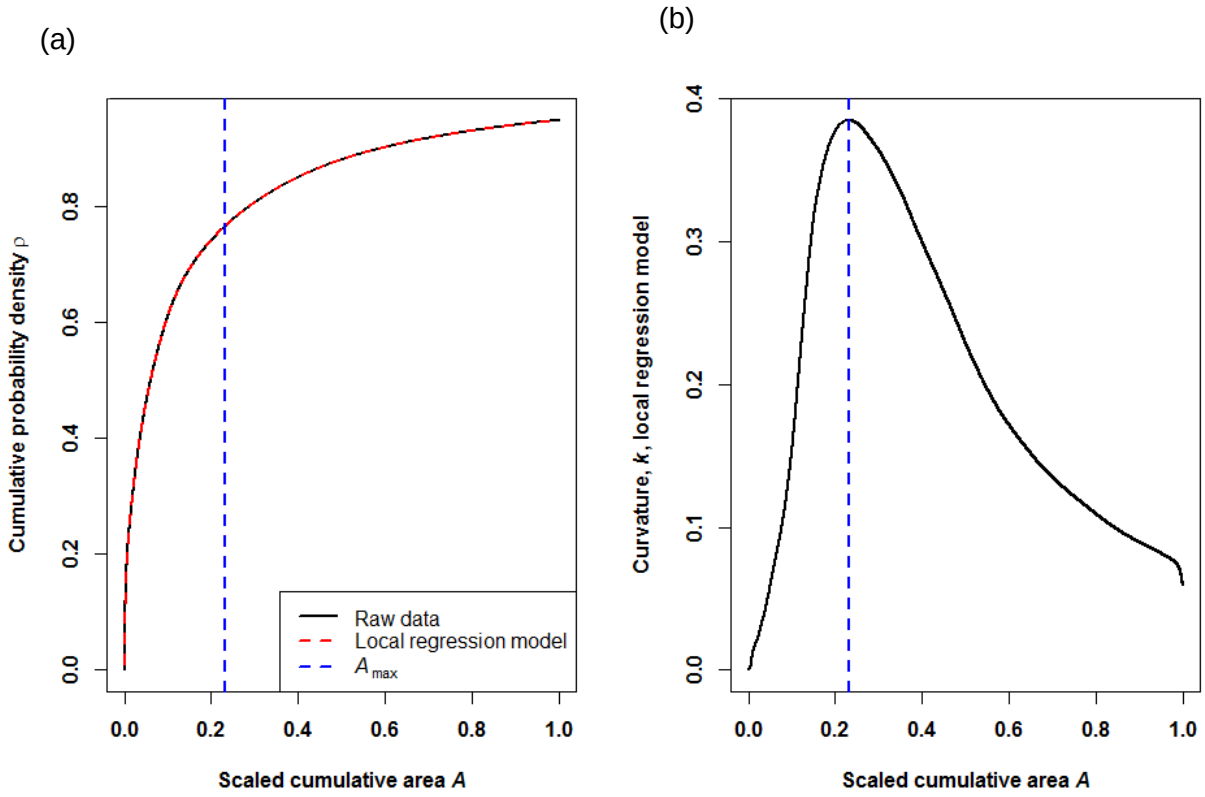

One key aspect of maximum curvature analysis is defining the spatial extent over which to perform the analysis, termed the analysis field, as this can have a marked effect upon the outcome (Webb 2009, Appendix, A5). The analysis field chosen might be all cells in which the density of a species was > 0 (O'Brien et al. 2012) or it might be all grid cells within the foraging range of birds from a particular breeding colony (Webb 2009). When performing maximum curvature

analysis at the UK-scale, we limited the analysis field to all those cells that satisfied two criteria: 1) cell must fall within the boundaries of the UK EEZ, 2) cell must fall within the 95% home range of at least one UK colony (Fig. 3). Similarly, when performing maximum curvature analysis at the SPA-level we restricted our analysis field to the 95% home range of birds originating from the SPA-colony in question (e.g. Fig. 1). Therefore, the SPA-level outputs show hotspots within the 95% home range of the SPA population in question (rather than within the UK EEZ). Understanding the spatial extent over which the analysis is performed is crucial to interpretation. We chose to focus on the 95% home range due to its long-standing use as measure of home range within ecology (Kie et al. 2010). Moreover, use of the 95% home range ensures we do not include a large number of low density or zero density cells in the analysis which reduces computing time considerably (Kranstauber et al. 2017).

Typically, the point of maximum curvature is identified using exponential growth models (O'Brien et al. 2012). However, Wakefield et al. (2017) found that exponential models often performed poorly and occasionally identified two maxima in k with neither corresponding well to the point of maximum curvature observed when plotting A vs. ρ. As a consequence, Wakefield et al. (2017) used a Loess smoothing approach (Loader 1999) as the means of estimating k_{max}. As we encountered the same problems with maximum curvature as those reported by Wakefield et al. (2017) we adopted the same approach. Loess smoothing is a highly flexible method of approximating non-linear responses using a local regression model,

$$\rho_i = \mu(A_i) + \varepsilon_i, \quad (1)$$

where $\mu(A_i)$ is a polynomial fitted in a sliding window. This model was fit and its first and second derivatives obtained using the R locfit package (Loader 2013). The degree of loess smoothing is

determined by the bandwidth, *h*, which ranges from 0 to 1 and determines how much of the data is used to fit each local polynomial. Exploratory analysis showed that the location of k_{max} and therefore the size of A_{max} were both sensitive to *h*. A value of $h = 0.001$ provided curves which approximated the data well (Fig. 2a) in a reasonable computing time (Wakefield et al. 2017). Decreasing *h* below this value resulted in little change in A_{max} but resulted in a prohibitive demand for computing power. Hence, $h = 0.001$ was used in all analyses.

2.4. Delineating hotspot boundaries via Getis-Ord analysis

Like maximum curvature, Getis-Ord analysis has previously been used to identify potential seabird MPAs (Kober et al. 2010, 2012). Getis-Ord, Gi* analysis works by looking at the value of the response variable in a given cell in the context of its neighbour's values and measures the intensity of clustering of high or low values in a cell relative to its neighbouring cells. The sum for a cell and its neighbours (local value) is then compared proportionally to the sum of all cells (global value). To be classified as a hotspot, a cell will have a high value and be surrounded by other cells with high values. Cold spots can also be discovered using Gi* though this is not pursued here. The formula for the Getis-Ord, Gi* statistic is:

$$G_i^*(d) = \frac{\sum_{j=1}^{N} w_{i,j}(d)\ x_j}{\sum_{j=1}^{n} x_j} \tag{2}$$

Where $w_{i,j}$ denotes a spatial weights matrix with elements i, j where:

$$w_{i,j}\,(d) = \begin{cases} 1, & if\ d_{i,j} < d\ for\ all\ i,j \\ 0, & otherwise \end{cases} \tag{3}$$

The numerator in (2) gives the local sum of the variable *x* within a circle of given radius (*d*) from the base point of region *i*. The denominator in (2) gives the total sum of variable *x* across the entire

region. In most statistical packages Gi* scores are automatically standardized and the resulting Gi* value reported is a standard normal deviate, equivalent to a *z*-score.

Getis-Ord analysis was conducted for each species at both the UK- and SPA-level in the R environment (R version 3.5.0, R Development Core Team 2018) via the usdm package (Naimi et al. 2014) using maps of the relative density of birds as the response variable (Appendix A4). Two key considerations when conducting Getis-Ord analysis are 1) Defining the analysis field over which to calculate Getis-Ord values and, 2) Defining *d*, the scale of the local neighbourhood over which to calculate local values. As with maximum curvature, Getis-Ord analysis is sensitive to the spatial extent over which the analysis is conducted (Appendix, A5). Therefore, at the UK-level we limited the analysis field to cells that fell within the boundaries of the UK EEZ and fell within the 95% home range at least one UK colony (Fig. 3b). This approach makes results comparable with those based on maximum curvature and prevents inclusion of cells in which the density of birds is extremely low, which speeds up computation time and prevents inclusion of large, low density areas. Similarly, at the SPA-level we restricted our analysis field to the 95% home range of birds originating from the SPA-colony in question. Hotspot analysis was run independently for each SPA colony in turn. However, to display identified SPA-level hotspots on the UK-scale the results from individual SPAs were overlaid and merged.

In many ecological applications the local neighbourhood of a cell is defined using a distance-based threshold, *d*. A cells neighbourhood is defined as all the cells within a given radius *d* from the centre of cell *x*. A larger radius will result in a greater smoothing of Gi* scores and larger hotspots (Nelson & Boots 2008), but fine-scale spatial patterns may be lost if over-smoothing occurs (Appendix, A6). Conversely, a small radius may reflect small-scale patterns well, but may not reflect the scale at which a particular species aggregates and hotspots may be

smaller than ideal. Many studies choose a value of *d* by estimating the distance at which spatial auto-correlation breaks down in the data and setting this as the value of *d* (Fischer & Getis 2009, Kober et al. 2012). However, when conducting hotspot analyses at the SPA-level spatial variograms failed to reach an asymptote at certain colonies, suggesting the variogram approach may not always be suitable. When tracking seabirds, an alternative approach might be to define *d* based on the characteristics and movement ecology of the species in question. One advantage to this approach is that Gi* scores could be estimated using a consistent value across populations. To do this, we performed a First-Passage Time (FPT) analysis, a standard analysis that uses data from tracked birds to identify zones of area restricted search (ARS) and determines the spatial scale at which individuals interact with the environment (Fauchald & Tveraa 2003, Suryan et al. 2006, Hamer et al. 2009, Lascelles et al. 2016, Appendix A7). The scale of ARS was determined across all trips recorded within a species during the study. To determine the value of *d*, the average scale of ARS for a species was estimated as the intercept from an intercept-only model of ARS scale in which colony identity and individual identity were included as random effects to control for potential pseudo-replication. Ultimately, this gave species-level *d* as: *d* = 10 km for kittiwakes, *d* = 9 km for guillemots, *d* = 7 km for razorbills and *d* = 4 km for shags. We subsequently used these FPT derived neighbourhood sizes when performing Getis-Ord analysis in the current report. A comparison of Gi* analysis conducted using FPT-based or spatial variogram-based neighbourhood sizes can be found in the appendix (A8), however, results were broadly similar between these methods.

In order to delineate seabird hotspots using Gi* scores we defined hotspots in three ways. Following, Kober et al. (2010) two different threshold values were used to define hotspots: 1) All cells within the top 5% of calculated Gi* scores and 2) all cells within the top 1% of calculated

Gi* scores. Polygons drawn around cells that satisfy these criteria provide the boundaries of hotspots. By choosing to select the top 1% or top 5% of cells on the basis of Gi* scores one also makes the implicit decision to select 1% or 5% of the analysis field for protection (essentially setting a target % area). 3) We exploited the fact that standardized Gi* scores are equivalent to *z*-values and can be used for statistical testing to determine whether a cell belongs to a hotspot or not with a given degree of significance. The naive use of *z* scores is problematic due to multiple statistical testing, particularly when assessing hotspots for species with large ranges. To address these problems, we calculated adjusted *p* values (*p. adj*) using false discovery rate (FDR) methods to control the error rate under multiple testing (Benjamini & Yekutieli 2001). FDR methods increase the threshold *z*-value required for a given level of statistical significance, reducing the Type-1 error rate. One caveat to the use of standardized Gi* scores for statistical testing is that typically the response variable being modelled is non-normal, thus standardized Gi* scores will also tend to be non-normal. However, using a conditional randomization approach Getis and Ord (1992) showed that Gi* scores are asymptotically normal provided a cell has at least eight neighbours (see also: Ord & Getis 1995; Nelson &Boots 2008). The neighbourhood sizes in the current work ensure that every cell has ≥8 neighbours. Here, we define cells as belonging to a hotspot if the probability of that cell belonging to a hotspot is *p. adj* <0.01. Drawing a boundary around cells that meet this criteria provides an alternate way to delineate a hotspot using Gi* scores that is based on statistical significance.

2.5. Assessing the performance of different hotspot delineation methods

To assess the performance of different hotspot delineation methods we compared the hotspots identified on the basis of: (i) hotspot area; (ii) hotspot area as a percentage of the total area of the analysis field used in the UK-level analysis (Fig. 3.); and (iii) the percentage of the reference

population contained within the hotspot area at a given time relative to total population size. In addition, we used the Jaccard Index of similarity (Intersection over Union, Jaccard 1912) to (iv) compare polygon boundaries of identified hotspots with different UD polygons. The Jaccard Index (J) was calculated as

$$J\ (A, B) = \frac{|A\ \cap B|}{|A\ \cup B|} \tag{4}$$

Where A ∩ B represents the area of the polygon formed by the intersection on polygons A and B and A ∪ B represents the area encompassed by the union of A and B. Thus the index represents the ratio of intersection and union areas and is scored from 0 to 1 with higher values denoting greater similarity. For each study population, the Jaccard Index was calculated based upon a comparison between the hotspots identified and a sequence of population-level UD contours ranging from the 5% UD to the 95% UD in 5% increments. We then identified for each hotspot method the corresponding % UD contour that it was most similar to (highest Jaccard similarity).

In addition, we (v) compared the size and location of hotspots identified at the SPA-level via maximum curvature and Getis-Ord analysis to areas identified using seabird foraging ranges to draw a foraging radius around a colony. Currently, the use of foraging radii is one method to ascertain the impact of marine renewables on seabird populations, particularly when detailed tracking data are unavailable (Thaxter et al. 2012). To create foraging radii around colonies we constructed buffers around each SPA colony using the mean foraging range, mean-maximum foraging range, mean-maximum foraging range + 1 standard deviation (SD) and the maximum foraging range using species-specific values reported in Thaxter et al. (2012). We use values taken from Thaxter et al. (2012) here as such values are commonly used to assess species foraging ranges

in the absence of tracking data (Eastham 2014). Foraging radii buffers for individual SPA colonies were then merged in order to plot UK-scale results. The area and expected proportion of the colony population contained within foraging radii were calculated and compared with similar values for SPA-level hotspots. The similarity between different hotspot methods and different foraging radii was assessed using the Jaccard Similarity Index.

Fig. 3. (a) Map displaying utilisation distribution for birds originating from the UK and the Republic of Ireland. At the UK-level maximum curvature and Getis-Ord analysis were based on the density estimates of birds originating from both the UK and Ireland. (b) To be included in UK-level analysis field a given grid cell had to fall within the UK EEZ and fall within the 95% home range of at least one UK-based colony. Cells selected for UK-level hotspot mapping (UK-level analysis field) are shown in green.

(a) (b)

Black-legged kittiwakes

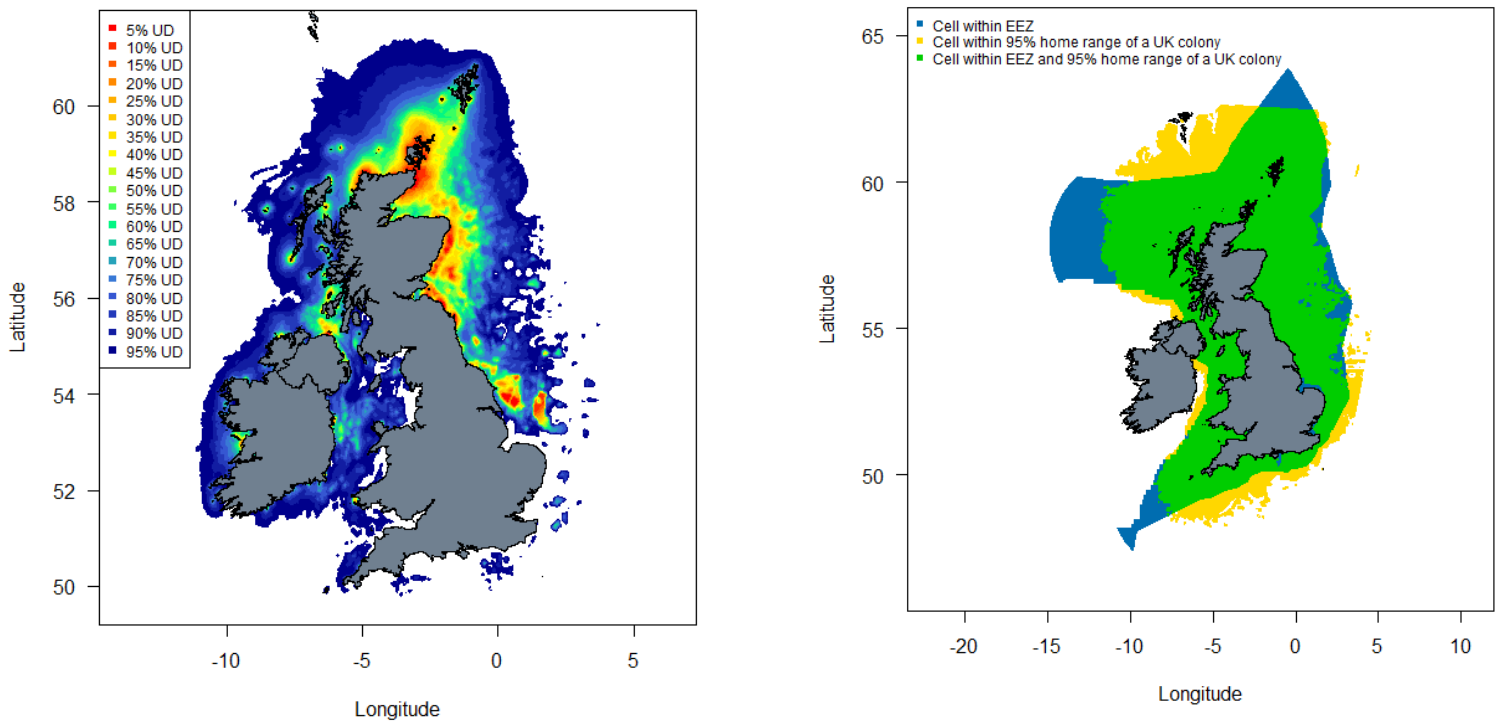

Common guillemots

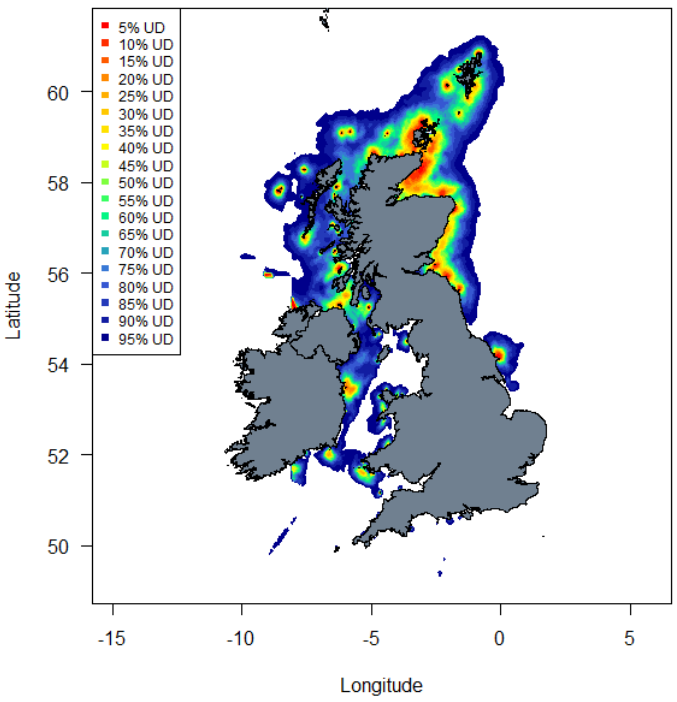

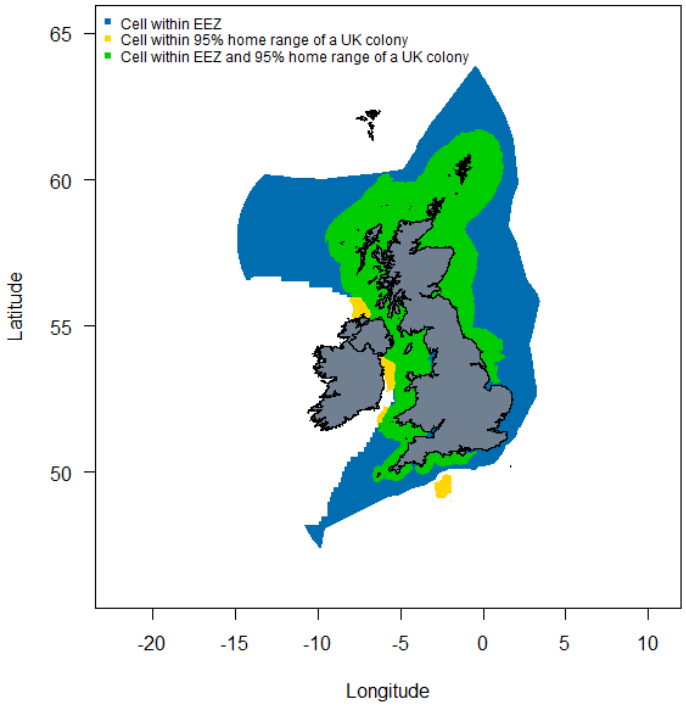

Razorbills

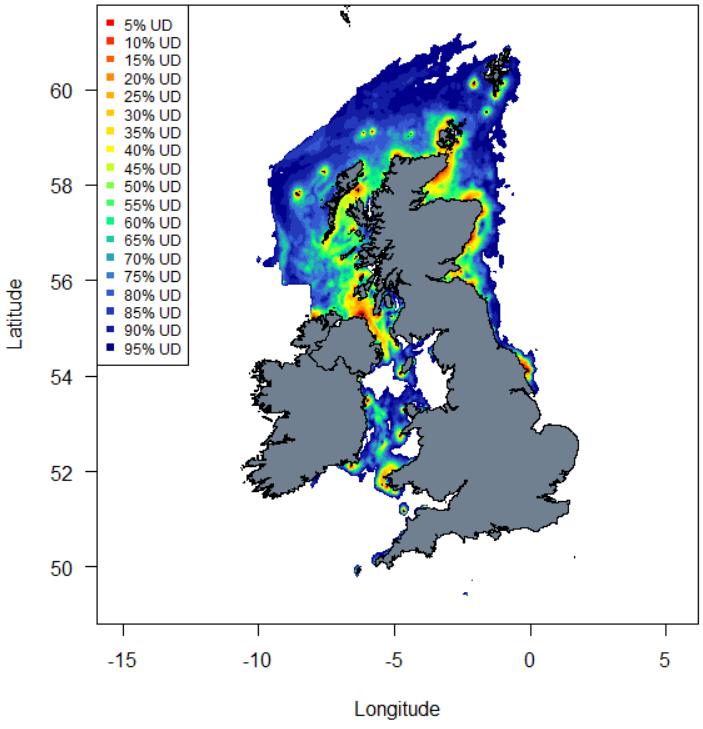

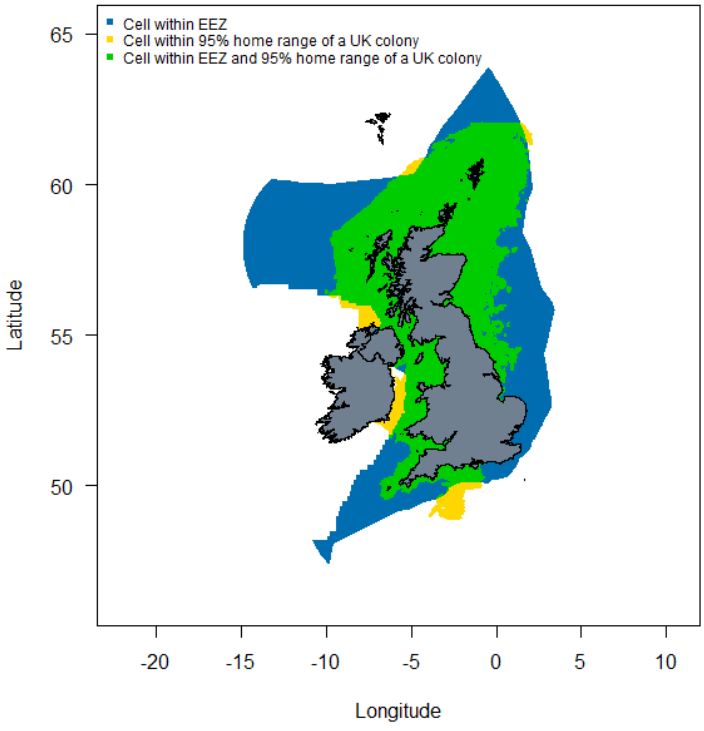

European shags

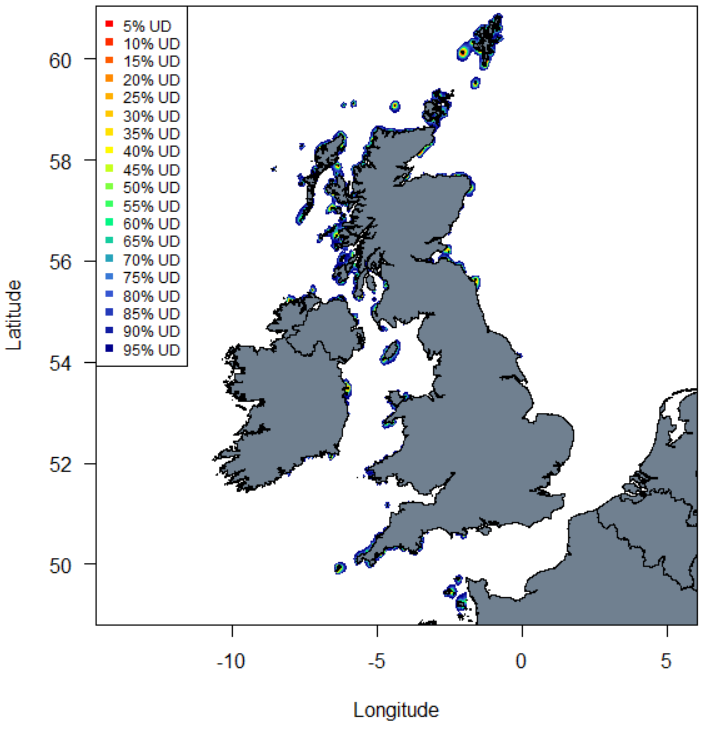

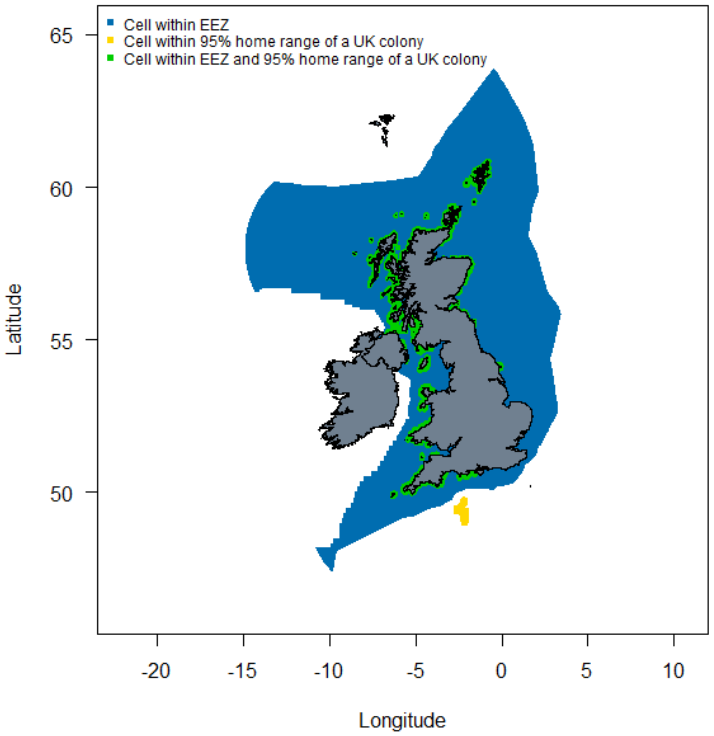

3. Results

3.1. Black-legged kittiwakes

3.1.1. UK-Level

At the UK-level, the top 1% and top 5 % Gi* methods emphasized the importance of areas along the entire east coast of Scotland and off the coast of Yorkshire (Fig. 4), where some of the largest kittiwake colonies are located. The larger areas identified by statistically significant Gi* values or maximum curvature also covered these regions, but included additional areas around the coast of Shetland, the Hebrides, Northern Ireland and North-East England.

Hotspots identified by loess-based maximum curvature encompassed the largest area (Table 1) and were most similar to the 85% UD contour of UK kittiwakes (J = 0.93). Defining hotspots as those cells within the top 1% or top 5% of Gi* scores gave smaller areas than hotspots defined on the basis of statistical testing (Table 1). When delineating hotspots as the top 1% of Gi* scores the area identified was most similar to the 20% UD of UK kittiwakes (J = 0.45). When using the top 5% of Gi* scores to delineate hotspots the area identified was most similar to the 40% UD of UK kittiwakes (J = 0.74). Finally, when delineating hotspots on the basis of statistical significant Gi* scores the areas identified was most similar to the 80% UD of UK kittiwakes (J = 0.86). The larger areas identified by maximum curvature or statistically significant Gi* scores contained high numbers of birds (> 70% of the at sea population at a given time), but even the smallest area, defined using the top 1% of Gi* scores, was expected to contain >10% of the at sea population at any given time.

3.1.2. SPA-level

To display SPA-level outputs on the UK-scale outputs from each of the SPA-level analyses were merged onto a single map (Fig. 5). Merging the outputs of SPA-level analyses resulted in larger hotspot areas than performing a single UK-wide analysis (in which all UK colonies were included), with a slight decline in the number of kittiwakes included (Table 1). Overall, the importance of the east coast of Scotland and the Yorkshire coast is apparent. However, the importance of areas around the coast of Shetland and the Hebrides is emphasized when looking at merged SPA-level hotspots relative to UK-wide analysis, reflecting the fact that a number of SPA-colonies are found within these regions.

As with the UK-level analysis, the size of the areas identified varied in a consistent manner between the different methods used. Hotspots based on the top 1% of Gi* scores provided hotspots with the smallest area, while hotspots based on statistically significant Gi* scores were bigger (Fig. 5, 6, Table 1). Areas delineated by maximum curvature provided the largest hotspot area for every single SPA colony, and covered the largest area when all SPA maximum curvature hotspots were merged. As expected, the area of hotspots defined as the top 1% or top 5% of Gi* scores covered 1% or 5% of the analysis field for each SPA colony (NB: analysis field was the 95% home range of the SPA in question). When using statistically significant Gi* values to determine hotspots the % area contained within identified hotspots had a median of 18.26% across SPA colonies (range: 9.67% - 31.17%). Similarly, if using maximum curvature the % area contained within identified hotspots had a median of 26.75% (range: 15.33% - 43.37%).

The % of the at sea population contained within a defined hotspot at any given time varied between colonies and between methods (Fig. 6). In general, areas defined by maximum curvature ensured that a large percentage of the at sea population was covered at any given time (median = 77.32%, range: 72.30% - 80.26%, Fig. 6). At the other extreme, areas defined by the top 1% of

Gi* scores gave the lowest % coverage of the at sea population (median = 15.18%, range: 2.78% - 33.83%). In addition, when using the top 1% or top 5% Gi* to delineate hotspots population coverage is less consistent across SPA colonies than seen when using maximum curvature or statistically significant Gi* scores.

Placing buffers around SPA colonies on the basis of foraging range estimates taken from Thaxter et al (2012) resulted in boundaries covering large areas (Fig. 5d, Table 2). Despite covering large areas, boundaries based upon foraging radii were less efficient in terms of protecting as many birds as possible per unit area. For example, creating buffers based on maximum foraging range from SPA colonies and merging outputs covered an area of 302, 934 km^2 and was estimated to contain 77.11% of the at sea population at any given time. However, merging maximum curvature boundaries for kittiwake SPAs covered an area of 219,285 km^2 (27% smaller) and was still predicted to contain an estimated 74.89 % of the at sea population.

Fig. 4. Maps displaying hotspots identified at the UK-scale for black-legged kittiwakes using a) Getis-Ord hotspot analysis with a neighbourhood size of d = 10 km based on FPT analysis and b) maximum curvature. UK EEZ also displayed.

(a)

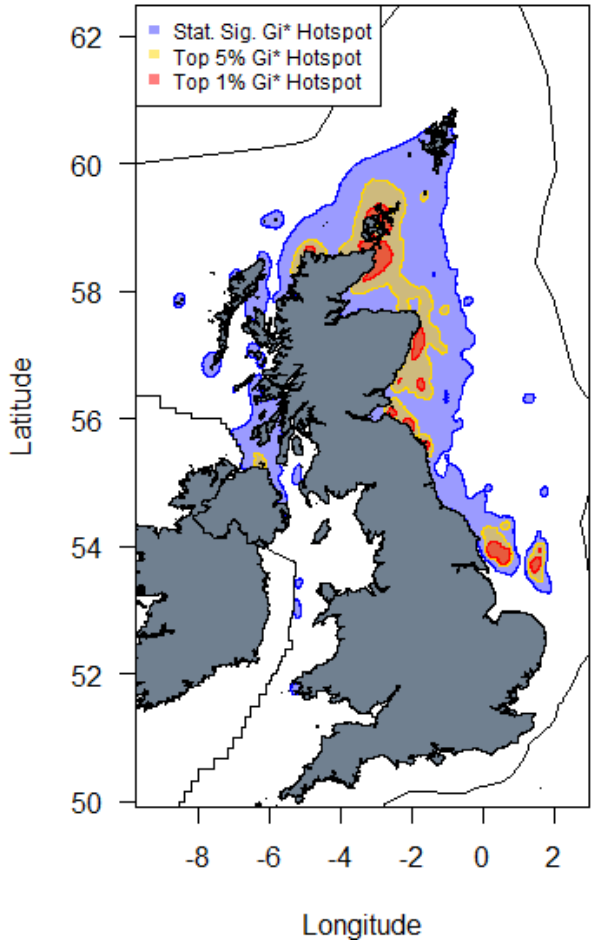

(b)

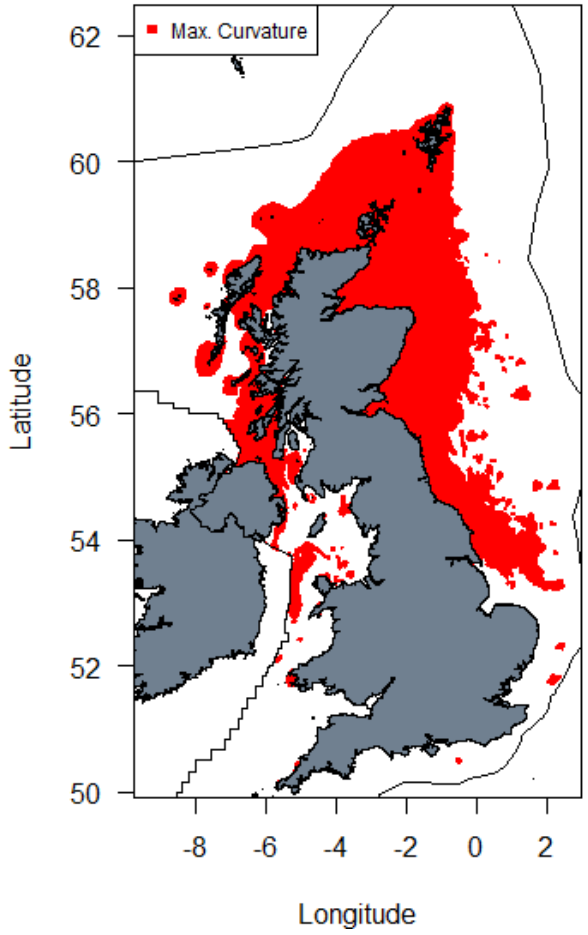

Table 1. Summary of the area and percentage of black-legged kittiwakes contained within different hotspots identified at the UK-scale. Hotspots were identified either by performing a single UK-level analysis or by conducting hotspot analysis at SPAs in which kittiwakes were listed as a feature and then merging the outputs from each SPA into a single map (SPA-level hotspots merged). UK analysis field comprises all cells within the UK EEZ and within the 95% home range of at least one UK colony (see Fig. 4). The % of at sea population within the hotspot at any given time refers to the entire UK and Ireland populations. % change between UK-level and SPA-level values calculated as $((V_2 - V_1) / V_1) \times 100$. V_1 = UK-level value, V_2 = SPA-level value. For Gi* hotspot data presented d = 10 km.

Analysis	Area of hotspots identified	Hotspot area as % of UK analysis field	% of at sea population within hotspot	Area of hotspots identified	Hotspot area as % of UK analysis field	% of at sea population within hotspot	% change UK-level vs. merged SPA-level hotspots
UK-level				**SPA-level hotspots merged**			
Top 1% Gi* hotspot	5, 852 km^2	1%	11.67%	14, 039 km^2	2.40%	10.66%	Area: 140 % increase No. Birds: 9 % decrease
Top 5% Gi* hotspot	29, 256 km^2	5%	35.78%	59, 972 km^2	10.25%	32.67%	Area: 105 % increase No. Birds: 9 % decrease
Statistically significant Gi* hotspot	122, 623 km^2	20.94%	74.08%	167, 098 km^2	28.55%	67.92%	Area: 36 % increase No. Birds: 8 % decrease
Maximum curvature	157, 802 km^2	26.95%	80.38%	219, 285 km^2	37.47%	74.89%	Area: 39 % increase No. Birds: 7 % decrease

Fig. 5. Maps displaying hotspots identified at the SPA-level for two example black-legged kittiwake SPA: a) Fowlsheugh SPA and b) Troup Head, Pennan and Lion's Heads SPA. c) Map displaying hotspots for all kittiwake SPA colonies throughout the UK. d) Map displaying kittiwake foraging ranges taken from Thaxter et al. (2012). For Gi* hotspots d = 10 km.

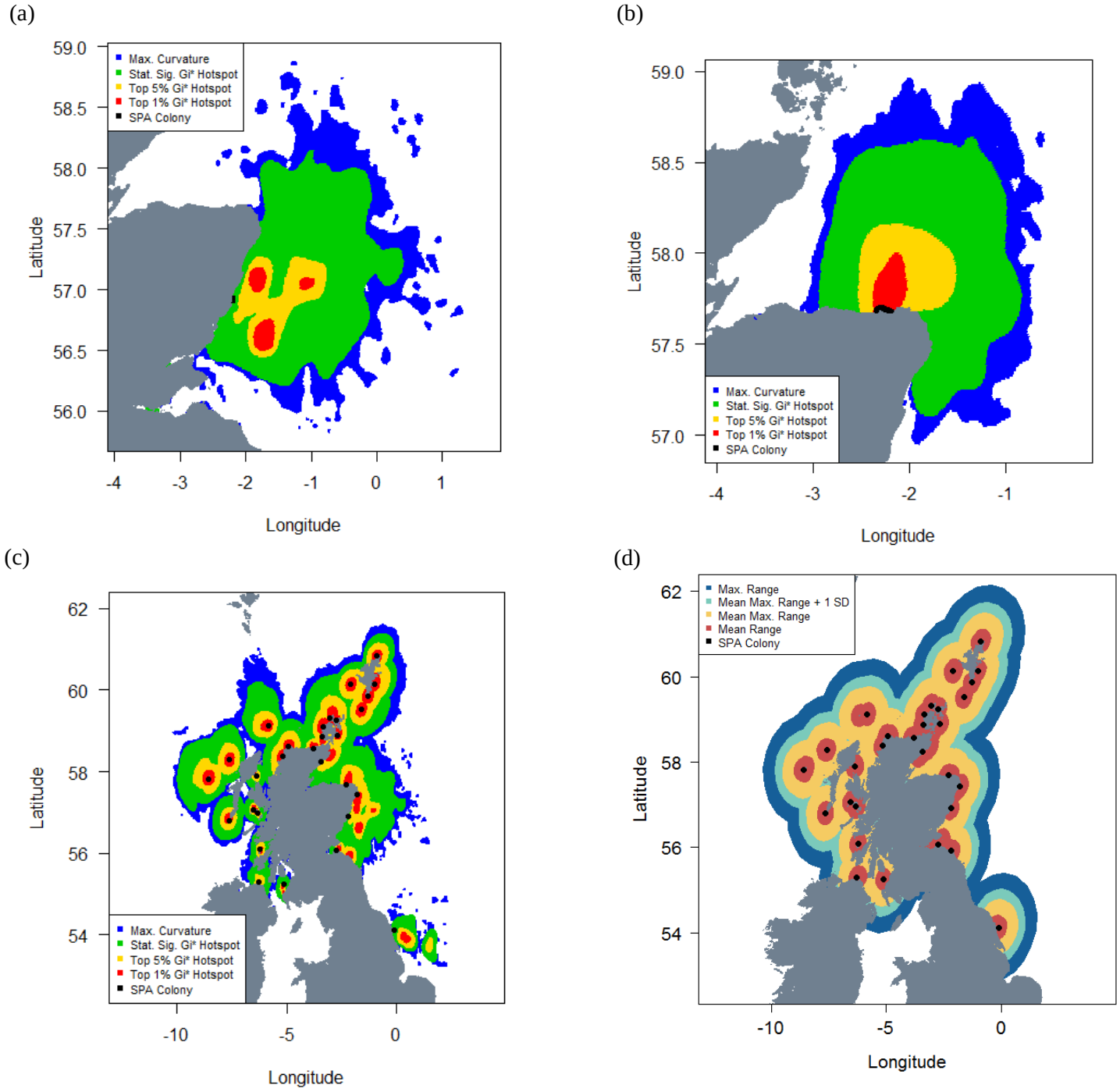

Fig. 6. Box and whisker plots showing a) area and b) % of SPA at sea population within hotspots identified using maximum curvature and Getis-Ord analysis (d = 10 km) at each SPA colony across the UK in which black-legged kittiwakes were listed as a feature. Box plots show the distribution of hotspot area and % at sea population included within a hotspot across each SPA colony included the analysis (n = 30 SPA colonies for kittiwakes). The solid line represents the median and the edges of the box show the upper and lower quartiles. Whiskers extend to the highest and lowest data extremes excluding outliers.

(a)

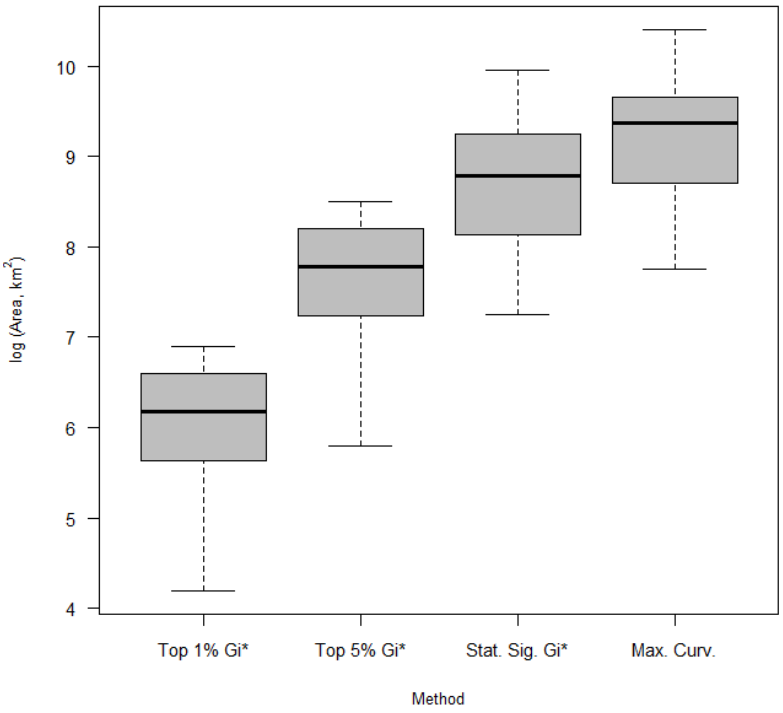

(b)

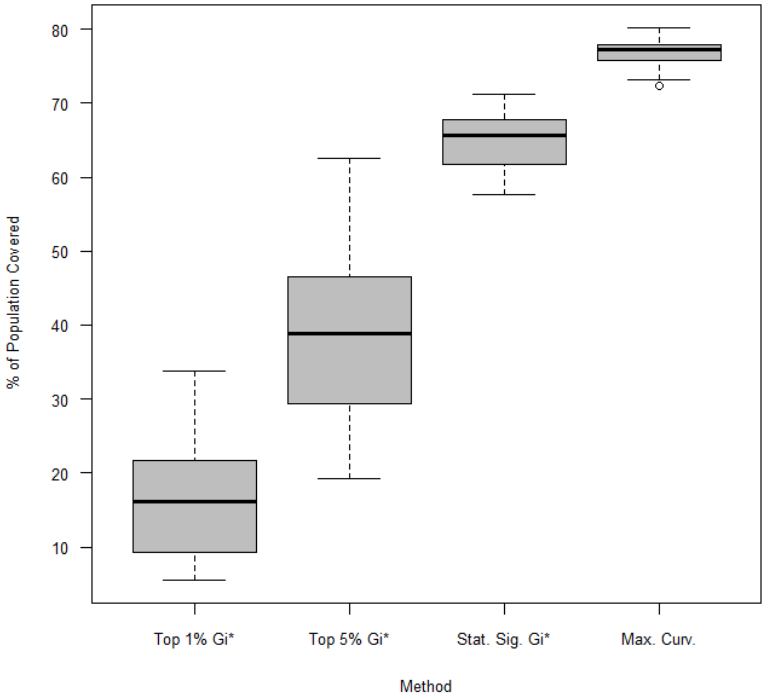

Table 2. The areas and % at sea population (UK and Republic of Ireland) contained within boundaries around UK black-legged kittiwake SPA colonies based upon foraging range (Fig. 5d). Based on foraging range data from Thaxter et al. (2012). Table also identifies which hotspot method (Fig. 5c) each foraging radius method shares the greatest similarity with.

Foraging Radius	Area within boundary	% of at sea population	Which hotspot most similar to
Mean foraging range	48, 013 km^2	29 %	Top 5% Gi* hotspot, J = 0.50
Mean-Maximum foraging range	156, 971 km^2	60 %	Stat. Sig. Gi* hotspot, J = 0.65
Mean-Maximum foraging range + 1 SD	212, 054 km^2	69 %	Max. Curv. hotspot, J = 0.69
Maximum foraging range	302, 934 km^2	77 %	Max. Curv, hotspot, J = 0.63

3.2. Common guillemots

3.2.1. UK-level

At the UK-level, the top 1% and top 5 % Gi* methods emphasized the importance of areas along the entire east coast of Scotland (Fig. 7). Using these methods, other hotspots were also evident around some of the larger UK colonies, e.g. Flamborough Head, Yorkshire or Rathlin Island, Northern Ireland. The larger areas identified by statistically significant Gi* values or maximum curvature covered these regions as well, but also encompassed almost the entirety of Scottish inshore waters. In addition, guillemot hotspots in the Irish Sea were identified, including areas off the Pembrokeshire coast and Anglesey when using either maximum curvature or statistically significant Gi* values to delineate hotspots.

Hotspots identified by loess-based maximum curvature encompassed the largest area (Table 3) and were most similar to the 80% UD contour of UK guillemots (J = 0.86). Defining

hotspots as those cells within the top 1% or top 5% of Gi* scores gave smaller areas than hotspots defined on the basis of statistical testing (Table 3). When defining hotspots as the top 1% of Gi* scores the area identified was most similar to the 15% UD of UK guillemots (J = 0.63). Similarly, when using the top 5% of Gi* scores the area identified was most similar to the 35% UD of UK guillemots (J = 0.78). Finally, when defining hotspots on the basis of statistical significant Gi* scores the area identified was most similar to the 70% UD of UK guillemots (J = 0.87). The larger areas identified by maximum curvature or statistically significant Gi* scores contained high numbers of birds (> 70% of the at sea population at any given time), but even the smallest area, defined using the top 1% of Gi* scores, was expected to contain >10% of the at sea population at any given time.

3.2.2. SPA-level

Merging the outputs of SPA-level analyses to the UK scale resulted in larger hotspots than performing a single UK-level analysis and an increase in the number of birds captured (Table 3). However, the % increase in the area covered exceeded the % increase in usage by birds in all cases. Overall, the importance of Scottish coastal waters and areas around Rathlin Island, Northern Ireland are apparent. However, the importance of areas such as the Yorkshire or Welsh coasts was reduced despite their importance at the UK-scale due to location of common guillemot colony SPAs (two in North-East England and none in Wales).

At the SPA-level, hotspots based on the top 1% of Gi* scores provided hotspots with the smallest area, while hotspots based on statistically significant Gi* scores were larger (Fig. 8, 9, Table 3). Areas delineated by maximum curvature provided the largest hotspot area for every single SPA colony, and the largest area when all SPA hotspots were merged onto a single map.

The area of hotspots defined as the top 1% or top 5% of Gi* scores covered, by definition, 1% or 5% of the analysis field across individual SPA colonies. When using statistically significant Gi* values to determine hotspots the % of the analysis field contained within identified hotspots had a median of 15 % across SPA colonies (range: 7 % - 25 %). Similarly, if using maximum curvature the % area contained within identified hotspots had a median of 25 % (range: 18 % - 47 %). The % of the at sea population contained within a given boundary at any given time varied between colonies and between methods. In general, areas defined by maximum curvature ensured that a large percentage of the at sea population was covered (median = 78 %, range: 69 % - 80 %, Fig. 9). At the other extreme, areas defined by the top 1% of Gi* scores gave the lowest % coverage of the at sea population (median = 18 %, range: 5 % - 36 %).

Placing buffers around SPA colonies on the basis of foraging range estimates taken from Thaxter et al (2012) resulted in boundaries covering large areas (Table 4). In particular, boundaries based on the Mean-Maximum or Maximum observed foraging range resulted in areas much larger than those identified by any of the hotspot methods used. The spatial similarity between different foraging range buffers and the most similar hotspot method is listed in Table 4.

Fig. 7. Maps displaying hotspots identified at the UK-level for common guillemots using a) Getis-Ord hotspot analysis with a neighbourhood size of d = 9 km based on FPT analysis and b) maximum curvature. UK EEZ also displayed.

(a)

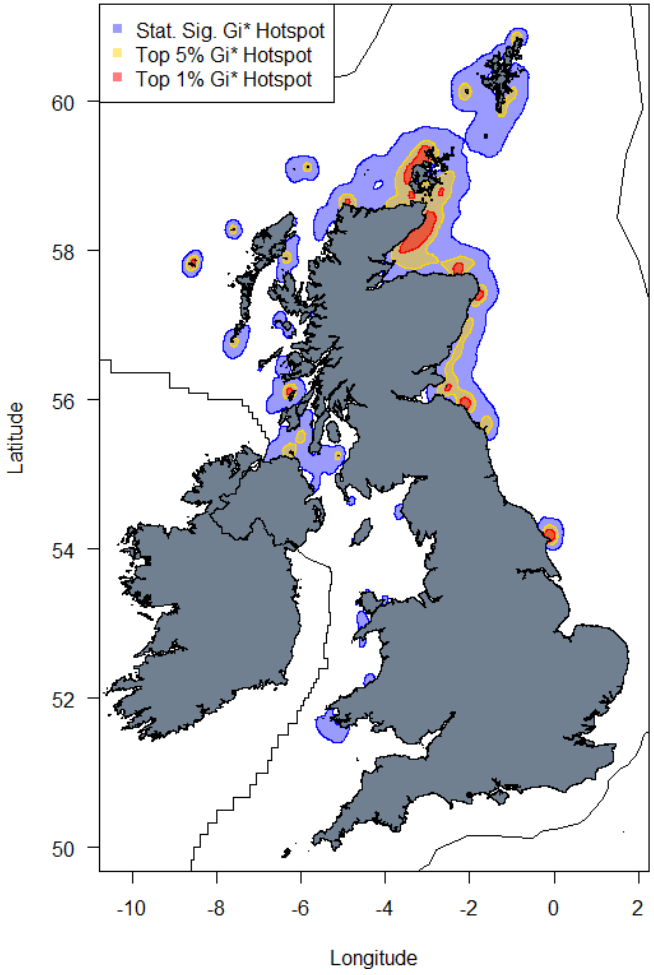

(b)

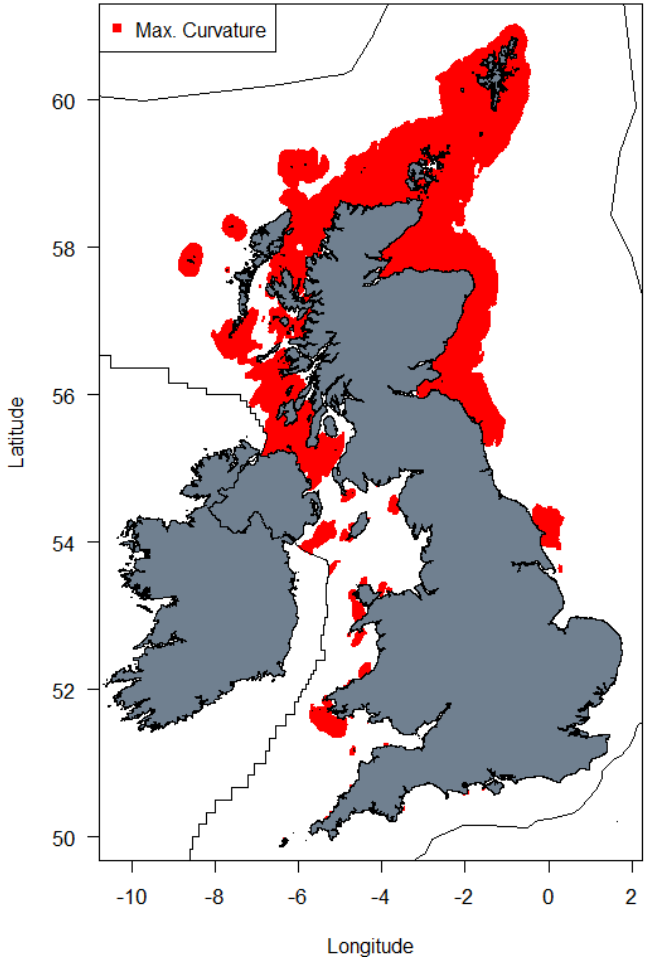

Table 3. Summary of the area and percentage of common guillemots contained within different hotspots identified at the UK-scale. Hotspots were identified either by performing a single UK-level analysis or by conducting hotspot analysis at SPAs in which guillemots were listed as a feature and then merging the outputs from each SPA into a single map (SPA-level hotspots merged). UK analysis field comprises all cells within the UK EEZ and within the 95% home range of at least one UK colony (see Fig. 4). The % of at sea population within the hotspot refers to the UK and Ireland populations. % change between UK-level and SPA-level values calculated as $((V_2 - V_1) / V_1) \times 100$. V_1 = UK-level value, V_2 = SPA-level value. For Gi* hotspot data presented d = 9 km.

Analysis	Area of hotspots identified	Hotspot area as % of UK analysis field	% of at sea population within hotspot	Area of hotspots identified	Hotspot area as % of UK analysis field	% of at sea population within hotspot	% change UK-level vs. merged SPA-level hotspots
UK-level				**SPA-level hotspots merged**			
Top 1% Gi* hotspot	2, 933 km^2	1%	10.50 %	7, 831 km^2	2.67%	16.33%	Area: 167 % increase No. Birds: 56% increase
Top 5% Gi* hotspot	14, 663 km^2	5%	33.54%	35, 653 km^2	12.15%	44.86%	Area: 143 % increase No. Birds: 34% increase
Statistically significant Gi* hotspot	62, 648 km^2	21.34%	71.12%	95, 480 km^2	32.53%	78.14%	Area: 52 % increase No. Birds: 10 % increase
Maximum curvature	95, 093 km^2	32.40%	83.12%	131, 858 km^2	44.92%	86.24%	Area: 39 % increase No. Birds: 4 % increase

Fig. 8. Maps displaying hotspots identified at the SPA-level for two example common guillemot SPA: a) Rathlin Island SPA and b) St Abb's Head to Fast Castle SPA. c) Map displaying hotpots for all guillemot SPA colonies throughout the UK. d) Map displaying guillemot foraging ranges taken from Thaxter et al. (2012). For Gi* hotspots d = 9 km.

(a)

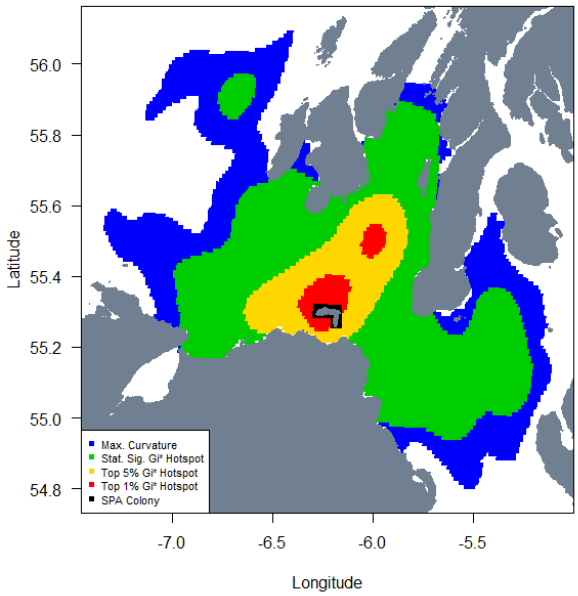

(b)

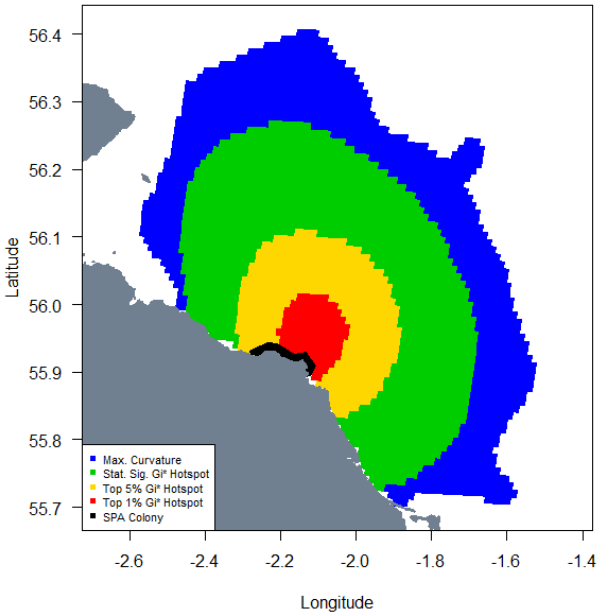

(c)

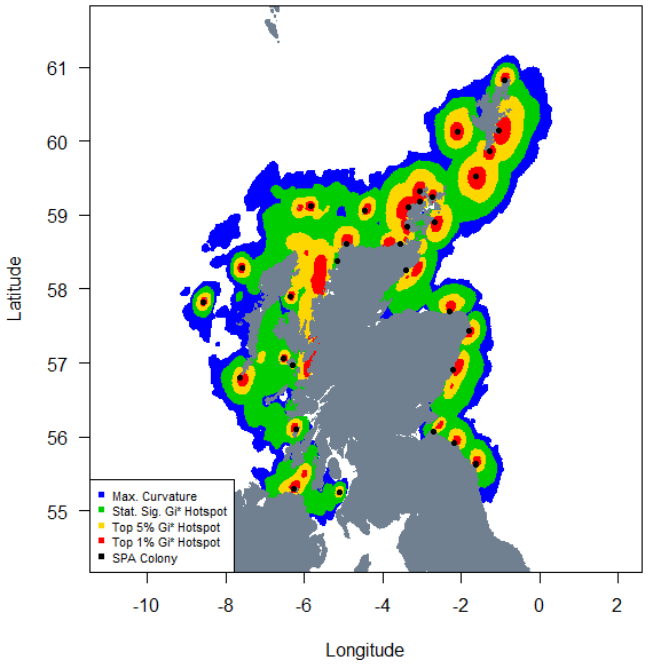

(d)

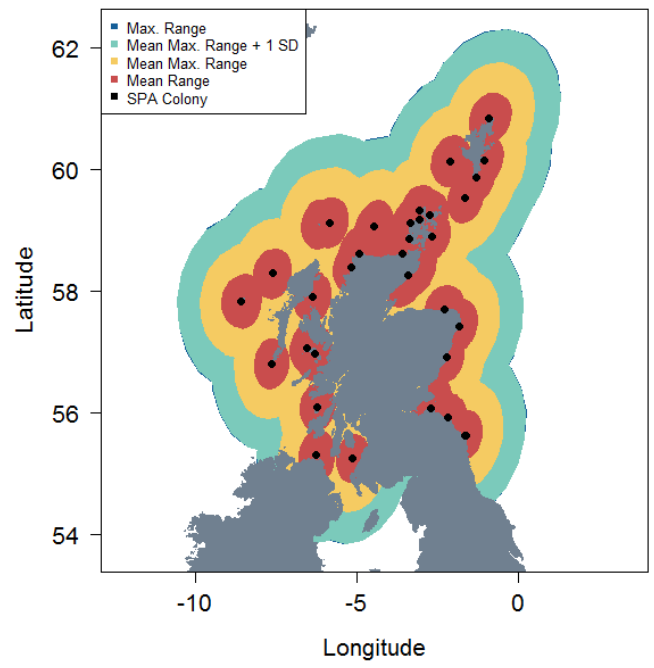

Fig. 9. Box and whisker plots showing a) area and b) % of SPA at sea population within hotspots identified using maximum curvature and Getis-Ord analysis at each SPA colony across the UK in which guillemots were listed as a feature. Box plots show the distribution of hotspot area and % at sea population included within a hotspot across each SPA colony included the analysis (n = 33 SPA colonies for guillemots). The solid line represents the median and the edges of the box show the upper and lower quartiles. Whiskers extend to the highest and lowest data extremes excluding outliers.

(a)

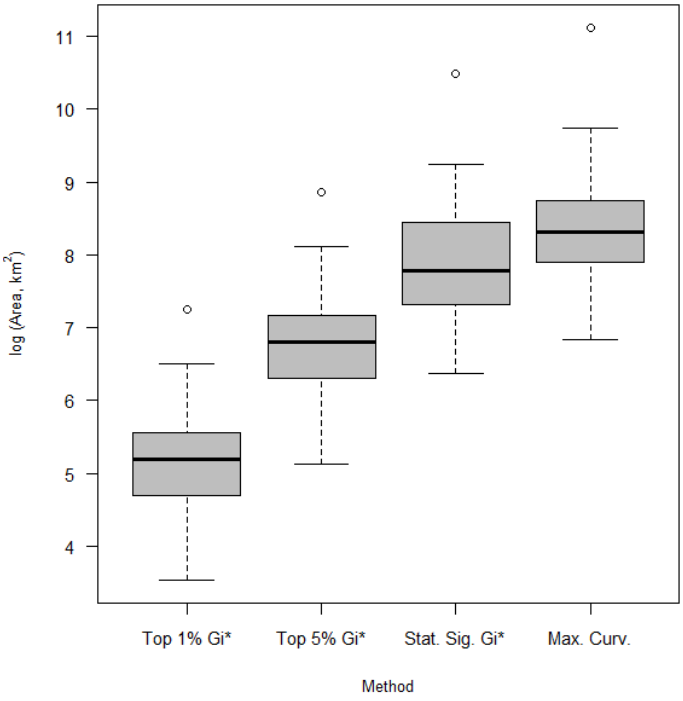

(b)

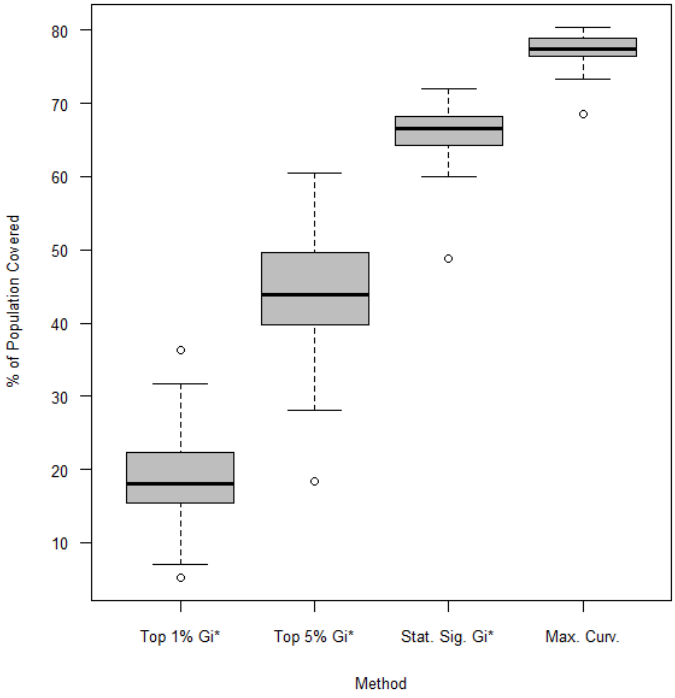

Table 4. The areas and % at sea population (UK and Republic of Ireland) contained within buffers around UK guillemot SPA colonies at any given time based upon foraging range (Fig. 8d). Foraging range data from Thaxter et al. (2012). Table also identifies which hotspot method (Fig. 8c) each foraging radius method shares the greatest similarity with.

Foraging Radius	Area within boundary	% of at sea population	Which hotspot most similar to
Mean foraging range	92, 678 km^2	64 %	Stat. Sig. Gi* hotspot, J = 0.63
Mean-Maximum foraging range	207, 991 km^2	79 %	Max. Curv. hotspot, J = 0.61
Mean-Maximum foraging range + 1 SD	316, 450 km^2	84%	Max. Curv. hotspot, J = 0.41
Maximum foraging range	318, 005 km^2	84%	Max. Curv, hotspot, J = 0.41

3.3. Razorbill

3.3.1. UK-level

At the UK-level, the top 1% and top 5 % Gi* methods emphasized the importance of a variety of areas across the UK. Multiple hotspots were identified along the east coast of Scotland and the Orkney Islands as well as hotspots in the Hebrides and around Foula, Shetland (Fig. 10). Outside of Scotland the top 1% and top 5% Gi* methods also identified hotspots along the Northern Irish coast, around the Yorkshire coast in England and around the Pembrokeshire coast in Wales. The larger areas identified by statistically significant Gi* values or maximum curvature covered these regions as well.

Hotspots identified by loess-based maximum curvature encompassed the largest area (Table 5) and were most similar to the 80% UD of UK razorbills (J = 0.86). Defining hotspots as those cells within the top 1% or top 5% of Gi* scores gave smaller areas than hotspots defined on the basis of statistical testing (Table 5). When defining hotspots as the top 1% of Gi* scores the area identified was most similar to the 20% UD of UK razorbills (J = 0.62). Similarly, when using the top 5% of Gi* scores the area identified was most similar to the 40% UD of UK razorbills (J = 0.74). Finally, when defining hotspots on the basis of statistical significant Gi* scores the areas identified was most similar to the 60% UD of UK razorbills (J = 0.83). The larger areas identified by maximum curvature or statistically significant Gi* scores contained high numbers of birds (> 60% of the at sea population at any given time), but even the smallest area, defined using the top 1% of Gi* scores, was expected to contain >10% of the at sea population at any given time.

3.3.2. SPA-level

Merging the outputs of SPA-level analyses to the UK scale resulted in larger hotspots than performing a single UK-wide analysis and resulted in an increase in the number of birds captured (Table 5). However, the % increase in the area covered exceeded the % increase in usage by birds in all cases. At the SPA-level, the importance of Scottish coastal waters and areas around Rathlin Island, Northern Ireland are apparent. However, the importance of areas such as the Yorkshire or the Welsh coast is less well reflected despite their importance at the UK-scale due to location of razorbill SPAs. Currently, there are no SPAs in which razorbills are designated as a feature in Wales (although they form part of a seabird assemblage at the Skomer, Skokholm and seas off Pembrokeshire SPA). Similarly, razorbills were not a designated feature in any English SPAs at the time of the analysis[2].

At the SPA-level, hotspots based on the top 1% of Gi* scores provided hotspots with the smallest area (Fig. 11). Unlike the previously examined species (kittiwakes and guillemots) there was often little difference between the areas of hotspots based on the top 5% Gi* scores or statistically significant Gi* scores at the level of individual SPA colonies (Fig. 12). Indeed, for certain SPA colonies hotspots based on the top 5% Gi* scores were actually larger than those based on statistical significance. Areas delineated by maximum curvature provided the largest hotspot area for every single SPA colony, as well as the largest area when all SPA hotspots were merged onto a single map. When using statistically significant Gi* values to determine hotspots the % of the analysis field contained within identified hotspots had a median of 7 % across SPA colonies (range: 5 % - 36 %). Similarly, if using maximum curvature the % area of the analysis field covered

[2] Note that razorbills have since been listed as feature in the new Flamborough and Filey Coast SPA which represents an extension to the existing Flamborough and Bempton Cliffs SPA.

by identified hotspots had a median of 20 % (range: 17 % - 53 %). In general, areas defined by maximum curvature ensured that a large percentage of the at sea population was covered at any one time (median = 78 %, range: 69 % - 80 %, Fig. 12). At the other extreme, areas defined by the top 1% of Gi* scores gave the lowest % coverage of the at sea population, although always included more than 1% of the population (median = 33 %, range: 3 % - 48 %).

Placing buffers around SPA colonies on the basis of foraging range estimates taken from Thaxter et al (2012) resulted in boundaries covering large areas (Table 5). In particular boundaries created around colonies using the maximum observed foraging range covered areas that were larger even than those identified using maximum curvature at the SPA-level. The spatial similarity between different foraging range buffers and the most similar hotspot method is listed in Table 6.

Fig. 10. Maps displaying hotspots identified at the UK-level for razorbills using a) Getis-Ord hotspot analysis with a neighbourhood size of d = 7 km based on FPT analysis and b) maximum curvature. UK EEZ also displayed.

(a)

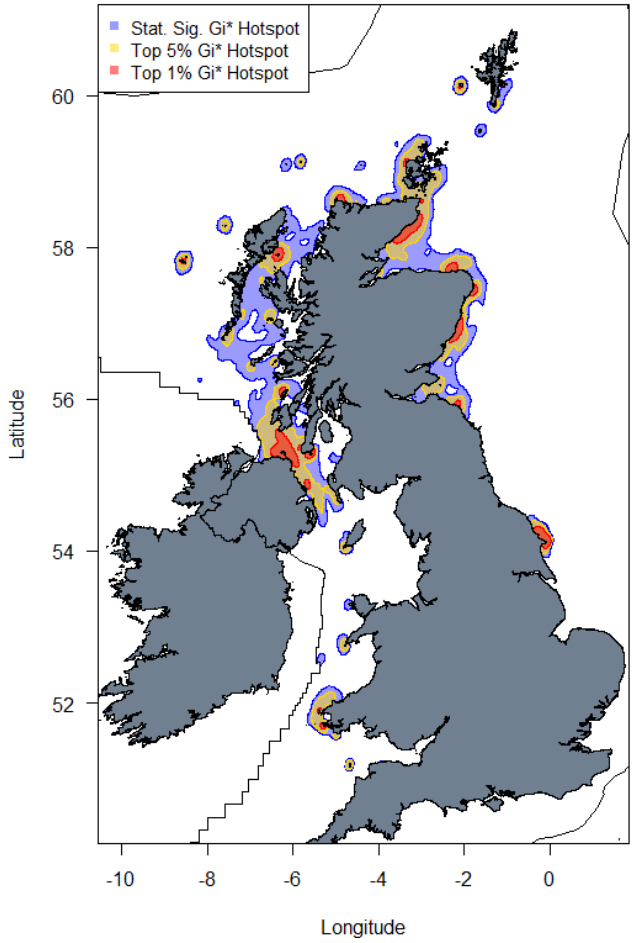

(b)

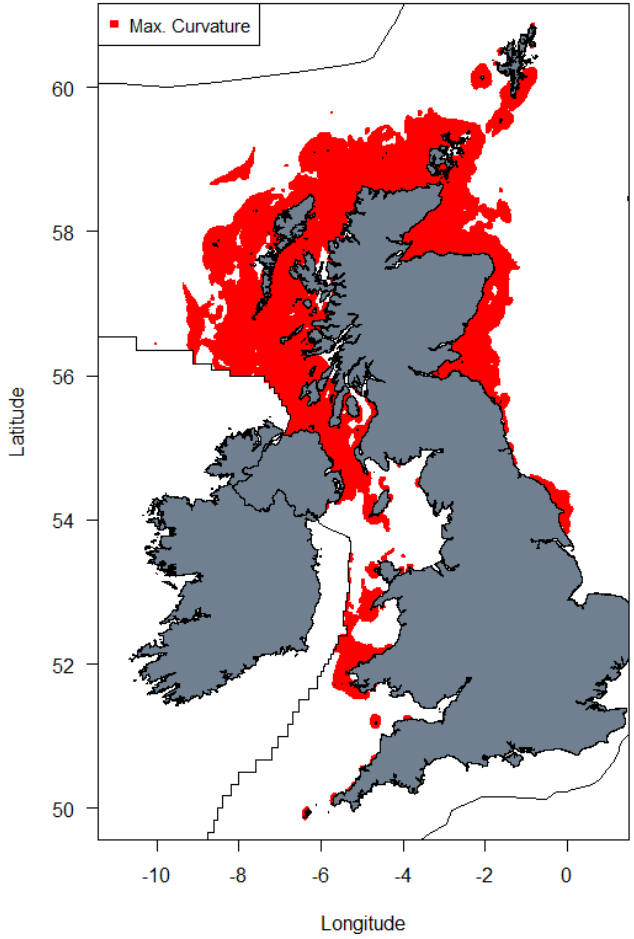

Table 5. Summary of the area and percentage of razorbills contained within different hotspots identified at the UK-scale. Hotspots were identified either by performing a single UK-level analysis or by conducting hotspot analysis at SPAs in which razorbills were listed as a feature and then merging the outputs from each SPA into a single map (SPA-level hotspots merged). UK analysis field comprises all cells within the UK EEZ and within the 95% home range of at least one UK colony (see Fig. 4). The % of at sea population within the hotspot refers to the UK and Ireland populations. % change between UK-level and SPA-level values calculated as $((V_2 - V_1) / V_1) \times 100$. V_1 = UK-level value, V_2 = SPA-level value. For Gi* hotspot data presented d = 7 km.

Analysis	Area of hotspots identified	Hotspot area as % of UK analysis field	% of at sea population within hotspot	Area of hotspots identified	Hotspot area as % of UK analysis field	% of at sea population within hotspot	% change UK-level vs. merged SPA-level hotspots
UK-level				**SPA-level hotspots merged**			
Top 1% Gi* hotspot	3, 570 km^2	1%	18.23 %	10, 934 km^2	3.06%	22.33%	Area: 206 % increase No. Birds: 21% increase
Top 5% Gi* hotspot	17, 848 km^2	5%	39.17%	49, 700 km^2	13.91%	48.05%	Area: 178 % increase No. Birds: 23 % increase
Statistically significant Gi* hotspot	46, 999 km^2	13.16%	59.53%	101, 963 km^2	28.54%	65.73%	Area: 117 % increase No. Birds: 10 % increase
Maximum curvature	108, 515 km^2	30.37%	80.52%	180, 948 km^2	50.65%	86.96%	Area: 67 % increase No. Birds: 8 % increase

Fig. 11. Maps displaying hotspots identified at the SPA-level for two example razorbill SPA: a) Rathlin Island SPA and b) Mingulay and Berneray SPA. c) Map displaying hotpots for all razorbill SPA colonies throughout the UK. d) Map displaying razorbill foraging ranges taken from Thaxter et al. (2012). For Gi* hotspots *d* = 7 km.

(a)

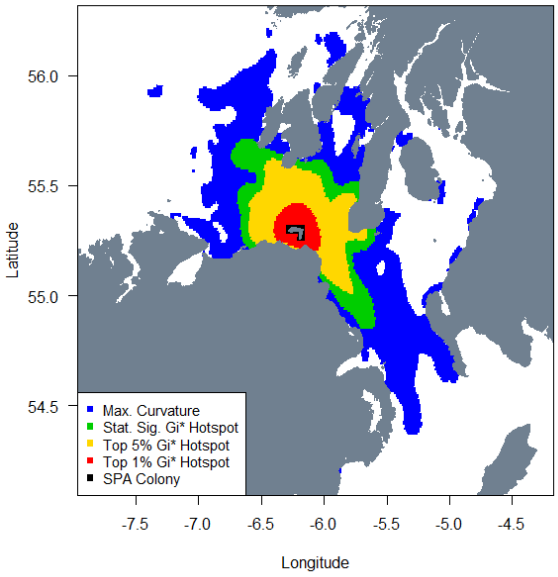

(b)

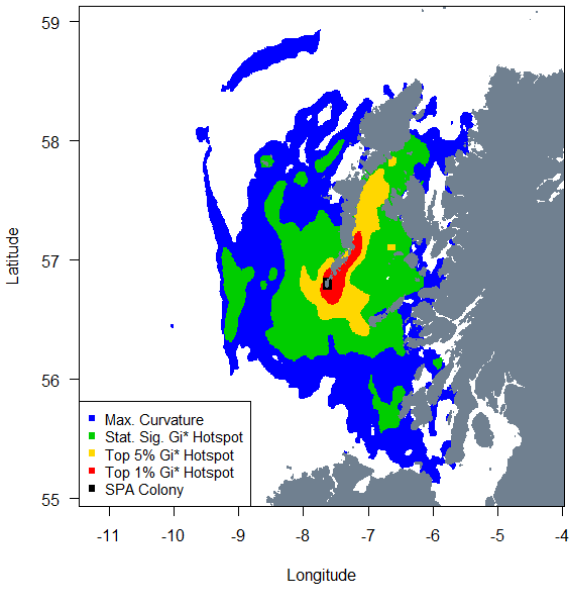

(c)

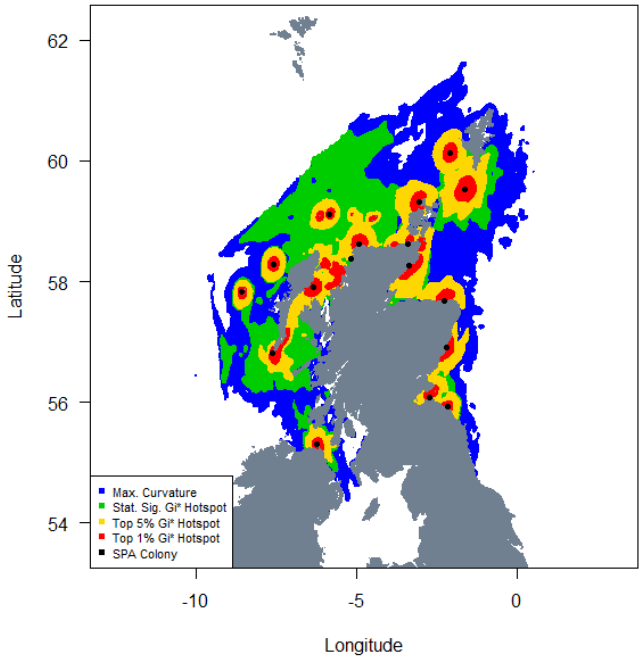

(d)

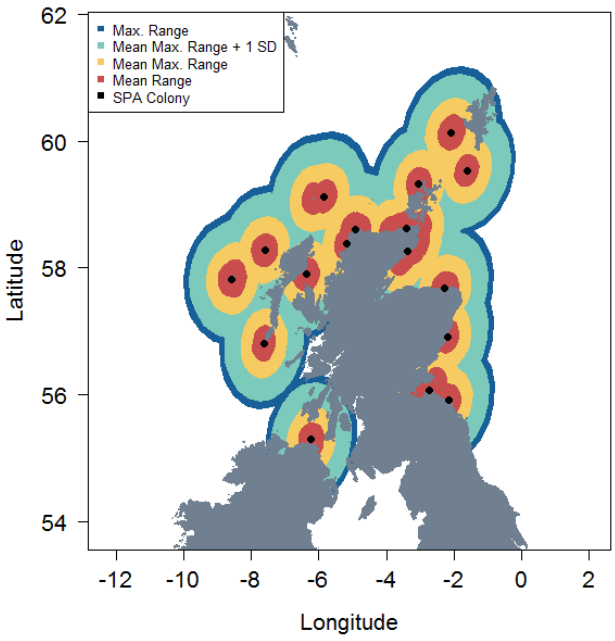

Fig. 12. Box and whisker plots showing a) area and b) % of SPA at sea population within hotspots identified using maximum curvature and Getis-Ord analysis at each SPA colony across the UK in which razorbills were listed as a feature. Box plots show the distribution of hotspot area and % at sea population included within a hotspot across each SPA colony included the analysis (*n* = 17 SPA colonies for razorbills). The solid line represents the median and the edges of the box show the upper and lower quartiles. Whiskers extend to the highest and lowest data extremes excluding outliers.

(a)

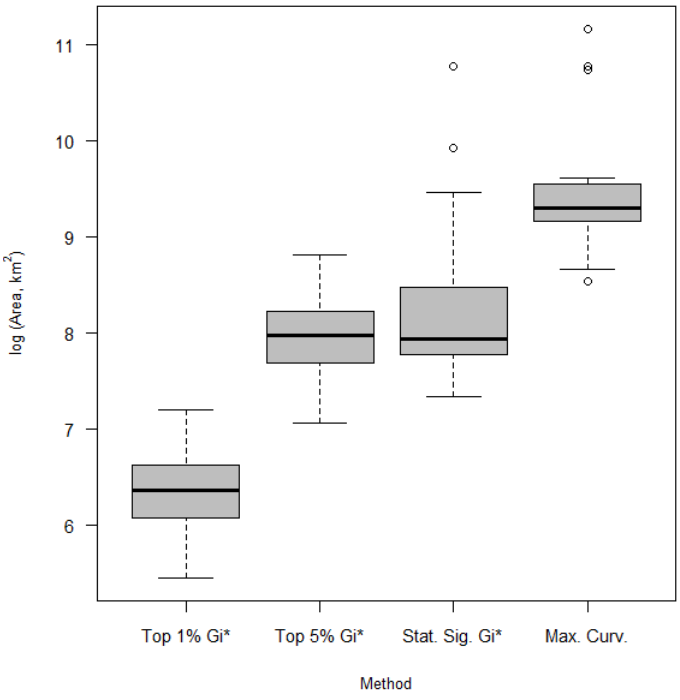

(b)

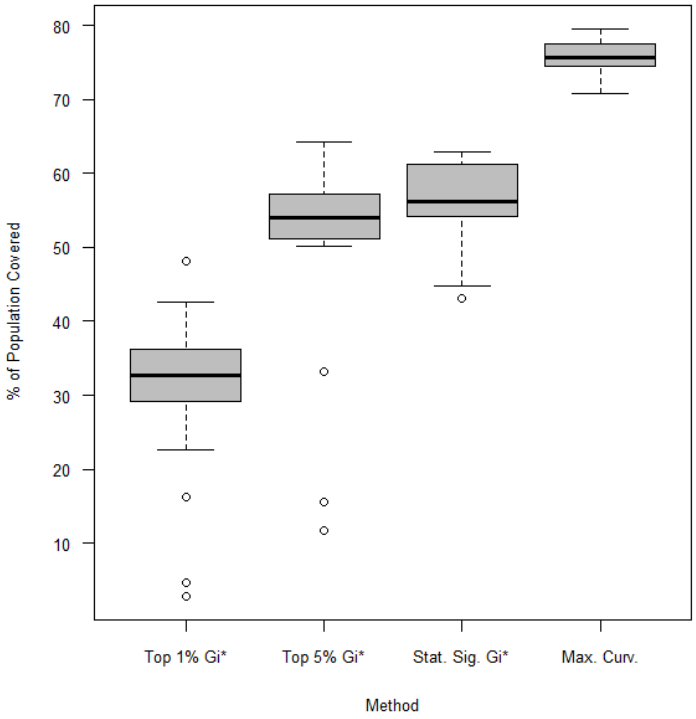

Table 6. The areas and % at sea population (UK and Republic of Ireland) contained within boundaries around UK razorbill SPA colonies based upon foraging range (Fig. 11d). Foraging range data from Thaxter et al. (2012). Table also identifies which hotspot method (Fig. 11c) each foraging radius method shares the greatest similarity with.

Foraging Radius	Area within boundary	% of at sea population	Which hotspot most similar to
Mean foraging range	29, 743 km^2	29 %	Top 5 Gi* hotspot, J = 0.49
Mean-Maximum foraging range	91, 520 km^2	51 %	Max. Curv. hotspot, J = 0.51
Mean-Maximum foraging range + 1 SD	169, 371 km^2	69%	Max. Curv. hotspot, J = 0.71
Maximum foraging range	193, 665 km^2	72%	Max. Curv, hotspot, J = 0.71

3.4. European shags

3.4.1. UK-level

At the UK-level, the top 1% and top 5 % Gi* methods emphasized the importance of a variety of areas across the UK (Fig. 13). However, the area of hotspots was small and their distribution reflected the location of the larger shag colonies. For example, top 1% Gi* hotspots were identified around Foula and the Isle of May in Scotland as well as the Isles of Scilly and the Farne Islands in England. The areas identified by statistically significant Gi* scores or maximum curvature covered larger areas, but were still restricted to coastal areas close to larger breeding colonies. Unlike the other species examined, results for shags are harder to visualise at the UK-scale, reflecting their highly localised foraging behaviour.

Hotspots identified by loess-based maximum curvature encompassed the largest area (Table 7) and were most similar to the 90% UD of UK shags (J = 0.38). Defining hotspots as those cells within the top 1% or top 5% of Gi* scores gave smaller areas than hotspots defined on the basis of statistical testing (Table 7). When defining hotspots as the top 1% of Gi* scores the area identified was most similar to the 55% UD of UK shags (J = 0.12). Similarly, when using the top 5% of Gi* scores the area identified was most similar to the 75% UD of UK shags (J = 0.12). Finally, when defining hotspots on the basis of statistical significant Gi* scores the areas identified was most similar to the 85% UD of UK shags (J = 0.21). The larger areas identified by maximum curvature or statistically significant Gi* scores contained high numbers of birds (> 60% of the at sea population), but even the smallest area, defined using the top 1% of Gi* scores, was expected to contain >15% of the at sea population.

3.4.2. SPA-level

In contrast to the other species examined, merging the outputs of SPA-level analyses resulted in smaller hotspots than performing a single UK-wide analysis and led to a concomitant reduction in the number of birds captured (Table 7). Such declines may be due to the relatively low number of colony SPAs across the UK in which shags are a designated feature (n = 11) and how they are arranged in space. For example, when merging the SPA-level hotspots at a UK scale, the importance of Scottish coastal waters is emphasized reflecting the distribution of designated shag SPA colonies, which are currently all found in Scotland (although shags will be a qualifying feature of the proposed Isles of Scilly SPA).

Hotspots based on the top 1% of Gi* scores provided hotspots with the smallest area (Fig. 14). The areas of hotspots based on the top 5% Gi* were generally smaller than those based upon statistically significant Gi* scores across SPA colonies. However, this difference in area was not always large and in one instance hotspots based on the top 5% Gi* scores identified larger areas than based on statistically significant Gi* values. As with the other species, areas delineated by maximum curvature provided the largest hotspot area for every single SPA colony, as well as the largest area when all SPA hotspots were merged onto a single map. When using statistically significant Gi* values to determine hotspots the % of the analysis field contained within identified hotspots had a median of 9 % across SPA colonies (range: 4 % - 11 %). Similarly, if using maximum curvature the % area contained within identified hotspots had a median of 28 % (range: 21 % - 35 %) across SPAs. The % of the at sea population contained within a given hotspot boundary at any given time varied between colonies and between methods (Fig. 15). In general, areas defined by maximum curvature ensured that a large percentage of the at sea population was covered (median = 78 %, range: 69 % - 80 %). At the other extreme, areas defined by the top 1%

of Gi* scores gave the lowest % coverage of the at sea population, although always included more than 1% of the at sea population (median = 12 %, range: 8 % - 25 %).

Placing buffers around SPA colonies on the basis of foraging range estimates taken from Thaxter et al (2012) resulted in boundaries covering large areas. Boundaries created around colonies using the maximum observed foraging range covered areas that were larger even than those identified using maximum curvature at either the UK-level or SPA-level. The spatial similarity between different foraging range buffers and the most similar hotspot method is listed in Table 8.

Fig. 13. Maps displaying hotspots identified at the UK-scale for shags using a) Getis-Ord hotspot analysis with a neighbourhood size of *d* = 4 km based on FPT analysis b) and maximum curvature. UK EEZ also displayed.

(a)

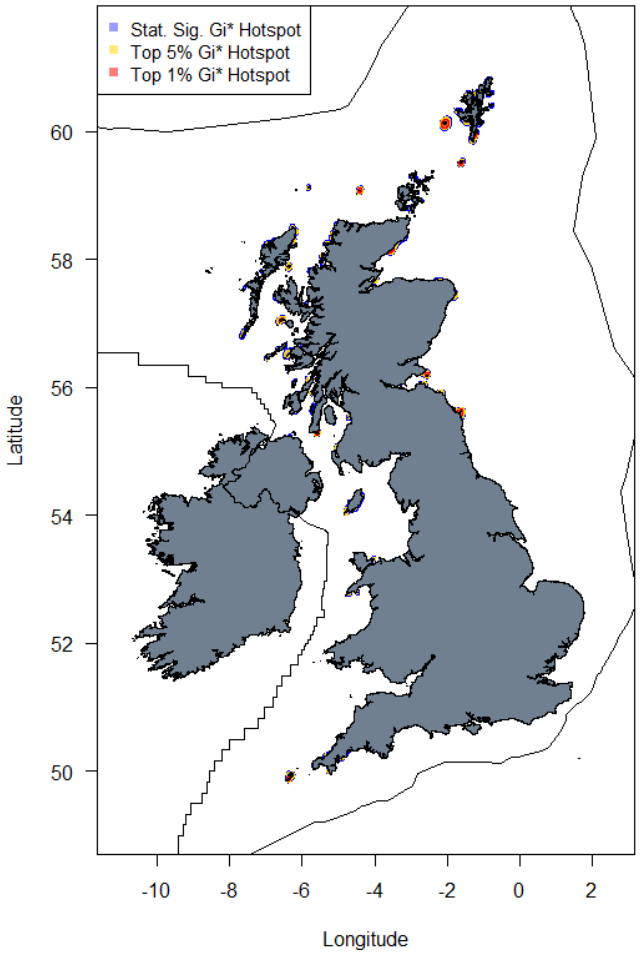

(b)

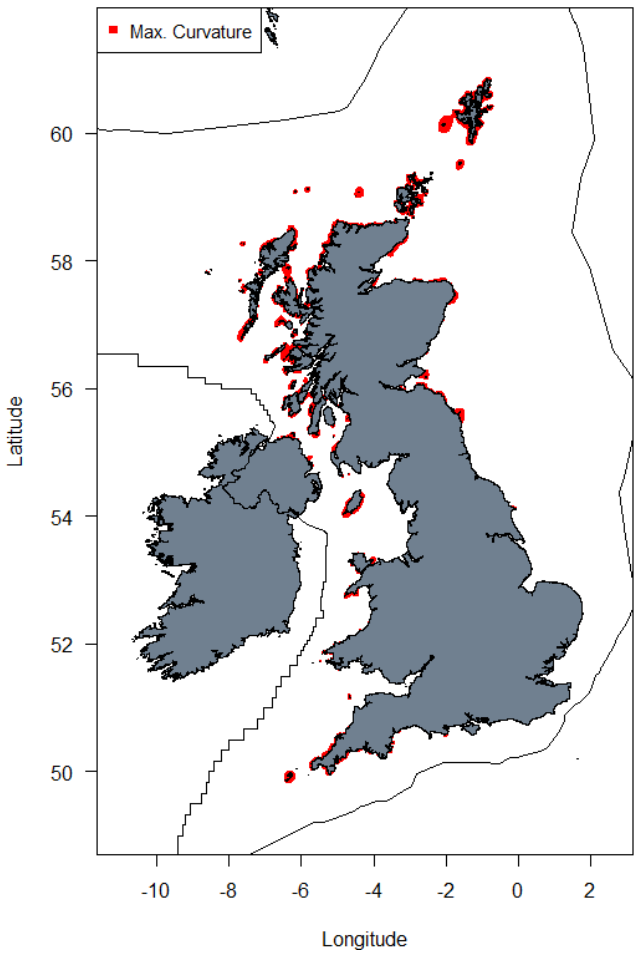

Table 7. Summary of the area and percentage of shags contained within different hotspots identified at the UK-scale. Hotspots were identified either by performing a single UK-level analysis or by conducting hotspot analysis at SPAs in which shags were listed as a feature and then merging the outputs from each SPA into a single map (SPA-level hotspots merged). UK analysis field comprises all cells within the UK EEZ and within the 95% home range of at least one UK colony (see Fig. 4). The % of at sea population within the hotspot refers to the UK and Ireland populations. % change between UK-level and SPA-level values calculated as $((V_2 - V_1) / V_1) \times 100$. V_1 = UK-level value, V_2 = SPA-level value. For Gi* hotspot data presented d = 4 km.

Analysis	Area of hotspots identified	Hotspot area as % of UK analysis field	% of at sea population within hotspot	Area of hotspots identified	Hotspot area as % of UK analysis field	% of at sea population within hotspot	% change UK-level vs. merged SPA-level hotspots
UK-level				**SPA-level hotspots merged**			
Top 1% Gi* hotspot	458 km^2	1%	20.35 %	36 km^2	0.078%	4.10%	Area: 92 % decrease No. Birds: 80% decrease
Top 5% Gi* hotspot	2, 288 km^2	5%	44.39%	176 km^2	0.38%	11.20%	Area: 92 % decrease No. Birds: 75 % decrease
Statistically significant Gi* hotspot	6, 235 km^2	13.51%	68.24%	706 km^2	1.53%	19.94%	Area: 89 % decrease No. Birds: 71 % decrease
Maximum curvature	10, 201 km^2	22.11%	85.41%	999 km^2	2.16%	23.93%	Area: 90 % decrease No. Birds: 72 % decrease

Fig. 14. Maps displaying hotspots identified at the SPA-level for two example shag SPA: a) Foula SPA and b) Forth Islands SPA. c) Map displaying hotpots for all shag SPA colonies throughout the UK. d) Map displaying shag foraging ranges taken from Thaxter et al. (2012), note no mean-max + 1 SD was reported for this species. For Gi* hotspots d = 4 km.

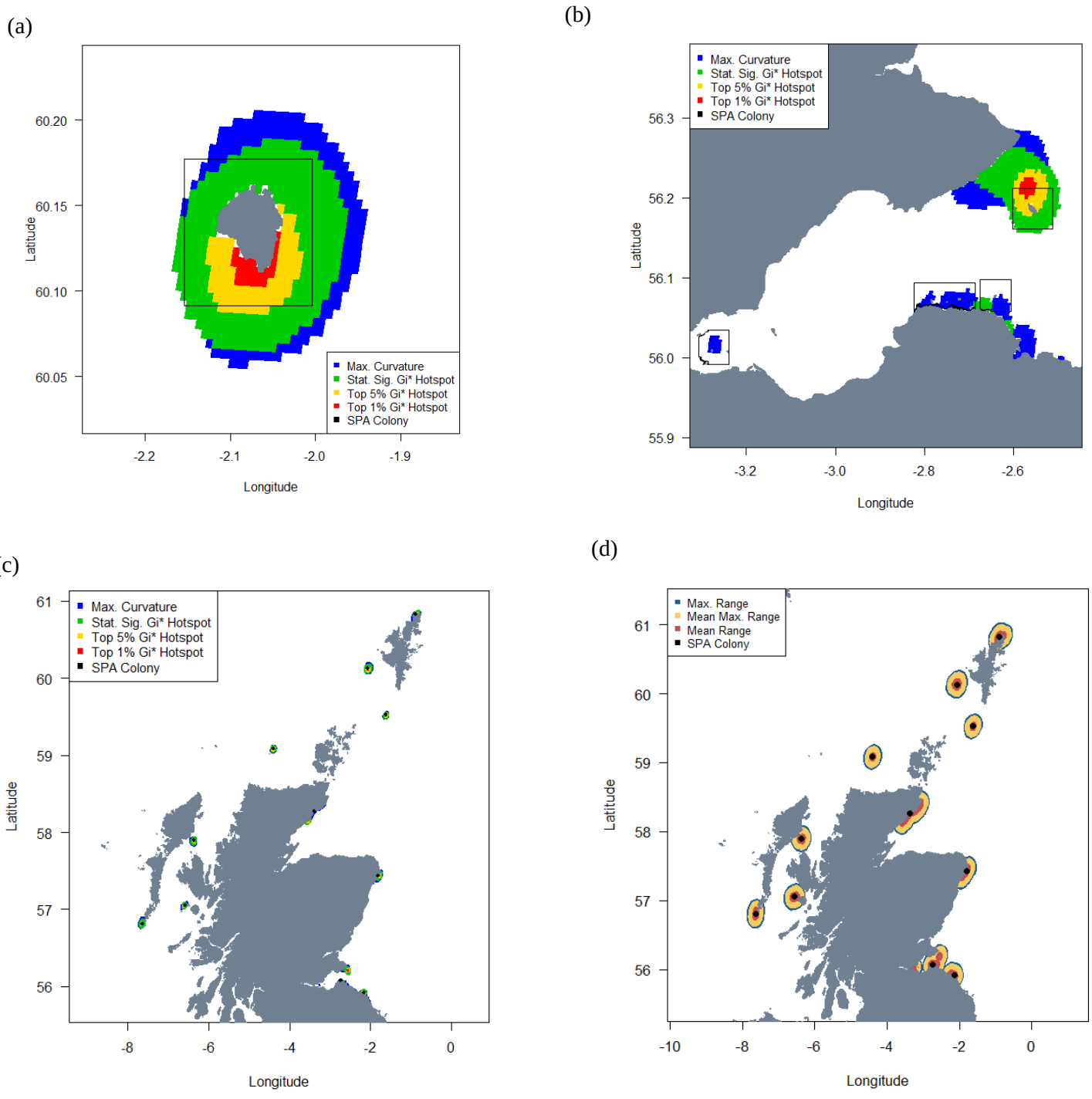

Fig. 15. Box and whisker plots showing a) area and b) % of SPA at sea population within hotspots identified using maximum curvature and Getis-Ord analysis at each SPA colony across the UK in which shags were listed as a feature. Box plots show the distribution of hotspot area and % population included within a hotspot across each SPA colony included the analysis (*n* = 11 SPA colonies for shags). The solid line represents the median and the edges of the box show the upper and lower quartiles. Whiskers extend to the highest and lowest data extremes excluding outliers.

(a)

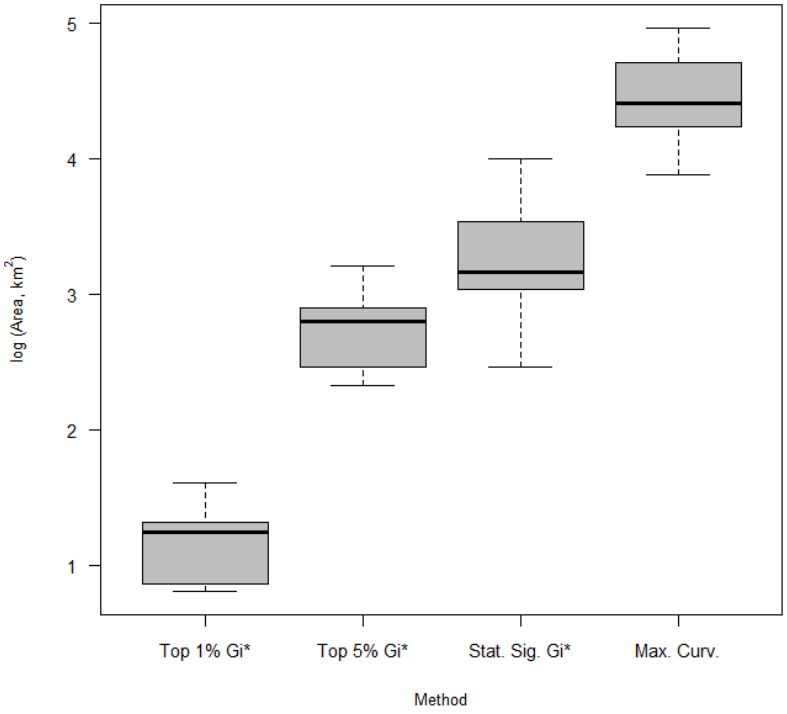

(b)

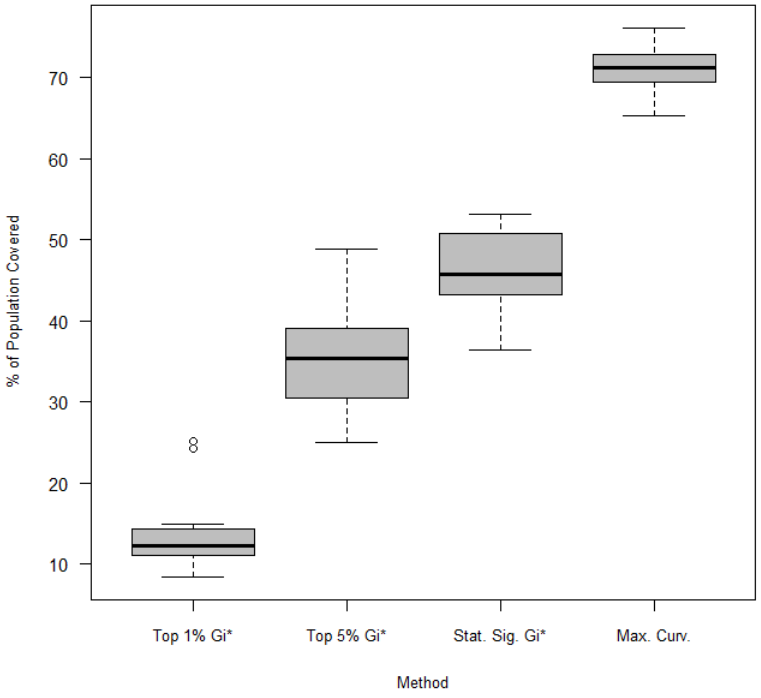

Table 8. The areas and % at sea population (UK and Republic of Ireland) contained within boundaries around UK shag SPA colonies based upon foraging range (Fig. 14d). Foraging range data from Thaxter et al. (2012). Note for shags Thaxter et al. (2012) does not report a value for Mean-max foraging range + 1 standard deviation. Table also identifies which hotspot method (Fig. 14c) each foraging radius method shares the greatest similarity with.

Foraging Radius	Area within boundary	% of at sea population	Which hotspot most similar to
Mean foraging range	2, 059 km^2	22 %	Max. Curv. hotspot, J = 0.41
Mean-Maximum foraging range	8, 601 km^2	27 %	Max. Curv. hotspot, J = 0.11
Mean-Maximum foraging range + 1 SD	NA	NA	NA
Maximum foraging range	11, 229 km^2	27 %	Max. Curv, hotspot, J = 0.09

4. Discussion

The current report demonstrates how GPS tracking data, processed via species distribution models (Wakefield et al. 2017), can be used to map seabird hotspots using previously established techniques (Kober et al. 2010, O'Brien et al. 2012). Key features of this are approach are that 1) species distribution modelling and, hence, hotspot mapping takes into account species-habitat relationships; 2) predictive modelling allows estimation of seabird distributions and the identification of potential hotspots even from colonies in which birds were not tracked and 3) hotspot mapping can be performed across a range of spatial scales (e.g. SPA-level or UK-level) depending on one's focus. Each of these features will assist in efforts to identify important at sea areas. For example, information on species-habitat relationships has proven important when designing protected areas (Hooker et al. 1999, Hyrenbach et al. 2000; Wilson et al. 2014); including the use of both static and/or persistent oceanographic features to define MPA boundaries (Louzao et al. 2006, Embling et al. 2013). Conditioning predicted seabird distributions on environmental variables to derive seabird hotspots also represents an improvement to the existing technique of drawing buffers around colonies in relation to foraging range and assuming birds are distributed uniformly within this buffer (Thaxter et al. 2012, Eastham 2014). Similarly, predicting usage in unsampled regions allows for hotspot mapping to be conducted at broad spatial scales. In addition, the ability to map seabird distributions and hotspots at local-scales permits the identification of important marine areas for seabirds already subject to various forms of protection (e.g. those birds originating from within designated breeding colony SPAs).

4.1. General performance of maximum curvature and Getis-Ord analysis

Across all species, maximum curvature consistently identified the largest hotspots and covered a greater percentage of the at sea population than any of the Getis-Ord methods, regardless of the

scale of the analysis (UK- or SPA-level). Likewise, hotspots defined using the top 1% of Gi* scores consistently provided hotspots with the smallest areas and population coverage. Hotspots based on the top 1% or top 5% of Gi* scores tended to emphasize inshore areas close to the largest colonies. In contrast, the larger areas identified by statistically significant Gi* scores or maximum curvature often extended further offshore. Maximum curvature also produced hotspots with more complex boundaries than the simpler shapes produced by Gi* hotspots. This behaviour arises because Getis-Ord analysis involves local smoothing whereas maximum curvature is conducted on a purely cell-by-cell basis. From a pragmatic perspective simpler boundaries may often be preferred when designing MPAs (Perrow et al. 2015), although the ubiquity of GPS tracking technology and remote sensing data may make defining complex and even dynamic boundaries increasingly feasible (Hooker et al. 2011).

At the UK-scale, the areas identified by the different hotspots methods were relatively large. For example, the combined area covered by UK SPAs[3] with marine components is currently 19, 449 km^2 with the largest single SPA (Outer Thames Estuary) covering 3, 922 km^2 (data source: http://jncc.defra.gov.uk/page-1409 - SPAs with marine components, date accessed 01/08/2018, last updated 12/12/2017). In comparison, the UK-level top 1% Gi* hotspot for kittiwakes covered 5, 852 km^2 in total and the corresponding maximum curvature boundary covered 157, 802 km^2 (Table 1). Similar results were observed in the remaining three species, with identified hotspots typically exceeding the size of the largest SPAs currently designated and often exceeding the area covered by all current marine UK SPAs (particularly if using maximum curvature). At the individual SPA-level, the size of identified hotspots was smaller than at the UK-level, as expected,

[3] Proposed SPA sites (pSPA) are afforded the same level of protection as when fully classified, thus the area covered by the combined SPA and pSPA suites will exceed this value.

but still frequently exceeded the size of existing individual marine SPAs. Nevertheless, the SPA-level approach demonstrates how hotspot mapping can be applied at more local-scales to identify important areas for specific colonies or colony aggregations. For kittiwakes, guillemots and razorbills merging the outputs of individual SPA-level hotspots onto a single UK-wide map resulted in larger areas being covered than when performing a single, UK-level hotspot analysis. However, despite covering a larger area, merged SPA-level hotspots were less efficient in terms of protecting as many birds as possible in the smallest possible area. In shags, merging the outputs of SPA-level hotspot analyses resulted in smaller hotspots than conducting a single UK-level analysis with a concomitant decrease in the number of birds captured. Across species, merging SPA-level outputs at the UK-scale also resulted in a distribution of hotspots that perforce reflected the location of SPA colonies. Consequently, areas in which no SPAs are designated may be under-represented at the UK-level if one were to focus solely upon SPA-level outputs. The differences in area covered between UK-level hotspot analysis and merged SPA-level outputs across species may be due to both the number of designated SPAs and their locations. For example, in shags the lower number of currently designated SPAs means that even when merging SPA-level outputs the total area covered is less than that covered by the single UK-level analysis. Moreover, a suite of SPAs that is regularly spread throughout the UK with non-overlapping hotspot boundaries is expected to cover a greater area than a similarly sized suite of SPAs that are clustered closer together with many overlapping hotspot boundaries.

Although maximum curvature has previously been used to help identify and design seabird SPAs in the UK (O' Brien et al. 2012) it may not always represent the most suitable method. For example, Kober et al. (2012) trialled maximum curvature on Poisson-kriged ESAS transect data but concluded that it selected areas so large that it was inappropriate for identifying important

seabird hotspots (the example given was for gannets). In the current study, as well as covering the largest areas, maximum curvature hotspots were most similar to the 80% - 90% UD of the different species, suggesting they cover the majority of the home range. Thus, the same issues identified by Kober et al. (2012) arise when applying maximum curvature to seabird distribution maps based upon telemetry data collected for the four species in our study during late incubation / early chick rearing. However for shags, although maximum curvature hotspots were most similar to the 90% UD, the absolute area encompassed was small relative to the other species. Therefore, the suitability of maximum curvature may rest partly on the degree to which a species aggregates while at sea and may work better for some species than others. Using exponential models to identify the point of maximum curvature (as per O'Brien et al. 2012) occasionally produced multiple maxima, necessitating the use of Loess smoothing (Wakefield et al. 2017). Thus, it is recommended that maximum curvature be estimated using Loess smoothing in the future alongside the exponential modelling approach outlined by O' Brien et al. (2012).

Previously Getis-Ord analysis has been used to assist in the design of potential UK SPAs by delineating hotspots as polygons that encompass the top x% of calculated Gi* scores. However, the threshold value of x% chosen influences both the size of hotspots identified and how many seabirds are contained therein. In turn, this will influence whether the areas identified hold numbers in excess of the thresholds set out in the UK SPA selection guidelines. Kober et al. (2010) trialled the use of the top 1% and top 5% and ultimately decided upon the top 1% as a suitable means for the identification of potential seabird SPAs (Kober et al. 2012). It should also be borne in mind that there is no correspondence between Getis-Ord thresholds and numerical population thresholds. That is, the top 1% Getis-Ord hotspot is not guaranteed to contain 1% of the at-sea population.

In our analysis, the location of the top 1% Gi* hotspots was typically centred around the largest breeding colonies, reflecting the fact that the largest density of birds is found close to such colonies. When basing density estimates on tracking data from breeding birds (particularly during the early chick rearing phase) the importance of areas close to the colony may be emphasized to a greater degree than when using other data sources which may include non-breeders (e.g. transect data, but see Sansom et al. 2018) or tracking non-breeders whose foraging ranges are less constrained by the need to provision young. Similarly, as the distribution of birds often shifts during the breeding cycle, distribution maps from the early chick rearing period may not reflect behaviour throughout the whole breeding season.

Using statistically significant Gi* scores to delineate hotspots has not previously been reported for seabirds, although the approach is used in other fields (Ord & Getis 1995, Harris et al. 2017). Using this approach we identified hotspots that were typically larger than those identified using the top 5% Gi* method and smaller than maximum curvature hotspots. It should also be noted that there is not necessarily a close correspondence between statistical significance and the top x% of Gi* scores. For example, a completely random spatial pattern will still produce Gi* scores in which it is possible to define a top 1% even though no statistically significant hotspots would be identified. As with maximum curvature, the area of hotspots identified using statistical significance may mean this approach is deemed unsuitable for SPA designation for more widely dispersed species. However, both maximum curvature and statistically significant Gi* hotspots may be suitable for more aggregated species and could also be used to identify important areas in which broader marine stewardship measures would best complement an existing MPA network (Roberts et al. 2003).

For each species and hotspot method, we identified the % UD contour that was most similar to each UK-level hotspot using the Jaccard Index of similarity. Identified hotspots often showed a relatively high degree of similarity to utilisation distributions for kittiwakes, guillemots and razorbills. In contrast, Getis-Ord hotspots showed much lower similarity with UDs in shags. One potential reason for this is that the spatial smoothing introduced by Getis-Ord analysis does not reflect the clumped and often highly localized nature of shag distributions (Bogdanova et al. 2014). Maximum curvature, which does not involve spatial smoothing, resulted in hotspots that were more similar to estimated UDs in shags, but even in this case similarity (0.38) was much lower than the corresponding similarity indices observed between maximum curvature hotspots and utilisation distributions in the other three species. It remains unclear why the results observed in shags differ from the three other species in this manner. One potential explanation is that the spatial scale (the interaction between extent and resolution, *sensu* Goodchild 2001) of our analyses differs between the species considered. Specifically, due to relatively limited foraging range of shags hotspots defined using maximum curvature or Getis-Ord analysis tend to be coarser or blockier than the underlying utilisation distributions resulting in relatively low similarity even when high density areas are successfully identified.

In comparison with maximum curvature and Getis-Ord analysis, the foraging radius approach tended to identify larger areas than either method but was less efficient in terms of protecting as much of a seabird population as possible in the smallest possible area. One drawback of the foraging radius is approach is that the distribution of birds is assumed to be symmetric around a given colony. However, in reality the distribution of birds departing from a colony is likely to be asymmetric as foraging trips may be targeted towards specific foraging areas or away from competitors from neighbouring colonies (Wakefield et al. 2013). A simple foraging radius

approach also does not take into account that seabird density is expected to decline with distance from the colony. Consequently, extending buffers to maximum foraging range or mean-maximum foraging range necessarily means including large areas of space towards the fringes of a species foraging distribution (Soanes et al. 2016) in which the expected distribution of seabirds is low. Soanes et al. (2016) demonstrates that the foraging radius approach can be refined by conditioning calculated foraging radii on key environmental variables such as water depth (see also Grecian et al. 2012). The species distribution models of Wakefield et al. (2017) represent a logical extension of this approach.

4.2. Sensitivity of maximum curvature and Getis-Ord analysis to analysis field and neighbourhood size

Both maximum curvature and Getis-Ord analysis were sensitive to how the analysis field was defined, which subsequently influenced the area of hotspots identified (Webb et al. 2009, Wang et al. 2014). For example, setting the analysis field as all cells within a colony's 95% home range resulted in hotspots of a different size (though in a similar location) than if analysis field was defined using a maximum foraging range buffer. One further caveat to using the top x% of Getis-Ord scores to designate hotspots is that, by design, the hotspots identified will cover x% of the analysis field, a point also made by Kober et al. (2012). Therefore, Gi* percentage thresholds are not closely linked to population-based thresholds, but are more akin to area-based thresholds and will therefore be highly sensitive to how the analysis field is defined. Previous work has tended to limit hotspot analyses to those grid cells in which the density of birds exceeds zero (O'Brien et al. 2012, Lawson et al. 2016) and/ or focus upon specific administrative regions (Kober et al. 2010). Here, we used the 95% home range to help define our survey field (along with the EEZ administrative region). The advantages of using this approach over using grid cells in which

density > 0 are that 1) the 95% home range represents a standard concept throughout ecology (Kie et al. 2010); and 2) Computationally such an approach is relatively efficient as it excludes large regions of low density beyond the 95% home range without impacting on results (Kranstauber et al. 2017). Ultimately, the choice of how to define analysis field may depend on both the nature of the data collected and the focus of a particular piece of work. However, given its importance, particularly when using Gi* % thresholds, we suggest the analysis field should be explicitly stated and that hotspots should be interpreted as hotspots within a given analysis field (e.g. hotspots within the 95% home range).

In addition to analysis field, Getis-Ord analysis requires that local neighbourhood size, *d*, be defined prior to running an analysis. Larger values of *d* involve calculating local Gi* scores over larger neighbourhoods and result in a greater degree of smoothing. Mis-specification of neighbourhood size runs the risk of under- or over-smoothing the underlying patterns in the data. In general, over-smoothing seems to be a more serious problem as when we set neighbourhood values at low levels the resulting hotspots still covered high density areas and were similar to estimated UDs (Appendix A6, Fig. A3). However, setting neighbourhood values at the highest levels resulted in hotspots that bore little resemblance to the underlying data (Fig. A3). At present, there are a variety of ways to define neighbourhood size (Haining & Haining 2003). For instance, certain studies use spatial correlograms/ variograms to define *d* (Kamdem et al. 2012, Mathur 2015), whereas others have chosen neighbourhood sizes that ensure each cell has a certain number of neighbours (Varga et al. 2015) or used Queens-case contiguity (Harris et al. 2017). Here, we used spatial variograms constructed from seabird density maps to identify the point at which spatial auto-correlation broke down to set *d* (as used in Kober et al. 2010, albeit a generic value was chosen across all species). In addition, we performed FPT analysis on raw tracking data to identify

the average scale of area-restricted search (Fauchauld & Tveraa 2003) across colonies for each species to set *d*. Results using both methods are presented and were broadly similar (Appendix A8), but ultimately we preferred the FPT-based approach for setting *d*. One reason for preferring the FPT-based approach is that spatial variograms did not always reach an asymptote or identified multiple peaks in spatial auto-correlation at different distances. Such a problem may arise due to patchiness or underlying trends in our response variable (Dale 1999, Crawley 2012) and suggests variograms did not always perform optimally. Similar problems were also reported for certain species in Kober et al. (2010). Alternatively, FPT analysis provided a quick way to estimate *d* and is more interpretable from an ecological perspective as the spatial-scale at which individuals forage (Hamer et al. 2009). In addition, the use of FPT analysis to identify local neighbourhood size has parallels with recently developed protocols to identify Important Bird Areas (IBA) from tracking data in which FPT analysis is used to identify species-specific smoothing parameters for kernel density estimation (Lascelles et al. 2016). Regardless of how *d* is defined, it is important that the value of *d* is reported in order to interpret the results of Getis-Ord analysis.

4.3. Temporal persistence of hotspots

To examine whether identified hotspot locations regularly held important numbers of birds Kober et al. (2010, 2012) classified hotspots based on the top 1% Gi* as regularly occurring if: 1) a hotspot was present during at least three years and 2) was hotspot found in at least 2/3 years for which sufficient data existed to test for its presence. The importance of temporal persistence of identified hotspots when trying to design seabird MPAs has also been raised elsewhere (Santora & Sydeman 2015). Recently developed methods also allow for Getis-Ord analyses to be performed incorporating both space and time when identifying hotspots (ESRI 2016). However, the species distribution models provided by Wakefield et al. (2017) provide distribution estimates that are

averaged across the years of the study. Thus, it is not possible to ascertain the temporal variability in hotspot location across years. Such a study is feasible, but would require a longer-term tracking dataset than currently available. For example, the ESAS dataset used by Kober et al. (2010) comprised 25 years of data, compared to the five years of tracking data used in Wakefield et al. (2017).

The current Wakefield et al. (2017) pools data across years as running separate species distribution model on a year-by-year basis would require more tracking data per year to ensure results are representative. Consequently, it is unclear whether the hotspots we identify here are consistent across years. However, many of the key explanatory variables within the models developed by Wakefield et al. (2017) were time-invariant (e.g. distance from coast, sediment type). Previous work has demonstrated that temperate, neritic seabirds often forage in consistent locations within and across years (Woo et al. 2008, Wakefield et al. 2015) suggesting that the time-averaged environmental covariates used by Wakefield et al. (2017) may be reasonable proxies for prey distributions. As foraging range often varies across years in seabirds (Bogdanova et al. 2014) the strength of the decline in habitat usage with distance from the colony may also vary. In Wakefield et al. (2017) the influence of colony distance is averaged across the years of the study. Averaging across variables may average across some of the between year variation seen in foraging range and environmental conditions, however the species distribution models of Wakefield et al. (2017) may perform less well if species undergo a systematic shift in their foraging ranges in the future (Weimerskirch et al. 2012). However, the general finding that the density of breeding birds is greatest in close vicinity to the largest colonies during the breeding season also reflects a general feature of central-place foragers (Dean et al. 2015, Briscoe et al. 2018) and comparison of high use areas identified from recent seabird tracking data versus at-sea transect datasets collected over

a longer temporal period have shown that agreement between them is greatest closest to the colonies (Sansom et al. 2018). Thus, the factors determining the marine distribution of breeding seabirds in Britain appear sufficiently consistent across time to permit reliable estimation of area usage from biotelemetry, environmental covariates, and central-place foraging theory (Wakefield et al. 2017).

4.4. Representativeness of tracking data

It should be borne in mind that the species distribution of Wakefield et al. (2017) were based on birds tracked during late incubation and the early chick rearing period. Thus, the distribution maps and the hotspots analyses presented here only represent the distribution of birds during this period of the annual cycle. Moreover, the behaviour and distribution of non-breeders and immature birds may also differ from patterns seen in breeding birds.

In addition, the species distribution models of Wakefield et al. (2017) did not distinguish between different behaviours whilst birds were at sea. Therefore, the hotspots identified in the current report are based upon commuting and loafing behaviour as well as foraging behaviour. As a consequence, the importance (in terms of foraging) of areas close to the colony may be upweighted as birds may spend a significant amount of time rafting close to the colony or commuting through such areas (Carter et al. 2016) even if these areas are not key foraging sites. To identify hotspots purely based on foraging behaviour species distribution models can be based solely on locations classified as foraging (Wilson et al. 2014; Cleasby et al. 2015), which may result in stronger associations between habitat and distribution (Wakefield et al. 2009) as well as allowing identification of areas that are particularly at risk from activities that disproportionately impact on foraging birds. At present, the RSPB is utilising data collected using Temperature-Depth

Recorders (TDR) fitted to guillemots, razorbills and shags to identify diving locations for each of these species in order to construct foraging distribution models. When completed these models could be used to create distribution maps based purely on foraging locations and compared with the species distributions from Wakefield et al. (2017) in which all behaviours were used.

When conducting a tracking study one of the key concerns is to ensure that adequate numbers of birds are tracked for long enough to obtain accurate estimates of population-level distributions. In terms of raw tracking data, Soanes et al. (2013) suggested large numbers of birds ($n > 100$ if only one trip per bird used; $n \sim 20 – 30$ if four trips per bird used) would need to be tracked in order to accurately predict home range area. However, the sampling regime required to obtain accurate calculations of the geographic location and layout (shape) of the home range as well as the utilisation distribution underpinning such estimates was not investigated. In order to assess whether tracking data are representative and allow inferences to be drawn about the spatial use patterns of a population Lascelles et al. (2016) provide a method for assessing the representativeness of tracking data based upon the overlap of UD contours. Lascelles et al. (2016) then used this approach to help identify important bird areas (IBA). An advantage of this method is the shape and location of home ranges are considered when assessing representativeness. Using this approach, we found that for the majority of colonies our tracking data exceeded the 70% representativeness threshold used by Lascelles et al. (2016) (Appendix, A9). Note that representativeness in this context refers to our ability to accurately reflect the distribution of the sampled population, i.e birds that were tracked during late incubation / early chick rearing at specific sites and during specific years. Consequently, it does not reflect the general representativeness of the dataset to assess derived foraging distributions for breeding birds elsewhere or at other points in the breeding cycle.

In the current study, a further consideration is that enough birds are sampled from across enough colonies to increase the power of species distribution models When fitting species distribution models, Wakefield et al. (2017) assessed model performance using a cross-validation procedure in which the results from each tracked colony in turn were excluded and the overlap between observed utilisation distributions and those based on model predictions for each colony was calculated. Colony-based measures of overlap were then averaged across all colonies, but weighted by the number of birds tracked per colony, to ensure that more emphasis was given to results from colonies in which more tracking data was available and hence more representative. Species distribution models fitted to data collected in one area may also predict usage poorly in another as habitat availability changes. To address this, the species distribution models of Wakefield et al. (2017) were fitted as generalized functional responses (GFR) in which the response of birds to environmental covariates was conditioned on their regional means. Generalized functional response (GFR) models can interpolate usage to unsampled sites more accurately than conventional habitat selection models, but require that usage is sampled under a range of availability regimes allowing the response to environmental covariates to be conditioned on regional averages. Therefore, colonies in which small numbers of birds were tagged were still included in species distribution models to provide information on habitat selection across as diverse a range of environmental condition as possible.

To assess the uncertainty of model estimates, Wakefield et al. (2017) plotted maps that showed the coefficient of variation of model predictions across the UK. In general, these maps showed that model uncertainty was greater in regions were the density of birds was predicted to be low. In contrast, model uncertainty was lower in high density regions close to breeding colonies, which are the areas that hotspot methods select (Appendix A9). Uncertainty arising from

uncertainty in model coefficients was also low with hotspots identified using simulated density surfaces based on model predictions consistently identifying the same areas as hotspots (Appendix, A10).

Sansom et al. (2018) show that the overlap in high use areas identified by modelled tracking and transect data increases as the percentile threshold defining high use decreases from the 99th to the 50th percentile. Putting this into context here, our results show that the top 1% Getis-Ord hotspots show the greatest similarity with the 15-20% UD in kittiwakes, guillemots and razorbills and the 55% UD in shags, roughly equivalent to the 80-85th percentile or 45th percentile of usage respectively. At these percentile thresholds, there was roughly 40-60% overlap in the areas identified as high use between Wakefield et al. (2017) and distributions based on transect data (Sansom et al. 2018), suggesting good agreement despite the multiple differences between the source datasets. Further work could include a more formal comparison of our hotspots with those identified from other data and /or further independent data could be collected to corroborate the importance of the hotspots as done previously for some proposed SPAs (Cook et al. 2015, Perrow et al. 2016).

4.5. Hierarchical hotspot mapping at different spatial scales

The ability to perform hotspot analyses at different spatial scales permits a hierarchical approach to identifying priority areas for conservation (Bailey & Thompson 2009). At the broadest scale, UK-wide analysis provides information on the location of the most important UK-hotspots. UK hotspots will reflect important areas used by UK seabird colonies regardless of whether birds originate from an SPA or not.

As birds from SPAs are subject to the strictest form of protection, identifying heavily used areas at sea by birds from those particular colonies is important for effective conservation (Lascelles et al. 2016). To achieve this, the hotspot mapping at the finer spatial scales presented here provides an improvement over the foraging radius approach. Firstly, hotspot maps based upon species distribution modelling will better reflect patterns of habitat usage. Secondly, SDMs provide density estimates across a two-dimensional surface upon which hotspot mapping is then based. In contrast, foraging range buffers typically assume seabirds are uniformly distributed in all directions around a colony and at all distances from it out to the limit of the defined buffer. Neither of these assumptions is likely ever to be true. As well as providing information on the areas birds from current colony SPAs use, hotspot mapping based on SDMs can also be used prospectively to examine the distribution of birds from proposed colony SPAs.

More generally, combining maps of identified hotspots or population UDs with other sources of marine data such as existing MPA boundaries and anthropogenic impacts will also help identify areas of high conservation priority, including within current MPAs that may not have originally been designated for the species in question (Bailey & Thompson 2009). By combining population UDs or hotspot maps that identify high density regions with sensitivity mapping we can target regions where management of threats would have the greatest impact on a species or colony (Bradbury et al. 2014; Wilson 2016; Bradbury et al. 2017).

4.6. Overview and additional approaches

An overview of the different hotspots approaches used in the current report is presented in Table 9. In terms of pros and cons, maximum curvature provides a relatively simple mathematical method for delineating potential hotspots. However, one has to choose a suitable method to

determine when the point of maximum curvature is reached (e.g. exponential growth models versus Loess smoothing). Moreover, how one defines the analysis field has a direct impact on the size of the area covered by the resulting maximum curvature boundaries. Typically, the maximum curvature areas identified are designed to protect as much of the population as possible in the smallest possible area, but typically cover large areas and can be relatively complex shapes.

When conducting Getis-Ord analysis one has to define two parameters carefully: the analysis field (as with maximum curvature) and the local neighbourhood size. Because Gi* scores for a focal cell are calculated over a local neighbourhood spatial correlation is incorporated to some extent. Unlike maximum curvature, an isolated focal cell in which a high density of birds was predicted may not be identified as a hotspot if predicted densities were low elsewhere in the local neighbourhood of the focal cell. On the other hand, one risk when performing Getis-Ord analysis is to set the neighbourhood size as too big, resulting in large-scale spatial smoothing that can obscure underlying patterns in the data (Appendix A6). This may be a particular concern when using Getis-Ord analysis on species with highly localized ranges or species that form very loose aggregations. One also needs to decide how to use Gi* scores to select potential hotspots. Treating Gi* scores as z-scores allows one to base hotspot identification on the basis of statistical significance. Hotspots defined on this basis tend to be relatively large, though smaller than those identified using maximum curvature.

Using the top 1% or top 5% Gi* scores to identify hotspots results in the smallest areas being selected. However, it should be borne in mind that the size of the hotspots selected will be directly proportional to the area of the analysis field used. In most cases the top 1% or 5% of Gi* scores will select cells in which there are high densities of individuals, however these percentage

thresholds are not related to statistical significance and in certain circumstances may identify cells as hotspots when statistical significance testing would not do so.

Finally, the hotspot approaches trialled here represent the methods by which marine SPAs in the UK have currently been identified and proposed (Kober et al. 2010, O'Brien et al. 2012) and subsequently been classified e.g. Outer Thames Estuary SPA, Liverpool Bay/Bae Lerpwl SPA and Irish Sea Front SPA. Furthermore, the use of SDMs applied to seabird tracking datasets has previously used successfully to identify and classify several other marine SPAs in UK waters e.g. Northumberland Marine SPA, Dungeness, Romney Marsh & Rye Bay SPA, and Morecambe Bay & Duddon Estuary SPA. A review of the sufficiency of the UK marine SPA network is currently underway by the Statutory Nature Conservation Bodies (Stroud et al. 2016, JNCC, pers. com.) and the work presented here has the potential to inform that work and the process of filling any gaps identified. Though beyond the scope of the current report, there are also a number of specialised decision support tools that have been developed to aid the planning of conservation networks. Typically, such approaches use optimization algorithms to design a network of protected sites that meets some predefined target whilst also minimising cost (Moilanen et al. 2005, Ball et al. 2009). Thus, such programs consider more than just the density of birds in an area. However, they typically require greater user input, including the development of pre-defined conservation targets and the construction of cost surfaces. Nevertheless, in certain circumstances they may be a useful additional approach.

5. Conclusions

Using a combination of cutting edge GPS tracking technology and predictive species distribution modelling, Wakefield et al. (2017) demonstrated it is possible to generate UK-wide distributions for guillemot, razorbill, kittiwake and shag based on a sample of tracking data (Wakefield et al. 2017). This followed on from previous work which focussed on applying SDMs to visually-tracked tern species, generating colony-specific distributions for both tracked and untracked colonies (Wilson et al. 2014). Such an approach is growing in popularity throughout ecology and is likely to become increasingly prevalent in the future (Hazen et al. 2017, Reynolds et al. 2017, Wilson et al. 2017). Here, we show how such distribution mapping can be used to identify potential seabird hotspots using previously established techniques for informing the identification of marine SPAs (Kober et al. 2010, O'Brien et al. 2012). Such hotspots have the advantage that they are conditioned upon species-habitat relationships, can be computed at a variety of spatial scales and do not require that birds from a given colony were tracked. As such, they represent a considerable advance over the use of simple buffers based upon maximum foraging range (Soanes et al. 2016). Ultimately, such work will contribute to our overall understanding of factors affecting seabird distributions at sea. The outputs from this work form a useful and valuable resource given the increasing political, environmental, moral and legal imperatives to identify protected areas at sea and improve the management of our marine environment.

Table 9. Summary of different hotspot methods used in current report.

Method	Outline	Details	Delineation	Spatial Smoothing?	Important parameters	Performance
Maximum Curvature	Outlines area that best balances protecting as much as the population as possible in the most efficient (smallest) area	Identify point of maximum curvature using exponential growth models or Loess smoothing.	Cells ordered by density and included within maximum curvature boundary up until the point of maximum curvature reached	No, analysis done on purely grid cell by grid cell basis	Size of analysis field partly determines the size of resulting hotspots	Selects large areas typically encompassing majority of home range and high % of at sea population. Selected boundaries relatively complex.
Getis-Ord Analysis	Identify areas in which clusters of density are distinct from patterns in the surrounding landscape.	Getis-Ord scores (Gi*) calculated for each grid cell in analysis by comparing density at the local level to overall global density	a) Select cells within top x% of Gi* scores OR b) Select cells in which Gi* score exceeds a critical significance threshold	Yes, local Gi* scores calculated on basis of density values in defined local neighbourhood rather than just a single, focal grid cell.	Size of analysis field partly determines the size of resulting hotspots Extent of local neighbourhood size, *d*, determines degree of smoothing when calculating Gi* scores	*Select top x% of Gi* scores:* Selects smallest areas for every species. Total area of hotspots defined equal to x% of analysis field. Selected boundaries relatively simple. *Select cells in which Gi* score exceeds significance threshold:* Selects relatively large areas typically exceeding boundaries of 50% home range (core range). Selected boundaries relatively simple. Sensitive to definition of analysis field and local neighbourhood size, but less so than top 1% or top 5% methods.
Foraging radius buffers	Draw buffers around colonies in relation to recorded foraging ranges	Foraging ranges typically estimated from tracking data.	Cells within foraging range buffer selected	No, focal cell selected if falls within buffer	Foraging range can be specified as max recorded range, mean-max foraging range or mean foraging range.	Typically selects large areas, but less efficient in terms of protecting most birds in smallest area. Between-individual and between-colony variation in foraging range means that values taken from one study may not always reflect behaviour at another colony.

6. Acknowledgments

We are grateful for the contributions received from the following attendees of meetings that discussed the analyses as it progressed and/or for comments on earlier versions of this report: Alex Banks and Richard Caldow (Natural England); Tom Evans and Jared Wilson (Marine Scotland Science); Kerstin Kober (Joint Nature Conservation Committee); Patrick Lindley and Matthew Murphy (Natural Resources Wales); Neil McCulloch and Ronan Owens (Northern Ireland Environment Agency); Emma Philip, Kate Thompson and Helen Wade (Scottish Natural Heritage); and Peadar O'Connell, Gareth Cunningham, Emily Williams, Kenny Bodles, Kate Jennings, Alice Groom and Alex Sansom (RSPB). We would also like to thank Ewan Wakefield for assistance and advice concerning species distribution modelling. We are grateful to all those who contributed funding and collected data as part of the FAME/STAR projects.

7. References

Anselin, L. 1995. Local indicators of spatial association — LISA. *Geographical analysis, 27*, 93-115.

Bailey, H. & Thompson, P.M. 2009. Using marine mammal habitat modelling to identify priority conservation zones within a marine protected area. *Marine Ecology Progress Series, 378*, 279-287.

Ball, I.R., Possingham, H.P. & Watts, M. 2009. Marxan and relatives: software for spatial conservation prioritisation. *Spatial conservation prioritisation: Quantitative methods and computational tools*, pp.185-195.

Becker, E.A., Foley, D.G., Forney, K.A., Barlow, J., Redfern, J.V. & Gentemann, C.L. 2012. Forecasting cetacean abundance patterns to enhance management decisions. *Endangered Species Research, 16*, 97-112.

Benjamini, Y. & Yekutieli, D. 2001. The control of the false discovery rate in multiple testing under dependency. *Annals of statistics*, *29*, 1165-1188.

Bogdanova, M.I., Wanless, S., Harris, M.P., Lindström, J., Butler, A., Newell, M.A., Sato, K., Watanuki, Y., Parsons, M. & Daunt, F. 2014. Among-year and within-population variation in foraging distribution of European shags Phalacrocorax aristotelis over two decades: implications for marine spatial planning. *Biological Conservation*, *170*, 292-299.

Bradbury, G., Trinder, M., Furness, B., Banks, A. N., Caldow, R. W. G. & Hume, D. 2014. Mapping Seabird Sensitivity to Offshore Wind Farms. *PLoS ONE, 9*, e106366. https://doi.org/10.1371/journal.pone.0106366

Bradbury G, Shackshaft M, Scott-Hayward L, Rexstad E, Miller D, Edwards D. 2017. Risk assessment of seabird bycatch in UK waters. Report to Defra under contract MB0126; Available from http:\\sciencesearch.defra.gov.uk

Briscoe, D.K., Fossette, S., Scales, K.L., Hazen, E.L., Bograd, S.J., Maxwell, S.M., McHuron, E.A., Robinson, P.W., Kuhn, C., Costa, D.P. & Crowder, L.B. 2018. Characterizing habitat suitability for a central-place forager in a dynamic marine environment. *Ecology and evolution*, *8*, 2788-2801.

Camphuysen, K.C., Shamoun-Baranes, J., Bouten, W. & Garthe, S. 2012. Identifying ecologically important marine areas for seabirds using behavioural information in combination with distribution patterns. *Biological Conservation*, *156*, 22-29.

Carter, M.I., Cox, S.L., Scales, K.L., Bicknell, A.W., Nicholson, M.D., Atkins, K.M., Morgan, G., Morgan, L., Grecian, W.J., Patrick, S.C. & Votier, S.C. 2016. GPS tracking reveals rafting behaviour of Northern Gannets (Morus bassanus): implications for foraging ecology and conservation. *Bird Study, 63,* 83-95.

CBD (Convention on Biological Diversity). 2004. Programme of work on protected areas. CBD, Montreal. Available from http:// www.cbd.int/protected/pow/learnmore/intro/ (accessed December 2017).

Cleasby, I.R., Wakefield, E.D., Bodey, T.W., Davies, R.D., Patrick, S.C., Newton, J., Votier, S.C., Bearhop, S. & Hamer, K.C. 2015. Sexual segregation in a wide-ranging marine predator is a consequence of habitat selection. *Marine Ecology Progress Series*, *518*, 1-12.

Crawley, M.J., 2012. *The R book*. John Wiley & Sons.

Croxall, J.P., Butchart, S.H. M., Lascelles, B, Stattersfield, A.J., Sullivan, B, Symes, A. & Taylor, P. 2012. Seabird conservation status, threats and priority actions: a global assessment. *Bird Conservation International*, *22*, 1-34.

Dale, M.R. 2000. *Spatial pattern analysis in plant ecology*. Cambridge university press.

Daunt, F., Afanasyev, V., Silk, J.R.D. & Wanless, S. 2006. Extrinsic and intrinsic determinants of winter foraging and breeding phenology in a temperate seabird. *Behavioral Ecology and Sociobiology*, *59*, 381-388.

Dean, B., Kirk, H., Fayet, A., Shoji, A., Freeman, R., Leonard, K., Perrins, C.M. & Guilford, T., 2015. Simultaneous multi-colony tracking of a pelagic seabird reveals cross-colony utilization of a shared foraging area. *Marine Ecology Progress Series*, *538*, 239-248.

Demšar, U., Buchin, K., Cagnacci, F., Safi, K., Speckmann, B., Van de Weghe, N., Weiskopf, D. & Weibel, R. 2015. Analysis and visualisation of movement: an interdisciplinary review. *Movement Ecology*, *3*, 5

Doney, S.C., Ruckelshaus, M., Duffy, J.E., Barry, J.P., Chan, F., English, C.A., Galindo, H.M., Grebmeier, J.M., Hollowed, A.B., Knowlton, N. & Polovina, J. 2012. Climate Change Impacts on Marine Ecosystems. *Annual Review of Marine Sci*ence *4*, 11-37.

Eastham, C. 2014. The use of breeding seabird foraging ranges for assessing impacts to Special Protection Areas (SPAs) from wave and tidal renewable energy proposals. *Proceedings of the 2nd International Conference on Environmental Interactions of Marine Renewable Energy Technologies (EIMR2014), 28 April – 02 May 2014, Stornoway, Isle of Lewis, Outer Hebrides, Scotland.*

Embling, C.B., Gillibrand, P.A., Gordon, J., Shrimpton, J., Stevick, P.T. & Hammond, P.S. 2010. Using habitat models to identify suitable sites for marine protected areas for harbour porpoises (Phocoena phocoena). *Biological Conservation*, *143*, 267-279.

Environmental Systems Research Institute (ESRI). 2016. ArcGIS Desktop 10.3. Space-time cluster analysis. http://pro.arcgis.com/en/pro-app/tool-reference/spatial-statistics/space-time-analysis.htm

EU. 2009. Directive 2009/147/EC of the European Parliament and of the Council of 30 November 2009 on the conservation of wild birds (codified version). Official Journal of the European Union L 20/7 (26.1.2010)

Fauchald, P. & Tveraa, T. 2003. Using first-passage time in the analysis of area-restricted search and habitat selection. *Ecology*, *84*, 282-288.

Fieberg, J. & Kochanny, C.O. 2005. Quantifying home-range overlap: the importance of the utilization distribution. *The Journal of Wildlife Management*, *69*, 1346-1359.

Fischer, M.M. & Getis, A. eds., 2009. *Handbook of applied spatial analysis: software tools, methods and applications*. Springer Science & Business Media.

Hooker, S.K., Cañadas, A., Hyrenbach, K.D., Corrigan, C., Polovina, J.J. & Reeves, R.R. 2011. Making protected area networks effective for marine top predators. *Endangered Species Research*, *13*, 203-218.

Game, E.T., Grantham, H.S., Hobday, A.J., Pressey, R.L., Lombard, A.T., Beckley, L.E., Gjerde, K., Bustamante, R., Possingham, H.P. & Richardson, A.J. 2009. Pelagic protected areas: the missing dimension in ocean conservation. *Trends in ecology & evolution*, *24*, 360-369.

Garthe, S., Markones, N., Mendel, B., Sonntag, N. & Krause, J.C. 2012. Protected areas for seabirds in German offshore waters: designation, retrospective consideration and current perspectives. *Biological conservation*, *156*, 126-135.

Getis, A. & Ord, J.K., 1992. The analysis of spatial association by use of distance statistics. *Geographical analysis*, *24*, 189-206

Goodchild, M.F. 2001. Metrics of scale in remote sensing and GIS. *International Journal of Applied Earth Observation and Geoinformation*, *3*, 114-120.

Grecian, W. J, Witt, M. J., Attrill, M. J., Bearhop, S., Godley, B. J., Grémillet, D., Hamer, K. C. & Votier, S. C. 2012. A novel projection technique to identify important at-sea areas for seabird conservation: An example using Northern gannets breeding in the North East Atlantic. *Biological Conservation*, 156, 43-52.

Gutowsky, S.E., Leonard, M.L., Conners, M.G., Shaffer, S.A. & Jonsen, I.D. 2015. Individual-level variation and higher-level interpretations of space use in wide-ranging species: an albatross case study of sampling effects. *Frontiers in Marine Science*, *2*, 93.

Habitats Directive, Council Directive 92/43/EEC of 21 May 1992 on the conservation of natural habitats and of wild fauna and flora, Off. J. Eur. Union 206 (1992) 7–50.

Haining, R. & Haining, R.P. 2003. *Spatial data analysis: theory and practice*. Cambridge University Press.

Hamer, K. C., E. M. Humphreys, M. C. Magalhaes, Stefan Garthe, J. Hennicke, G. Peters, D. Grémillet, H. Skov, & S. Wanless. Fine-scale foraging behaviour of a medium-ranging marine predator. *Journal of Animal Ecology*, 78, 880-889.

Harris, M.P., Newell, M.A. & Wanless, S., 2015. The use of k values to convert counts of individual Razorbills Alca torda to breeding pairs. *Seabird*, *28*, 30-36.

Harris, N.L., Goldman, E., Gabris, C., Nordling, J., Minnemeyer, S., Ansari, S., Lippmann, M., Bennett, L., Raad, M., Hansen, M. & Potapov, P. 2017. Using spatial statistics to identify emerging hot spots of forest loss. *Environmental Research Letters*, *12*, p.024012.

Hazen, E.L., Palacios, D.M., Forney, K.A., Howell, E.A., Becker, E., Hoover, A.L., Irvine, L., DeAngelis, M., Bograd, S.J., Mate, B.R. & Bailey, H. 2017. WhaleWatch: a dynamic management tool for predicting blue whale density in the California Current. *Journal of Applied Ecology*, *54*, 1415-1428.

Hooker, S.K., Whitehead, H. & Gowans, S. 1999. Marine protected area design and the spatial and temporal distribution of cetaceans in a submarine canyon. *Conservation Biology*, *13*, 592-602.

Hooten, M.B., Johnson, D.S., McClintock, B.T. & Morales, J.M. 2017. *Animal movement: statistical models for telemetry data*. CRC Press.

Hyrenbach, K.D., Forney, K.A. & Dayton, P.K. 2000. Marine protected areas and ocean basin management. *Aquatic conservation: marine and freshwater ecosystems*, *10*, 437-458.

Jaccard, P., 1912. The distribution of the flora in the alpine zone. 1. *New phytologist*, *11*, 37-50.

Johnston, R.J. & Ramachandran, M. 2014. Modeling spatial patchiness and hot spots in stated preference willingness to pay. *Environmental and Resource Economics*, *59*, 363-387.

Jones, H.P., Tershy, B.R., Zavaleta, E.S., Croll, D.A., Keitt, B.S., Finkelstein, M.E. & Howald, G.R. 2008. Severity of the effects of invasive rats on seabirds: a global review. *Conservation Biology*, *22*, 16-26.

Jones, E.L., McConnell, B.J., Smout, S., Hammond, P.S., Duck, C.D., Morris, C.D., Thompson, D., Russell, D.J., Vincent, C., Cronin, M. & Sharples, R.J. 2015. Patterns of space use in sympatric marine colonial predators reveal scales of spatial partitioning. *Marine Ecology Progress Series*, *534*, 235-249.

Kamdem, C., Fouet, C., Etouna, J., Etoa, F.X., Simard, F., Besansky, N.J. & Costantini, C. 2012. Spatially explicit analyses of anopheline mosquitoes indoor resting density: implications for malaria control. *PloS one*, *7*, p.e31843.

Kie, J.G., Matthiopoulos, J., Fieberg, J., Powell, R.A., Cagnacci, F., Mitchell, M.S., Gaillard, J.M. & Moorcroft, P.R. 2010. The home-range concept: are traditional estimators still relevant with modern telemetry technology?. *Philosophical Transactions of the Royal Society of London B: Biological Sciences*, *365*, 2221-2231.

Kober, K., Webb, A., Win, I., Lewis, M., O'Brien, S., Wilson, L.J. & Reid, J.B. 2010. An analysis of the numbers and distribution of seabirds within the British Fishery Limit aimed at identifying areas that qualify as possible marine SPAs. *JNCC report*, *431*.

Kober, K., Wilson, L.J., Black, J., O'Brien, S., Allen, S., Win, I., Bingham, C. & Reid, J.B. 2012. JNCC Report No. 461.

Kranstauber, B., Smolla, M. & Safi, K. 2017. Similarity in spatial utilization distributions measured by the earth mover's distance. *Methods in Ecology and Evolution*, *8*, 155-160.

Lascelles, B.G., Langham, G.M., Ronconi, R.A. & Reid, J.B. 2012. From hotspots to site protection: Identifying Marine Protected Areas for seabirds around the globe. *Biological Conservation*, *156*, 5-14

Lascelles, B.G., Taylor, P.R., Miller, M.G.R., Dias, M.P., Oppel, S., Torres, L., Hedd, A., Le Corre, M., Phillips, R.A., Shaffer, S.A. & Weimerskirch, H. 2016. Applying global criteria to tracking data to define important areas for marine conservation. *Diversity and Distributions*, *22*, 422-431.

Lawson, J., Kober, K., Win, I., Allcock, Z., Black, J. Reid, J.B., Way, L. & O'Brien, S.H. 2016. An assessment of the numbers and distribution of wintering waterbirds and seabirds in Liverpool Bay/Bae Lerpwl area of search. JNCC Report No 576

Loader, C.R., 1999. Bandwidth selection: classical or plug-in? *The Annals of Statistics*, *27*, 415-438.

Loader, C. 2013 locfit: Local Regression, Likelihood and Density Estimation.. R package version 1.5-9.1. https://CRAN.R-project.org/package=locfit

Louzao, M., Hyrenbach, K.D., Arcos, J.M., Abelló, P., de Sola, L.G. & Oro, D. 2006. Oceanographic habitat of an endangered Mediterranean procellariiform: implications for marine protected areas. *Ecological applications*, *16*, 1683-1695.

Mathur, M., 2015. Spatial autocorrelation analysis in plant population: An overview. *Journal of Applied and Natural Science*, *7*, 501-513.

McSorley, C.A., Dean, B.J., Webb, A. & Reid J.B. 2006. Extending the boundaries of seabird breeding colony protected areas into the marine environment. In: Waterbirds around the world. Eds. G.C. Boere, C.A. Galbraith & D.A. Stroud. The Stationery Office, Edinburgh, UK. pp. 752-753.

Mitchell, P.I., Newton, S.F., Ratcliffe, N. & Dunn, T.E. 2004. Seabird populations of Britain and Ireland. *T. & AD Poyser, London*

Moilanen, A., Franco, A.M., Early, R.I., Fox, R., Wintle, B. & Thomas, C.D. 2005. Prioritizing multiple-use landscapes for conservation: methods for large multi-species planning problems. *Proceedings of the Royal Society of London B: Biological Sciences*, *272*, 1885-1891.

Montevecchi, W.A., Hedd, A., Tranquilla, L.M., Fifield, D.A., Burke, C.M., Regular, P.M., Davoren, G.K., Garthe, S., Robertson, G.J. & Phillips, R.A. 2012. Tracking seabirds to identify ecologically important and high risk marine areas in the western North Atlantic. *Biological Conservation*, *156*, 62-71.

Naimi, B., Hamm, N.A., Groen, T.A., Skidmore, A.K. & Toxopeus, A.G. 2014. Where is positional uncertainty a problem for species distribution modelling? *Ecography*, *37*, 191-203

Nelson, T.A. & Boots, B. 2008. Detecting spatial hot spots in landscape ecology. *Ecography*, *31*, 556-566.

O'Brien, S.H., Webb, A., Brewer, M.J. & Reid, J.B. 2012. Use of kernel density estimation and maximum curvature to set Marine Protected Area boundaries: Identifying a Special Protection Area for wintering red-throated divers in the UK. *Biological Conservation*, *156*, 15-21.

Ord, J.K. & Getis, A. 1995. Local spatial autocorrelation statistics: distributional issues and an application. *Geographical analysis*, *27*, 286-306

OSPAR Commission. 1992. Ospar Convention for the Protection of the Marine Environment of the North-East Atlantic. OSPAR Commission, London, UK.

Perrow, M.R., Harwood, A.J., Skeate, E.R., Praca, E. & Eglington, S.M. 2015. Use of multiple data sources and analytical approaches to derive a marine protected area for a breeding seabird. *Biological Conservation*, *191*, 729-738.

Perrow, M.R., Harwood, A.J.P. & Caldow, R.W.G. 2016. Tern verification surveys for marine sites. Natural England Commissioned Reports, Number212.

Reynolds, S.D., Norman, B.M., Beger, M., Franklin, C.E. & Dwyer, R.G. 2017. Movement, distribution and marine reserve use by an endangered migratory giant. *Diversity and Distributions*, *23*, 1268-1279.

Roberts, C. M., Gell, F. & Hawkins, J. P. 2003. Protecting nationally important marine areas in the Irish Sea Pilot Project Region. JNCC, Peterborough.

R Core Team. 2018. R: A language and environment for statistical computing. R Foundation for Statistical Computing, Vienna, Austria. URL https://www.R-project.org/.

Sansom, A., Wilson, L. J., Caldow, R. W. G. & Bolton, M. 2018. Comparing marine distribution maps for seabirds during the breeding season derived from different survey and analysis methods. *PLoS ONE*, *13*, e0201797. https://doi.org/10.1371/journal.pone.0201797

Soanes, L.M., Arnould, J.P., Dodd, S.G., Sumner, M.D. & Green, J.A. 2013. How many seabirds do we need to track to define home-range area?. *Journal of Applied Ecology*, *50*, 671-679.

Soanes, L. M., J. A. Bright, L. P. Angel, J. P. Y. Arnould, M. Bolton, M. Berlincourt, B. Lascelles, E. Owen, Benoit Simon-Bouhet, & J. A. Green. 2016. Defining marine important bird areas: Testing the foraging radius approach. *Biological conservation*, *196*, 69-79.

Sokal, R.R., Oden, N.L. & Thomson, B.A. 1998. Local spatial autocorrelation in a biological model. *Geographical Analysis*, *30*, 331-354.

Stroud, D.A., Chambers, D., Cook, S., Buxton, N., Fraser, B., Clement, P., Lewis, P., McLean, I., Baker, H. & Whitehead, S. (eds). 2001. *The UK SPA network: its scope and content.* JNCC, Peterborough.

Stroud, D.A., Bainbridge, I.P., Maddock, A., Anthony, S., Baker, H., Buxton, N., Chambers, D., Enlander, I., Hearn, R.D., Jennings, K.R, Mavor, R., Whitehead, S. & Wilson, J.D. - on behalf of the UK SPA & Ramsar Scientific Working Group (eds.) 2016. *The status of UK SPAs in the 2000s: the Third Network Review*. JNCC, Peterborough.

Suryan, R.M., Sato, F., Balogh, G.R., Hyrenbach, K.D., Sievert, P.R. & Ozaki, K. 2006. Foraging destinations and marine habitat use of short-tailed albatrosses: A multi-scale approach using first-passage time analysis. *Deep Sea Research Part II: Topical Studies in Oceanography*, *53*, 370-386.

Sydeman, W.J., Thompson, S.A., Santora, J.A., Koslow, J.A., Goericke, R. & Ohman, M.D. 2015. Climate–ecosystem change off southern California: time-dependent seabird predator–prey numerical responses. *Deep Sea Research Part II: Topical Studies in Oceanography*, *112*, 158-170.

Thaxter, C.B., Lascelles, B., Sugar, K., Cook, A.S., Roos, S., Bolton, M., Langston, R.H. & Burton, N.H. 2012. Seabird foraging ranges as a preliminary tool for identifying candidate Marine Protected Areas. *Biological Conservation*, *156*, 53-61

Varga, C., Pearl, D.L., McEwen, S.A., Sargeant, J.M., Pollari, F. & Guerin, M.T. 2015. Area-level global and local clustering of human Salmonella enteritidis infection rates in the city of Toronto, Canada, 2007–2009. *BMC infectious diseases*, *15*, 359.

Wakefield, E.D., Phillips, R.A. & Matthiopoulos, J. 2009. Quantifying habitat use and preferences of pelagic seabirds using individual movement data: a review. *Marine Ecology Progress Series*, *391*, 165-182.

Wakefield, E.D., Phillips, R.A., Trathan, P.N., Arata, J., Gales, R., Huin, N., Robertson, G., Waugh, S.M., Weimerskirch, H. & Matthiopoulos, J. 2011. Habitat preference, accessibility, and competition limit the global distribution of breeding Black-browed Albatrosses. *Ecological Monographs*, *81*, 141-167.

Wakefield, E.D., Bodey, T.W., Bearhop, S., Blackburn, J., Colhoun, K., Davies, R., Dwyer, R.G., Green, J.A., Grémillet, D., Jackson, A.L. & Jessopp, M.J. 2013. Space partitioning without territoriality in gannets. *Science*, *341*, 68-70.

Wakefield, E.D., Cleasby, I.R., Bearhop, S., Bodey, T.W., Davies, R.D., Miller, P.I., Newton, J., Votier, S.C. & Hamer, K.C., 2015. Long-term individual foraging site fidelity—why some gannets don't change their spots. *Ecology*, *96*, 3058-3074.

Wakefield, E.D., Owen, E., Baer, J., Carroll, M.J., Daunt, F., Dodd, S.G., Green, J.A., Guilford, T., Mavor, R.A., Miller, P.I. & Newell, M.A. 2017. Breeding density, fine-scale tracking, and large-scale modeling reveal the regional distribution of four seabird species. *Ecological Applications*, *27*, 2074-2091.

Wang, Z., Du, Q., Liang, S., Nie, K., Lin, D.N., Chen, Y. & Li, J.J. 2014. Analysis of the spatial variation of hospitalization admissions for hypertension disease in Shenzhen, China. *International journal of environmental research and public health*, *11*, 713-733.

Webb, A., Dean, B.J., O'Brien, S.H., Söhle, I., McSorley, C., Reid, J.B., Cranswick, P.A., Smith, L.E. & Hall, C. 2009. The numbers of inshore waterbirds using the Greater Thames during the non-breeding season; an assessment of the area's potential for qualification as a marine SPA. JNCC Report No. 374.

Weimerskirch, H., Louzao, M., De Grissac, S. & Delord, K. 2012. Changes in wind pattern alter albatross distribution and life-history traits. *Science*, *335*, 211-214.

Wilcox, C., Van Sebille, E. & Hardesty, B.D. 2015. Threat of plastic pollution to seabirds is global, pervasive, and increasing. *Proceedings of the National Academy of Sciences*, *112*, 11899-11904.

Wilson, L.J., McSorley, C.A., Gray, C.M., Dean, B.J., Dunn, T.E., Webb, A. & Reid, J.B. 2009. Radio-telemetry as a tool to define protected areas for seabirds in the marine environment. *Biological Conservation*, *142*, 1808-1817.

Wilson L. J., Black J., Brewer, M. J., Potts, J. M., Kuepfer, A., Win I., Kober K., Bingham C., Mavor R. & Webb A. 2014. Quantifying usage of the marine environment by terns Sterna sp. around their breeding colony SPAs, JNCC Report 500

Wilson, B. 2016. Might marine protected areas for mobile megafauna suit their proponents more than the animals? *Aquatic Conservation: Marine and Freshwater Ecosystems, 26*, 3-8.

Wilson, A.M., Brauning, D.W., Carey, C. and Mulvihill, R.S. 2017. Spatial models to account for variation in observer effort in bird atlases. *Ecology and Evolution, 7*, 6582-6594.

Woo, K. J., Elliott, K. H., Davidson, M., Gaston, A. J. & Davoren, G. K. 2008. Individual specialization in diet by a generalist marine predator reflects specialization in foraging behaviour. Journal of Animal Ecology 77:1082 – 1091

Žydelis, R., Small, C. and French, G. 2013. The incidental catch of seabirds in gillnet fisheries: A global review. *Biological Conservation, 162,* 76-88.

8. Appendix

Appendix Contents

A1. Details on when birds were tracked as part of Wakefield et al. (2017)

The species distributions models of Wakefield et al. (2017) were based upon tracking data collected during the late incubation and early chick rearing period. Thus, the predictions derived by Wakefield et al. (2017) show the distribution of breeding birds during this period. The distribution of breeding birds at other points of the breeding season or the distribution of non-breeders is not incorporated. Details on the dates at which birds were tracked are given in Table A1 below.

Table A1. Table showing the dates at which birds were tracked at each tracked colony across the years of the study. The earliest trip records the date at which recording of the first track commenced and latest trip records the date at which the last track was recorded. Dates are split by breeding colony and year of study. Colony ID: ANN = Annet, BAR = Bardsey, BEM = Bempton, BOB = Bullers of Buchan, CAW = Cape Wrath, COP = Copinsay, COQ = Coquet, CSY = Colonsay, FAI = Fair Isle, FAN = Flannans, FIL = Filey, FOW = Fowlsheugh, GTS = Great Saltee, IOM = Isle of May, LAM = Lambay, LUN = Lunga, MKS = Muckle Skerry, PUF = Puffin Island, RAT = Rathlin, SAB = St Abbs, SAM = Samson, SHI = Shiants, SKO = Skomer, STA = St Agnes, STM = St Martins, SUM = Sumburgh Head, SUS = Sule Skerry, SWO = Swona, WIN = Whinnyfold.

Year	Colony	Earliest Trip	Latest Trip
2010	ANN	29/5/2010	29/5/2010
2011	ANN	12/5/2011	3/6/2011
2012	ANN	14/5/2012	15/5/2012
2011	BAR	15/5/2011	11/7/2011
2010	BEM	8/6/2010	3/7/2010
2011	BEM	2/6/2011	22/6/2011
2012	BEM	28/6/2012	4/7/2012
2013	BEM	5/6/2013	3/7/2013
2014	BEM	24/6/2014	30/6/2014
2012	BOB	4/6/2012	9/6/2012
2014	CAW	29/6/2014	1/7/2014
2010	COP	30/5/2010	30/6/2010
2011	COP	6/6/2011	5/7/2011
2012	COP	18/5/2012	20/7/2012
2014	COP	28/5/2014	10/7/2014

2011 2012	COQ COQ	14/6/2011 23/5/2012	16/6/2011 6/7/2012
2010 2011 2012 2013 2014	CSY CSY CSY CSY CSY	20/5/2010 3/5/2011 2/5/2012 8/5/2013 28/5/2014	12/7/2010 23/7/2011 21/7/2012 20/7/2013 20/7/2014
2010 2011 2012 2013 2014	FAI FAI FAI FAI FAI	6/7/2010 18/5/2011 19/5/2012 25/5/2013 12/5/2014	10/7/2010 23/6/2011 2/7/2012 21/6/2013 10/7/2014
2014	FAN	22/6/2014	24/6/2014
2013 2014	FIL FIL	6/6/2013 24/6/2014	4/7/2013 28/6/2014
2012	FOW	19/6/2012	25/6/2012
2013	GTS	29/4/2013	10/5/2013
2012 2013 2014	IOM IOM IOM	29/5/2012 25/6/2013 19/6/2014	20/6/2012 14/7/2013 7/7/2014
2010 2011	LAM LAM	6/5/2010 31/5/2011	19/7/2010 8/7/2011
2014	LUN	5/6/2014	11/6/2014
2010 2011 2012 2013 2014	MKS MKS MKS MKS MKS	5/6/2010 1/6/2011 21/5/2012 16/6/2013 9/6/2014	23/6/2010 2/7/2011 5/7/2012 14/7/2013 4/7/2014
2010 2011 2012 2013	PUF PUF PUF PUF	10/5/2010 12/5/2011 2/5/2012 3/6/2013	14/7/2010 11/7/2011 10/7/2012 20/7/2013
2013	RAT	3/6/2014	24/7/2014
2012	SAB	16/5/2012	1/6/2012
2010 2011 2012	SAM SAM SAM	18/5/2010 18/5/2011 27/5/2012	23/5/2010 30/5/2011 28/5/2012
2014	SHI	27/5/2014	29/5/2014
2011 2012	SKO SKO	2/6/2011 1/6/2012	25/6/2011 4/6/2012
2011 2012	STA STA	23/6/2011 26/6/2012	24/6/2011 27/6/2012
2010 2011 2012	STM STM STM	22/6/2010 16/6/2011 18/6/2012	18/7/2010 29/6/2011 19/6/2012

2014	SUM	25/6/2014	25/6/2014
2011	SUS	12/7/2011	13/7/2011
2010	SWO	18/6/2010	21/6/2010
2011	SWO	8/6/2011	16/6/2011
2012	SWO	6/6/2012	10/6/2012
2013	SWO	26/6/2013	28/6/2013
2014	SWO	26/6/2014	27/6/2014
2012	WIN	6/6/2012	8/7/2012

A2. Brief description of the modelling approach in Wakefield et al. (2017)

The approach used in Wakefield et al. (2017) involved modelling the intensity of tracking locations at a given point in space by using numerical quadrature methods to fit an Inhomogeneous Poisson Process (IPP) model. The response variable for the IPP was created by scoring all point locations in which tracking was observed as 1 and then creating a set of quadrature or dummy points on a regular grid across the study area and scoring them as 0. Weights were then assigned to quadrature points in relation to how many points (quadrature and data points) occurred within the same grid cell as a given point. Thus, the response variable is proportional to the expected density of tracking locations and the IPP model is equivalent to a weighted Poisson model. Separate models were run for each species, but within a species data was provided by multiple colonies. Birds from different colonies are likely to experience different environmental conditions/ habitat availability and may respond differently to habitat covariates as a consequence. To address this, the expected values of environmental covariates at a given colony were added as predictors to the models; expected covariate values were defined as the mean value of a covariate over the waters accessible from a given colony. The use of expected values partially implements the GFR model described in Matthiopoulos et al. (2011), which can predict usage in unsampled sites more accurately than conventional habitat selection models. To assess the performance of the fitted models, the predicted distribution of birds from tracked colonies was compared with the observed distribution of birds calculated using raw tracking data. A high degree of overlap (based on Bhattacharyya's Affinity, (Bhattacharyya 1943)) indicated good model fit. Covariates that improved the overlap between predicted and observed distribution of birds were retained as part of the best fitting model, but covariates that had no effect or decreased overlap were removed.

A3. Variation in the proportion of time spent at sea across colonies

Currently, the outputs from Wakefield et al. (2017) do not account for differences in time spent at sea among different colonies. To examine the extent of variation in time at sea between tracked colonies, we modelled the proportion of time birds spent at sea per day for each species using binomial mixed effects models in which the response variable was specified as a two-column matrix of successes (number of fixes at sea per day) and failures (number of fixes on land per day)

using the R package MCMCglmm (Hadfield 2010). Only days in which birds were tracked for the full 24 hours were included in the analysis. As random effects we included individual ID and colony ID to account for between-individual and between-colony variation in the proportion of time spent at sea. Colony ID was included as a random effect because we were specifically interested in estimating the degree of between-colony variation in proportion of time at sea across colonies. As a fixed effect predictor we included $\log^{10}$ colony size and latitude. Overall, we found that neither colony size or latitude associated with the proportion of time spent at sea per day in any species (Table A1). However, there was evidence of between-individual variation and between-colony variation in the proportion of time spent at sea per day across species.

Table A2. Analysis of proportion of time spent at sea across colonies for each of the four species included in the technical report. Point estimates are given along with Bayesian 95% credible intervals (95% CRI). Variance components are reported as between-individual or between colony standard deviations (σ).

Species	Intercept (95% CRI)	β: $\log^{10}$ Colony Size (95% CRI)	β: Latitude (95% CRI)	σ Individual ID (95% CRI)	σ Colony ID (95% CRI)	*n* = individuals/ colonies
Kittiwakes	-0.55 (-1.72 – 0.53)	0.21 (-0.17 – 0.62)	0.09 (-0.12 – 0.31)	1.45 (1.35 – 1.56)	0.501 (0.23 – 0.72)	*n* = 424/ 20
Guillemots	- 0.059 (- 1.35 – 1.34)	0.029 (-0.33 – 0.36)	0.32 (-0.13 – 0.76)	1.27 (1.21 – 1.34)	0.42 (0.14 – 0.65)	*n* = 183/ 12
Razorbills	-0.16 (-2.11 – 1.77)	-0.11 (-0.71 – 0.56)	0.27 (-0.18 – 0.71)	1.54 (1.47 – 1.61)	0.82 (0.44 – 1.17)	*n* = 299/ 14
Shags	-0.15 (-0.96 – 0.52)	0.032 (-0.37 – 0.36)	0.14 (-0.17 – 0.46)	1.17 (1.11 – 1.22)	0.69 (0.37 – 0.98)	*n* = 243/ 14

A4. Calculating relative density and utilisation distributions over a set of selected colonies.

Relative Density:

The relative density of birds originating from a selected set of colonies was calculated as:

$$RD_{P,i} = \sum_{All\ x} UD_{s,x}\, N_s.$$

Where $RD_{P,i}$ represents the relative density surface for a defined population *P* for the *i*th species. The population in question is defined by a list of colonies, *set x*, over which to perform the operation. For example, at the UK-level, set *x* contains all Seabird 2000 sites that are located within the UK. Similarly, at the SPA-level set x contain all Seabird 2000 sites that are located within the boundaries of a specified SPA. $UD_{s,x}$ represents the UD for the *s*th colony for all colonies included within the set *x*. *Ns* represents the size of colony *s* and is calculated as two times the number of Apparently Occupied Nests (AON) recorded during the Seabird 2000 census for kittiwakes and shags or the number of individuals recorded for guillemots and razorbills. Note that we did not use a conversion of factor of 0.67 to convert he numbers of guillemots and razorbills into pairs (see main text).

Utilisation Distribution:

The utilisation distribution (UD) of a given population is calculated by normalizing the relative density estimates (described above) for said population to generate a probability distribution that sums to one. This is achieved as:

$$UD_{P,i} = \frac{\sum_{All\ x} UD_{s,x}\, N_s}{\sum_{s=1}^{N.\ Sites} N_s}$$

Where $UD_{P,i}$ represents the population-level UD *P* for the *i*th species and *N. Sites* denotes the total number of sites included within set *x*. Note that the numerator here is the same as the equation for relative density.

A5. Influence of analysis field on hotspot methods

When performing either maximum curvature or Getis-Ord analysis how one specifies the analysis field can have a noticeable impact on the size of the subsequent hotspots identified. We provide an example of this by comparing hotspots identified at the Fowlsheugh SPA for black-legged kittiwakes and the Foula SPA for European shags. At Fowlsheugh both maximum curvature and Getis-Ord analysis were conducted by setting the analysis field as either the 95% home range (the approach used in the main technical report) or by drawing a maximum foraging radius around the colony (Fig. A1). At the Foula SPA a similar procedure was conducted for European shags (Fig. A2). Data on foraging range was taken from Thaxter et al. (2012). We took data from Thaxter et al. (2012) rather than our own tracking data as, in the absence of tracking data, these values are often used as the benchmark for identifying which areas colonies use (Eastham 2014).

The size of identified hotspots reflects the size of the analysis field used. At Fowlsheugh the 95% home range of kittiwakes was larger than the maximum foraging radius buffer resulting in larger hotspots being identified. Conversely, at Foula the 95% home range of shags was smaller than the maximum foraging radius buffer resulting in smaller hotspots. Differences between the size of 95% home ranges and buffers based on maximum environmental variables, coastal geography and density dependence are taken into consideration when estimating colony-specific home ranges. In contrast, such considerations are not taken into account when using a point estimate of maximum foraging range.

Fig. A1. Plots showing the influence of changing the analysis field on hotspots identified for kittiwakes originating from within the Fowlsheugh SPA. a) Comparison of the area covered by two different analysis fields, 95% home range and maximum foraging range radius. b) Top 1% Getis-Ord hotspots using different analysis fields. c) Top 5% Getis-Ord hotspots using different analysis fields. d) Statistically significant Getis-Ord hotspots using different analysis fields. e) Maximum curvature hotspots using different analysis fields.

a)

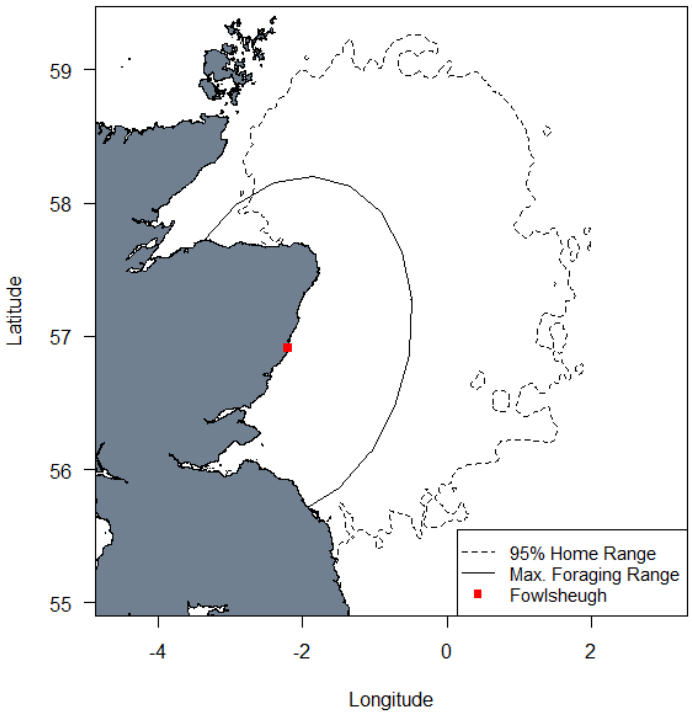

b)

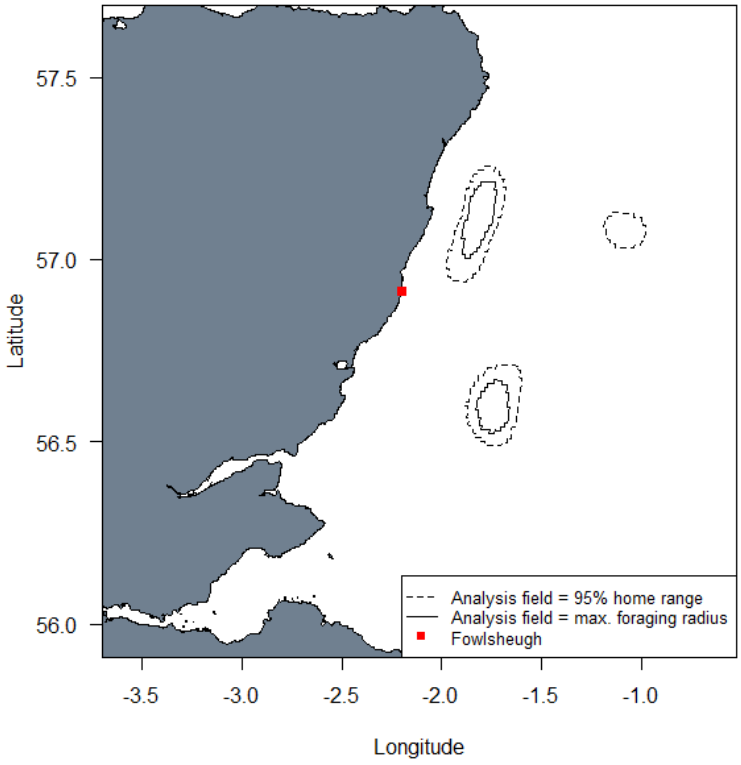
57.5
57.0
56.5
56.0
Latitude
-3.5
-3.0
-2.5
-2.0
-1.5
-1.0
Longitude
Analysis field = 95% home range
Analysis field = max. foraging radius
Fowlsheugh

c)

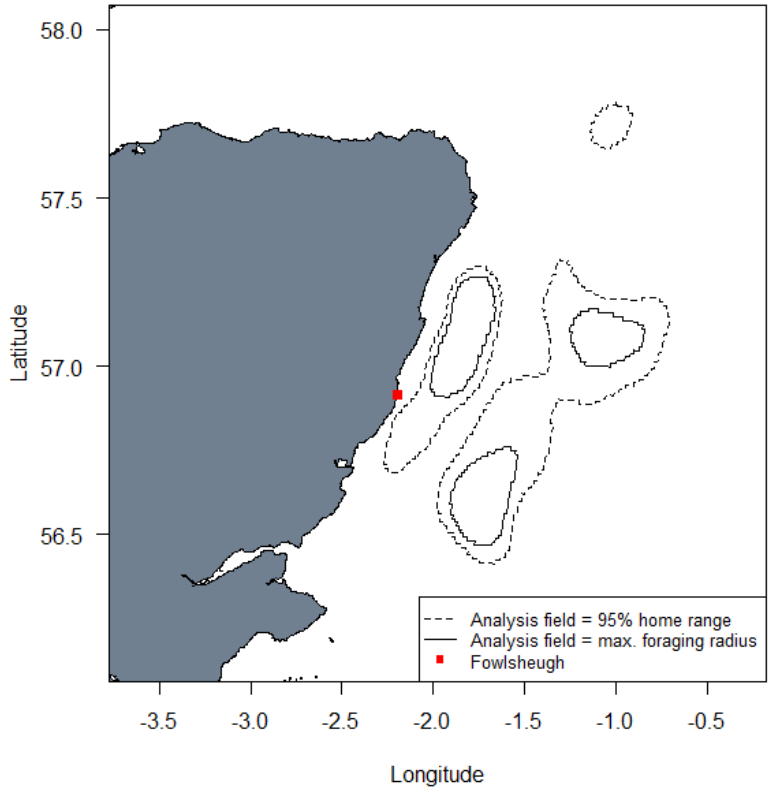
58.0
57.5
57.0
56.5
Latitude
-3.5
-3.0
-2.5
-2.0
-1.5
-1.0
-0.5
Longitude
Analysis field = 95% home range
Analysis field = max. foraging radius
Fowlsheugh

d)

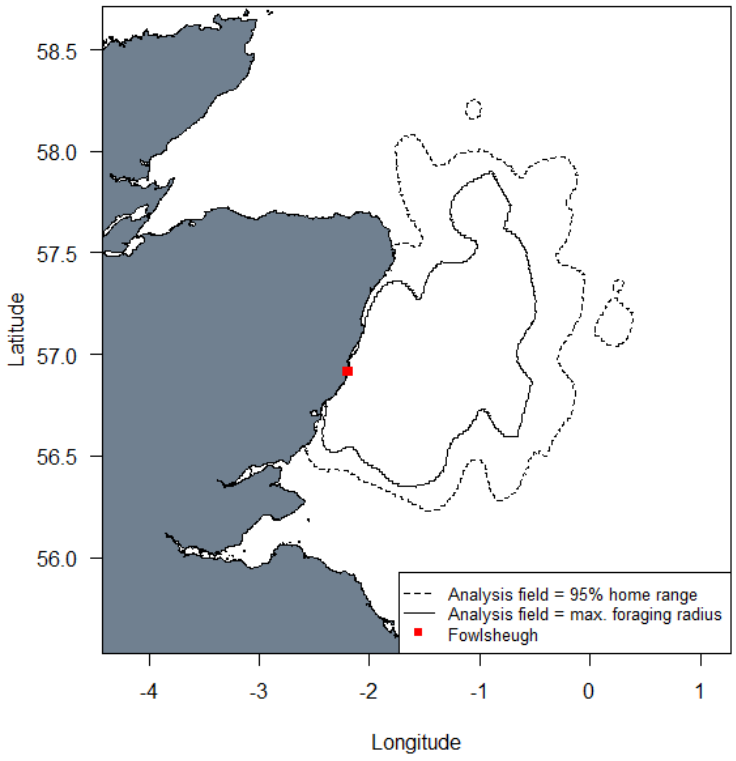
58.5
58.0
57.5
57.0
56.5
56.0
Latitude
-4
-3
-2
-1
0
1
Longitude
Analysis field = 95% home range
Analysis field = max. foraging radius
Fowlsheugh

e)

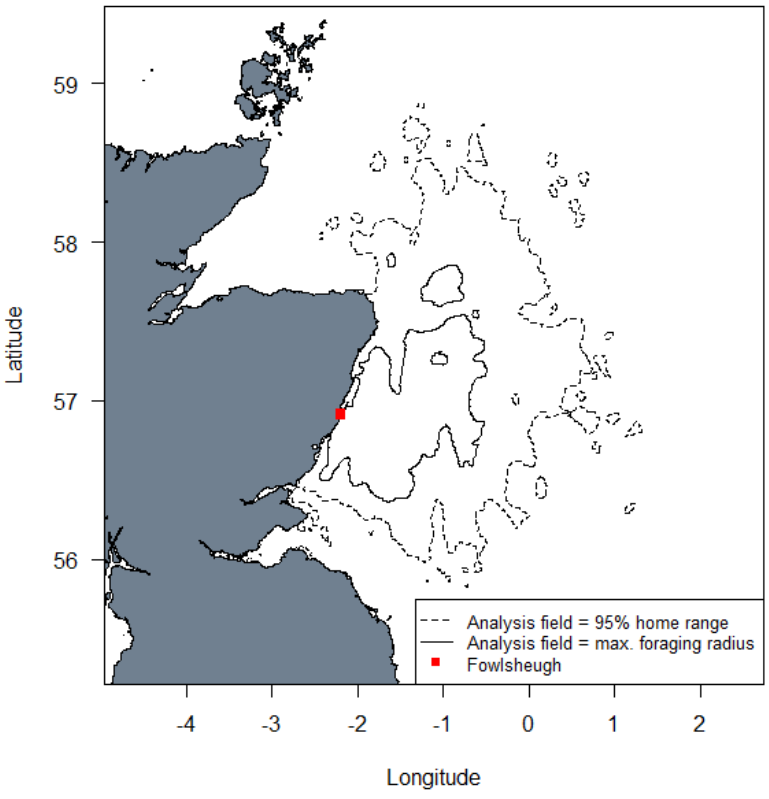
59
58
57
56
Latitude
-4
-3
-2
-1
0
1
2
Longitude
Analysis field = 95% home range
Analysis field = max. foraging radius
Fowlsheugh

Fig. A2. Plots showing the influence of changing the analysis field on hotspots identified for shags originating from within the Foula SPA. a) Comparison of the two different analysis fields trialled 95% home range and maximum foraging range radius. b) Top 1% Getis-Ord hotspots using different analysis fields. c) Top 5% Getis-Ord hotspots using different analysis fields. d) Statistically significant Getis-Ord hotspots using different analysis fields. e) Maximum curvature hotspots using different analysis fields.

a)

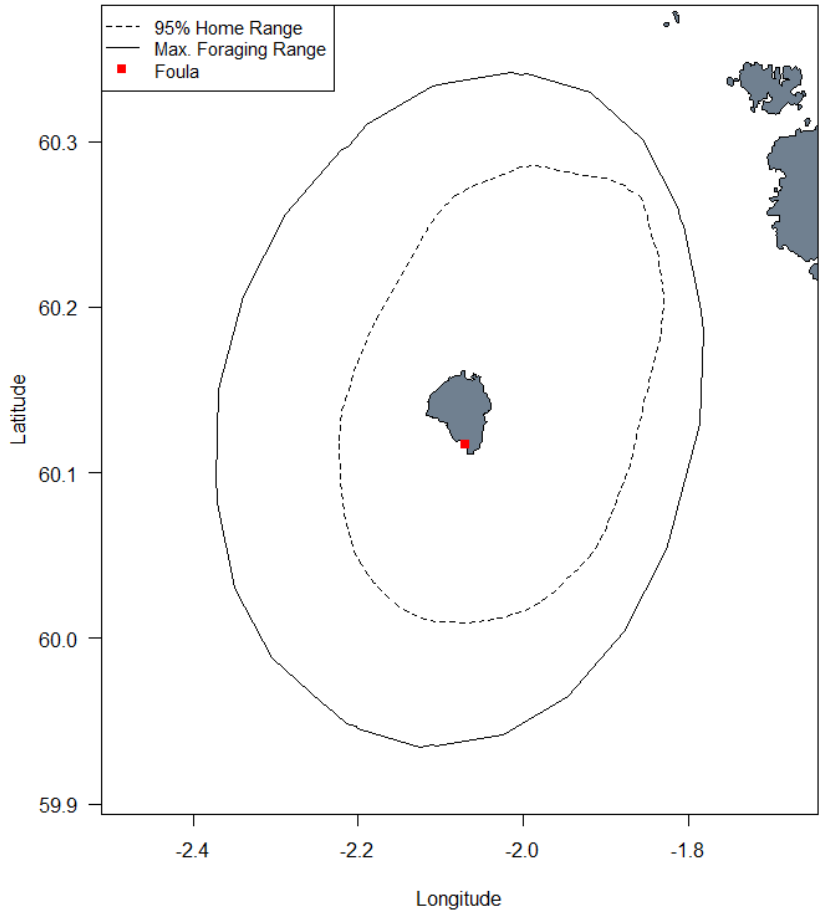

b)

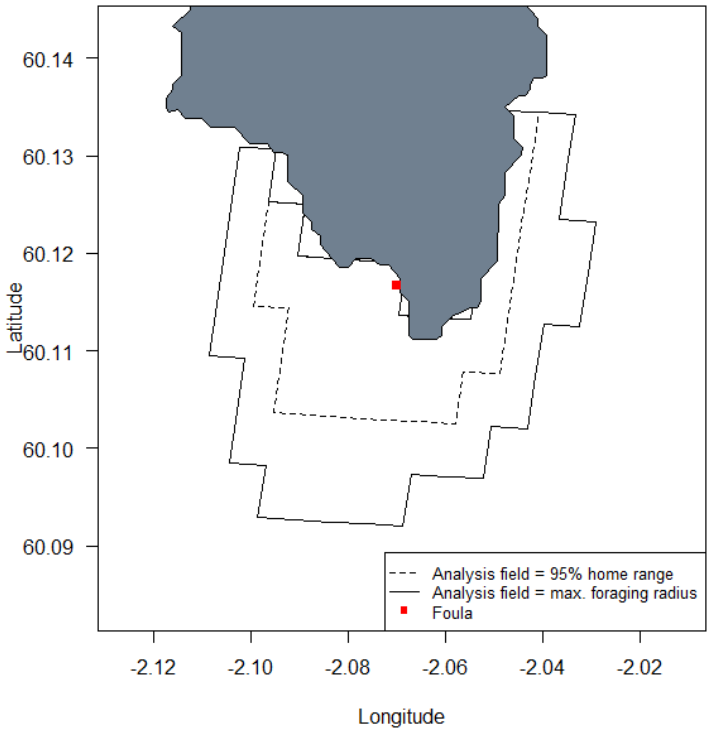
60.14
60.13
60.12
60.11
60.10
60.09
Latitude
-2.12
-2.10
-2.08
-2.06
-2.04
-2.02
Longitude
Analysis field = 95% home range
Analysis field = max. foraging radius
Foula

c)

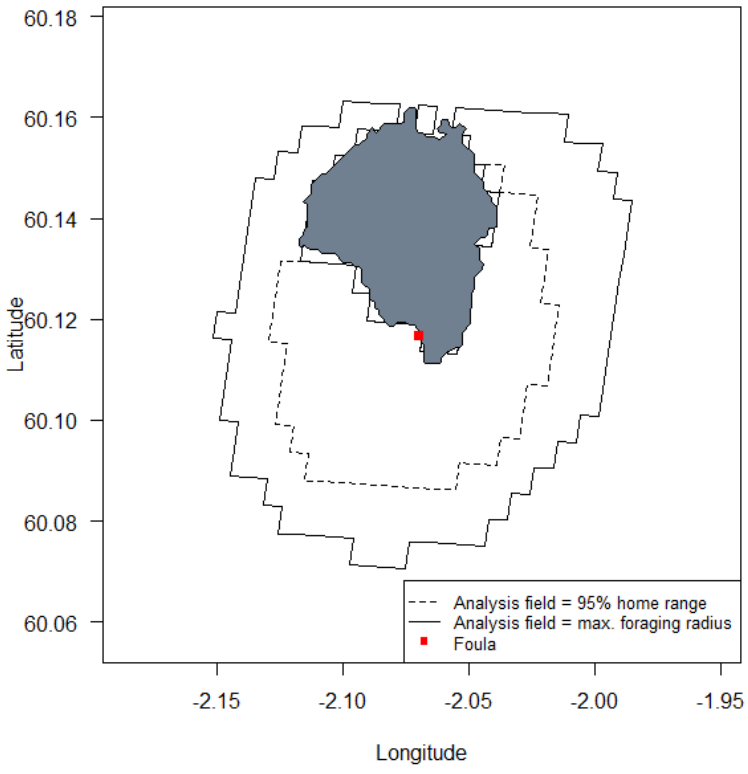
60.18
60.16
60.14
60.12
60.10
60.08
60.06
Latitude
-2.15
-2.10
-2.05
-2.00
-1.95
Longitude
Analysis field = 95% home range
Analysis field = max. foraging radius
Foula

d)

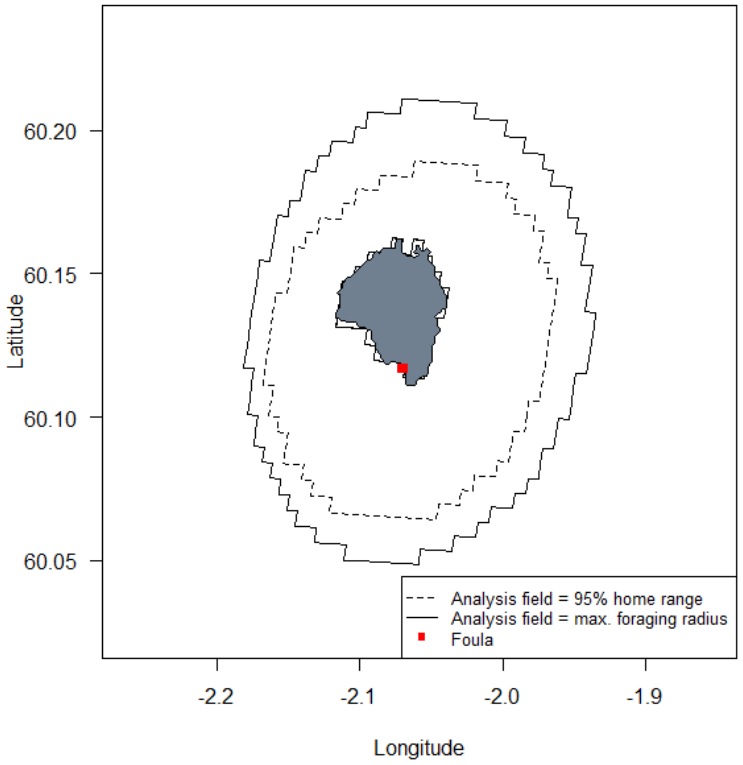
60.20
60.15
60.10
60.05
Latitude
-2.2
-2.1
-2.0
-1.9
Longitude
Analysis field = 95% home range
Analysis field = max. foraging radius
Foula

e)

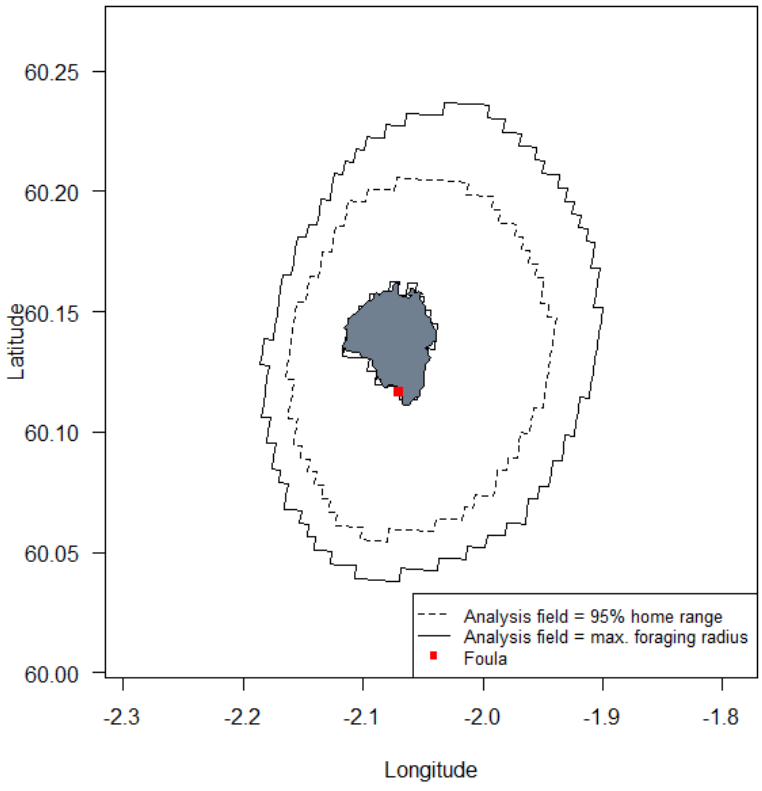
60.25
60.20
60.15
60.10
60.05
60.00
Latitude
-2.3
-2.2
-2.1
-2.0
-1.9
-1.8
Longitude
Analysis field = 95% home range
Analysis field = max. foraging radius
Foula

A6. Influence of neighbourhood size on Getis-Ord analysis

When performing Getis-Ord analysis the choice of appropriate neighbourhood size plays a key role in determining the size and location of hotspots identified. Here, we examined how changing the neighbourhood size altered the Getis-Ord hotspots for kittiwakes nesting within the Flamborough and Bempton Cliffs SPA. For the current analysis the analysis field was defined as the 95% home range of birds originating from within the Flamborough and Bempton Cliffs SPA and range of different neighbourhood sizes were trialled: d = 8 km, 10 km, 12 km, 15 km, 18 km, 20 km, 23 km, 25 km, 30 km, 35 km, 40 km, 50 km and 60 km. Using these neighbourhood sizes Getis-Ord hotspots were defined using the top 1% and top 5% of Getis-Ord scores as well as on the basis of the statistical significance of Getis-Ord scores.

Plots (Fig. A3) show examples of the hotspots identified using different neighbourhood values over-laid with density estimates from the models of Wakefield et al. (2017). When using the top 1% or top 5% of Getis-Ord scores to delineate hotspots we found that using a small neighbourhood size (8 – 10 km) generally gave hotspots that showed a high degree of similarity (Jaccard similarity) to specific population UDs. In this case, top 1% Getis-Ord hotspots were most similar to the 20% UD and top 5% Getis-Ord hotspots were most similar to the 45% UD (Fig. A4). However, as neighbourhood size increased similarity between hotspots and UDs decreased and at the largest neighbourhood sizes (d = 50 – 60 km) hotspots bore very little resemblance to estimated UDs. Such a relationship can also be seen by plotting identified hotspots and over-laying estimated distribution data. When using statistical significance to delineate hotspots we found that as neighbourhood size increased the similarity between hotspots and estimated UDs decreased slightly, though not to the same extent as when using the top 1% or top 5% of Getis-Ord scores. In addition, as neighbourhood size was increased the hotspots identified became more similar to larger population-level UDs. For example, when neighbourhood size was set at 8 km statistically significant Gi* hotspots were most similar to the 60% UD, but when neighbourhood size was 60 km hotspots were most similar to the 80% UD. In general, over-estimating neighbourhood size appears of greatest concern when conducting Getis-Ord analysis than specifying too small a neighbourhood. In particular, the top 1% or 5% methods of delineating hotspots appear particularly sensitive to over-estimation of neighbourhood size. In the current example neighbourhood sizes above 30 km appeared to give very poor results. Similar results were seen in other populations/

species with larger neighbourhood sizes generating hotspots that did not resemble underlying distribution well, particularly when using the top 1% or top 5% of Getis-Ord scores to delineate hotspots. We note that the selection of large neighbourhood sizes was not supported by the use of either spatial variograms (maximum *d* across species = 16km) or FPT analysis (maximum *d* across species = 10km).

Fig. A3. Maps showing estimated density of kittiwakes per km^2 at sea originating from colonies within the Flamborough and Bempton Cliffs SPA over-laid with Getis-Ord hotspots calculated using different neighbourhood size values.

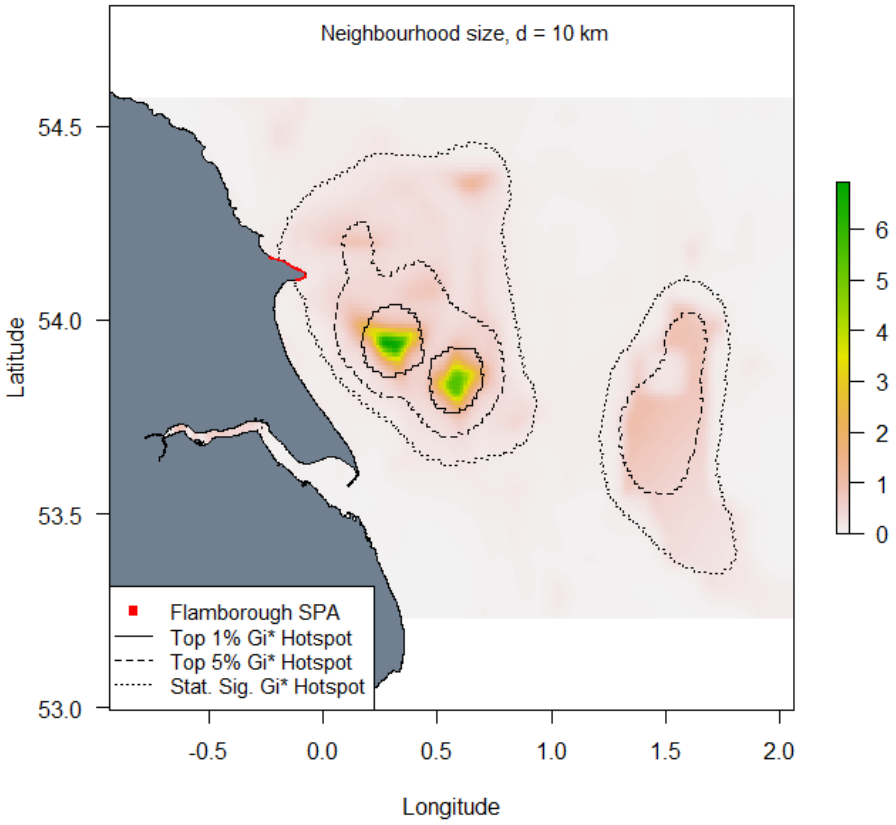

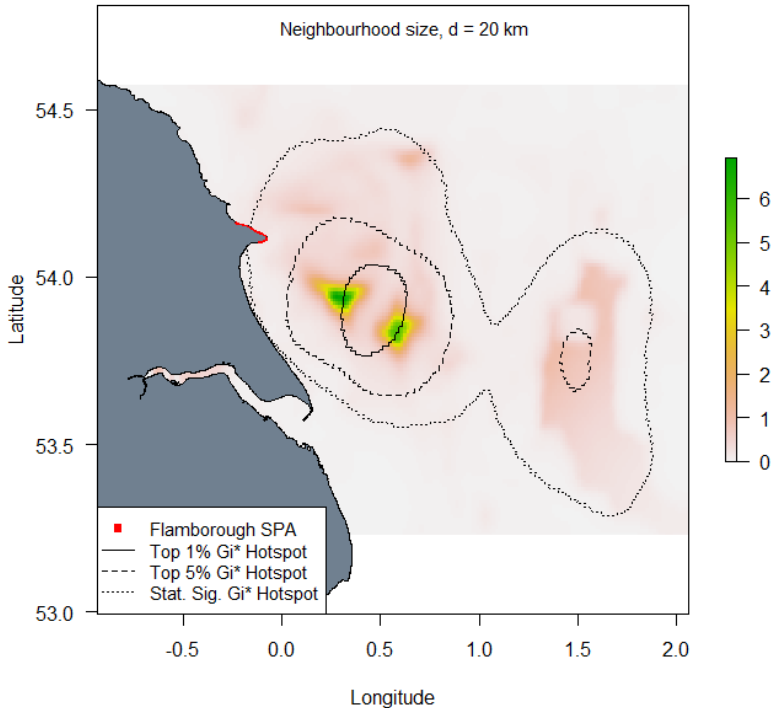
Neighbourhood size, d = 20 km
54.5
54.0
53.5
53.0
Latitude
-0.5
0.0
0.5
1.0
1.5
2.0
Longitude
6
5
4
3
2
1
0
Flamborough SPA
Top 1% Gi* Hotspot
Top 5% Gi* Hotspot
Stat. Sig. Gi* Hotspot

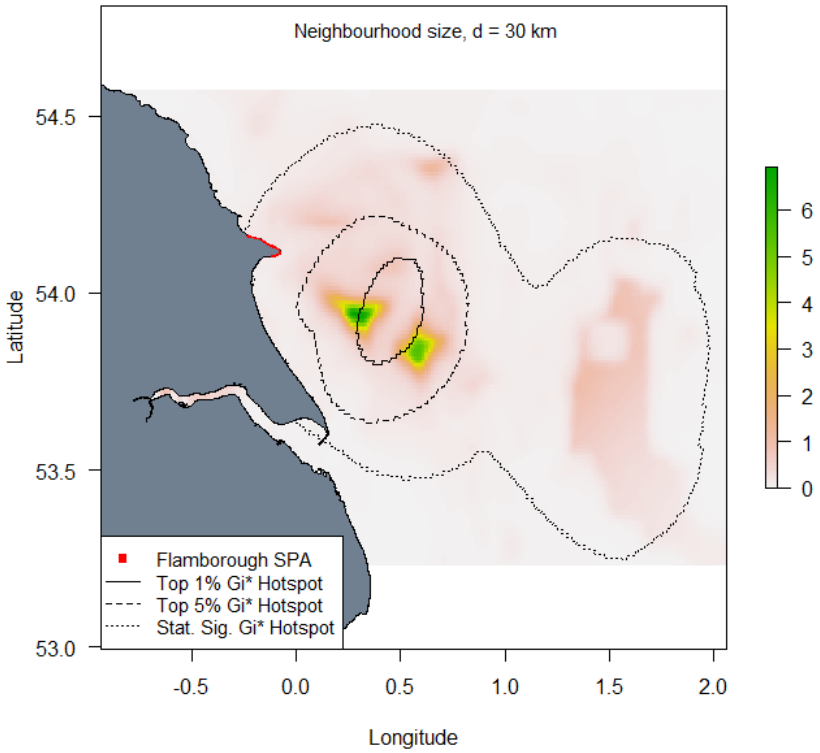
Neighbourhood size, d = 30 km
54.5
54.0
53.5
53.0
Latitude
-0.5
0.0
0.5
1.0
1.5
2.0
Longitude
6
5
4
3
2
1
0
Flamborough SPA
Top 1% Gi* Hotspot
Top 5% Gi* Hotspot
Stat. Sig. Gi* Hotspot

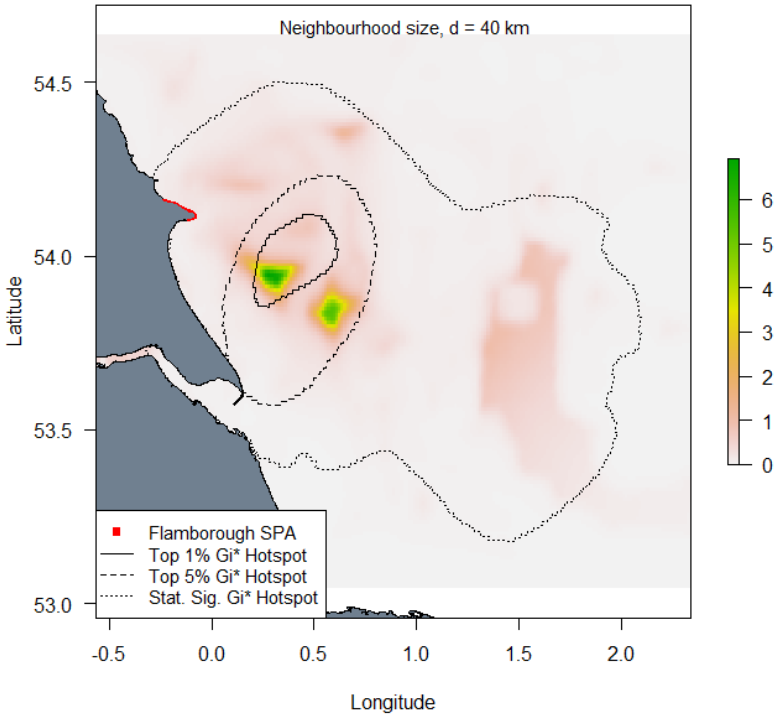
Neighbourhood size, d = 40 km
54.5
54.0
53.5
53.0
Latitude
-0.5
0.0
0.5
1.0
1.5
2.0
Longitude
Flamborough SPA
Top 1% Gi* Hotspot
Top 5% Gi* Hotspot
Stat. Sig. Gi* Hotspot
6
5
4
3
2
1
0

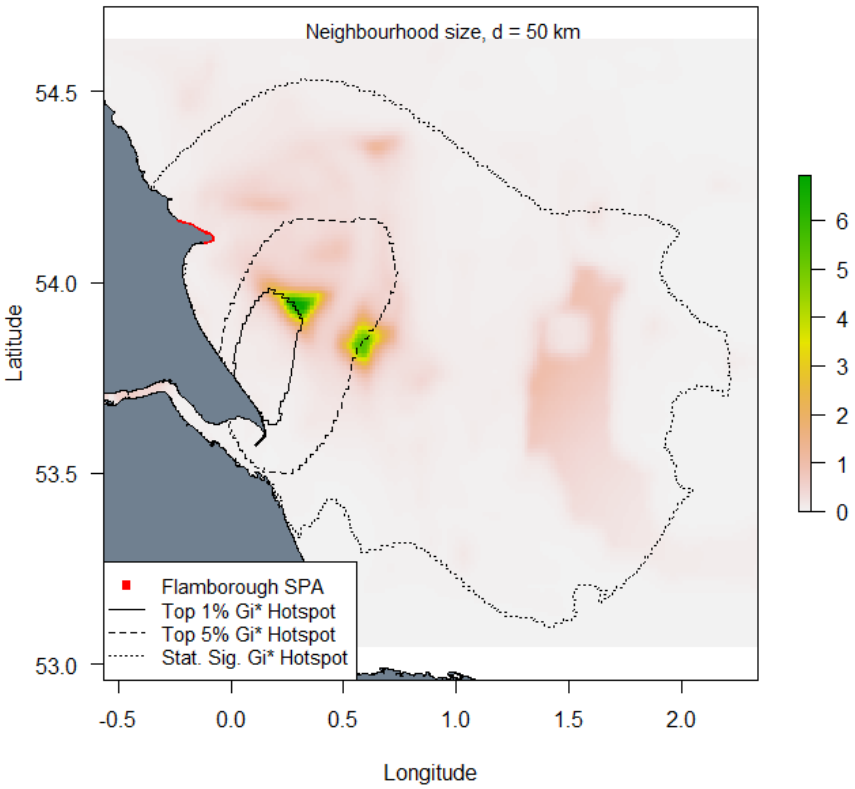
Neighbourhood size, d = 50 km
54.5
54.0
53.5
53.0
Latitude
-0.5
0.0
0.5
1.0
1.5
2.0
Longitude
Flamborough SPA
Top 1% Gi* Hotspot
Top 5% Gi* Hotspot
Stat. Sig. Gi* Hotspot
6
5
4
3
2
1
0

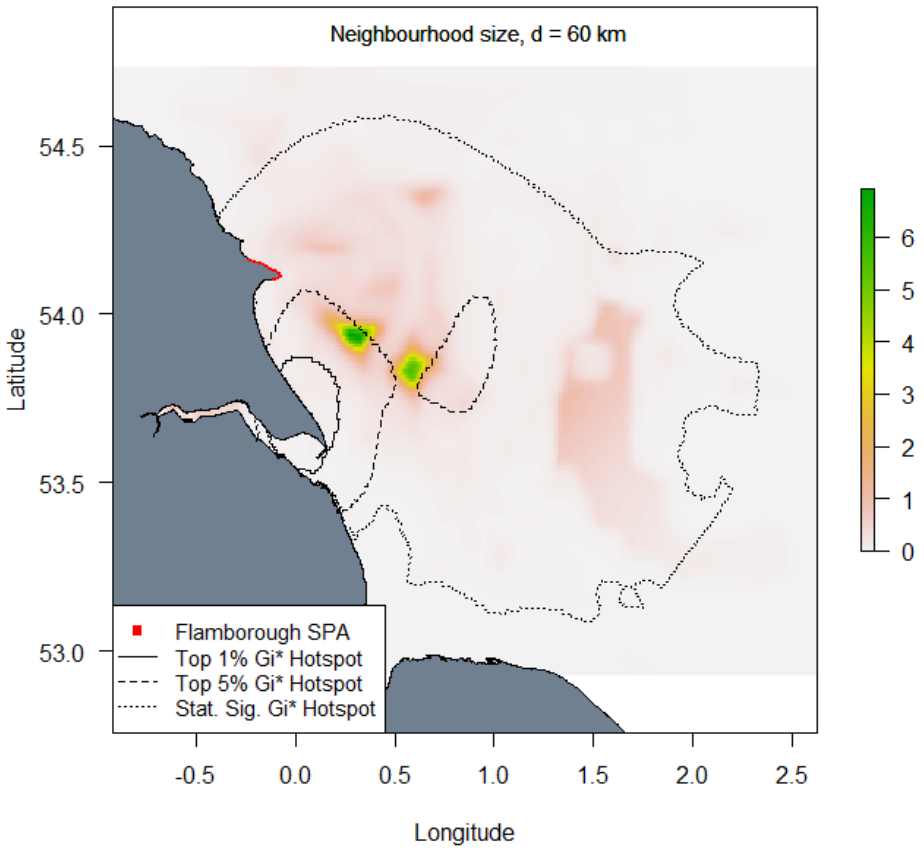
Neighbourhood size, d = 60 km
54.5
54.0
53.5
53.0
Latitude
-0.5
0.0
0.5
1.0
1.5
2.0
2.5
Longitude
Flamborough SPA
Top 1% Gi* Hotspot
Top 5% Gi* Hotspot
Stat. Sig. Gi* Hotspot
6
5
4
3
2
1
0

Fig. A4. Figures showing the Jaccard similarity between Getis-Ord hotspots calculated using different neighbourhood sizes, *d*, and % UDs for kittiwakes at the Flamborough and Bempton Cliffs SPA. a) Getis-Ord hotspots calculated using top 1% of Getis-Ord scores; similarity peaks at the 20% UD when using a small neighbourhood size, but peak similarity declines as neighbourhood size increases. b) Getis-Ord hotspots calculated using top 5% of Getis-Ord scores; similarity peaks at the 45% UD when using a small neighbourhood size, but peak similarity declines as neighbourhood size increases. c) Getis-Ord hotspots calculated using statistically significant Getis-Ord scores; similarity peaks at different values depending on neighbourhood size and declines as neighbourhood size increases.

a)

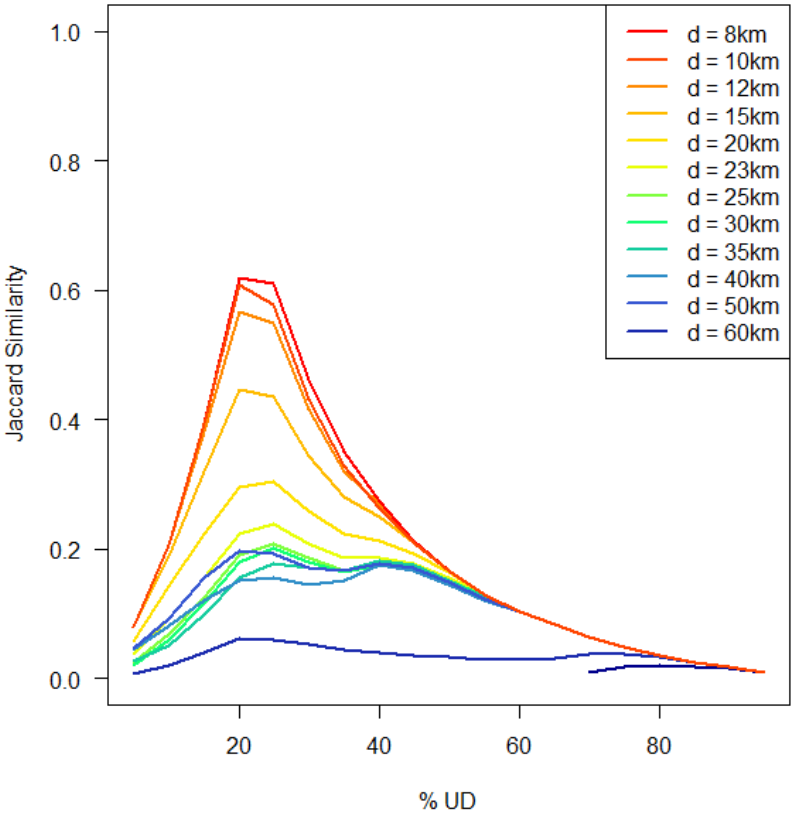

b)

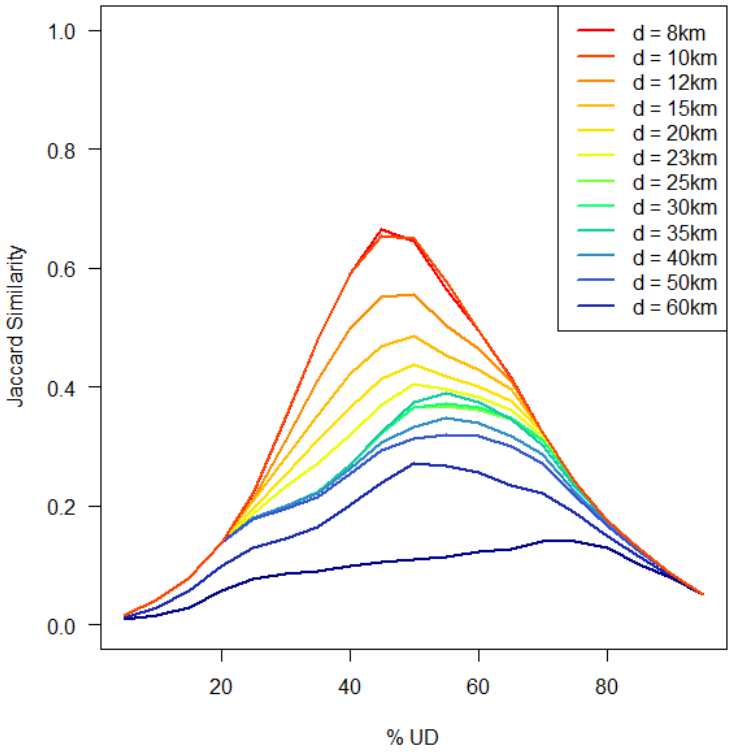
d = 8km
d = 10km
d = 12km
d = 15km
d = 20km
d = 23km
d = 25km
d = 30km
d = 35km
d = 40km
d = 50km
d = 60km
Jaccard Similarity
1.0
0.8
0.6
0.4
0.2
0.0
20
40
60
80
% UD

c)

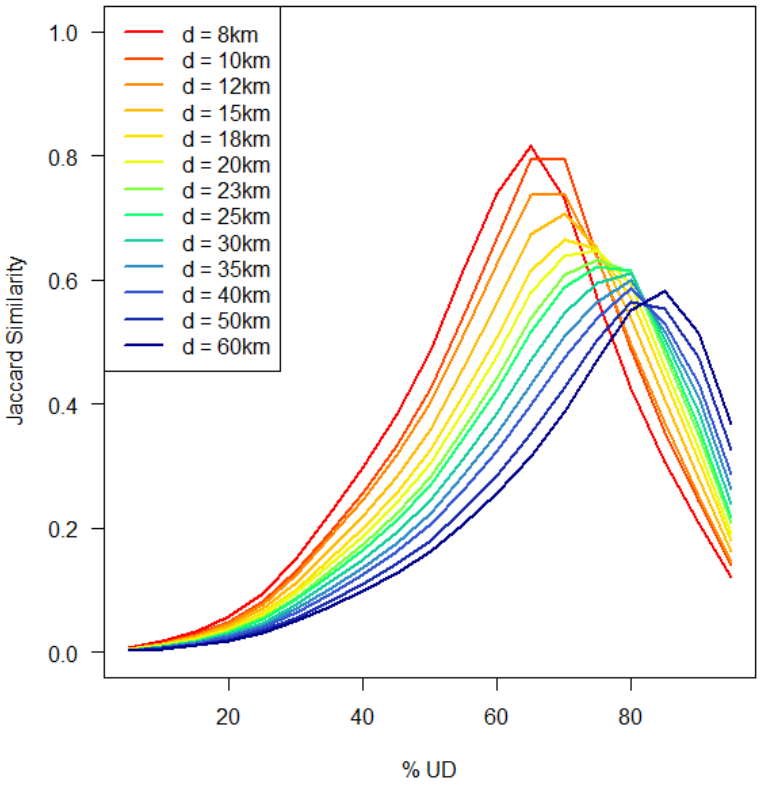
d = 8km
d = 10km
d = 12km
d = 15km
d = 18km
d = 20km
d = 23km
d = 25km
d = 30km
d = 35km
d = 40km
d = 50km
d = 60km
Jaccard Similarity
1.0
0.8
0.6
0.4
0.2
0.0
20
40
60
80
% UD

A7. Description of First-Passage Time

The first passage time (FPT) is a parameter often used to describe the scale at which patterns occur in a movement trajectory and is frequently used to identify foraging areas in both terrestrial and marine systems (Battaile, Nordstrom, Liebsch, & Trites, 2015; Byrne & Chamberlain, 2012; Hamer et al., 2009; Le Corre, Dussault, & Côté, 2014). FPT is defined as the time required by the animals to pass through a circle of radius *r* centred on a given point within the trajectory. The mean first passage time scales proportionately to the square of the radius of the circle for an uncorrelated random walk (Johnson et al. 1992).

Fauchald and Tverra (2003) proposed that, instead of computing the mean of FPT, one could calculate the variance of the log (FPT). Consider a trajectory composed of *n* points where each point is separated by a small given distance in space. Assume that each point is also associated with a circle of given radius, *r*. By measuring the time taken between entering and exiting this circle we get a measure of search effort/ time at each point along a trajectory. As mentioned above, increasing *r* will increase the time taken to cross the circle. However, this increase will be larger in areas with higher tortuosity and lower speed (associated with search effort) than areas in which an animal moves faster in more straight lines. Therefore, the relative variance in FPT for all points along a trajectory will increase as *r* increases. The variance in log (FPT) is given as *Var* [log (*t*) *r*], where *t*(*r*) is the time taken to cross a circle of given radius. When *r* increases beyond the spatial scale at which search effort occurs then the relative difference between *t*(*r*) between points within and outside of the area will decrease resulting in a decrease in the log (FPT) variance. Thus, whenever search effort is concentrated in a particular area we expect to find a peak in the log (FPT) variance, with *r* corresponding to the spatial scale of the intensively searched area.

Using the *adehabitatLT* package in R (Calenge 2009), FPT values were calculated for each trip scales ranging from *r* = 2 km to 100 km at 1 km intervals for kittiwakes, guillemots and razorbills. For shags *r* ranged from *r* = 1 km to 50 km at 0.5 km intervals. The variance in FPT was calculated as a function of radius, and maxima in the log-transformed variance indicated the scale at which the bird interacted with the environment. This value was averaged across all trip within a species and taken to represent the scale at searching behaviour. Occasionally, FPT analysis identifies multiple maxima (peaks) in log (FPT) variance, which may occur when species exhibit hierarchical searching strategies (Hamer et al. 2009). When this occured we chose the value at which the

variance in log (FPT) first peaked as our measure of the scale of search effort provided that this peak was at least one third of the size of the largest peak in the variance of log (FPT). In most cases, the first peak in log (FPT) variance is the greatest. Moreover, choosing the first peak means that we focus on smaller scale foraging effort and because FPT is used to determine the neighbourhood size for Getis-Ord analysis it helps us avoid the risk of over-estimating neighbourhood size (see below).

A8. Variogram versus FPT neighbourhood size

Across species performing Getis-Ord analysis at the UK-level using either FPT analysis or spatial variograms to define neighbourhood size, *d*, resulted in broadly similar hotspots being identified. However, FPT-based analysis consistently identified smaller neighbourhood sizes than spatial variograms reflecting a lower level of smoothing. As a result, FPT based analysis was occasionally able to identity small hotspots at a few locations that were not highlighted when using a larger neighbourhood size.

In kittiwakes, guillemots and razorbills the choice of neighbourhood size had most effect when defining hotspots as the top 1% of Getis-Ord scores. In contrast, the choice of neighbourhood size had less effect when hotspots were defined as the top 5% of Getis-Ord scores or on the basis of statistical significance. In shags, there was little evidence that the method used to define Gi* thresholds influenced the similarity of identified hotspots as neighbourhood size was changed. Table A2 shows the spatial similarity between Gi* hotspots identified using a neighbourhood size define by FPT analysis or spatial variograms.

Our rationale for preferring FPT is that it has a common ecological interpretation as the spatial scale at which birds interact with their environment. Moreover, the fact that spatial variograms occasionally failed to reach an asymptote of identified multiple peaks in spatial auto-correlation suggested that they did not always fit the patterns seen in the data particularly well. Finally, because over-estimating the size of the local neighbourhood resulted in poor performance of Getis-Ord analysis the smaller neighbourhood sizes derived from FPT analysis were judged more reliable.

Table A3. Table showing estimated similarity between Getis-Ord hotspots calculated using a neighbourhood size, *d*, estimated via FPT analysis or spatial variograms.

Species	Neighbourhood Size (*d*) comparison, FPT vs. variogram	Getis-Ord method	Jaccard Similarity
Black-legged kittiwake	10 km vs. 15 km	Top 1% Gi*	J = 0.71
		Top 5% Gi*	J = 0.90
		Stat. Sig. Gi*	J = 0.90
Common guillemot	9 km vs. 16 km	Top 1% Gi*	J = 0.54
		Top 5% Gi*	J = 0.75
		Stat. Sig. Gi*	J = 0.82
Razorbill	7 km vs. 11 km	Top 1% Gi*	J = 0.67
		Top 5% Gi*	J = 0.82
		Stat. Sig. Gi*	J = 0.77
European Shag	4 km vs. 5 km	Top 1% Gi*	J = 0.77
		Top 5% Gi*	J = 0.76
		Stat. Sig. Gi*	J = 0.79

Fig. A5. Maps displaying Getis-Ord hotspots identified at the UK-level for a) black-legged kittiwakes using using a neighbourhood size of d = 15 km; b) common guillemots using a neighbourhood size of 16 km; c) razorbills using a neighbourhood size of 11 km; d) European shags using a neighbourhood size of 5 km. UK EEZ also displayed.

a)

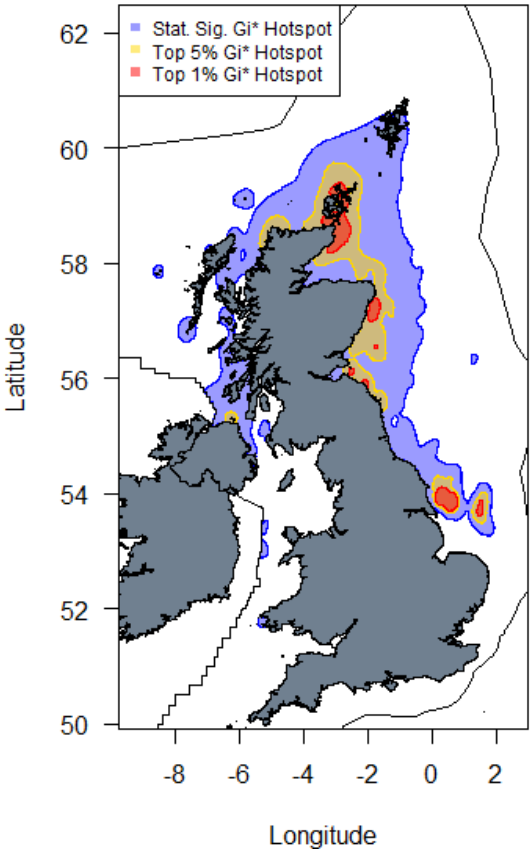

b)

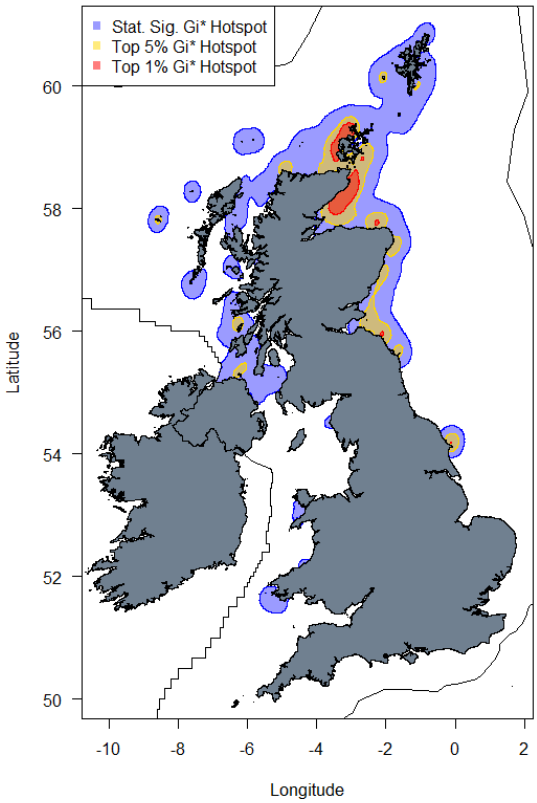

c)

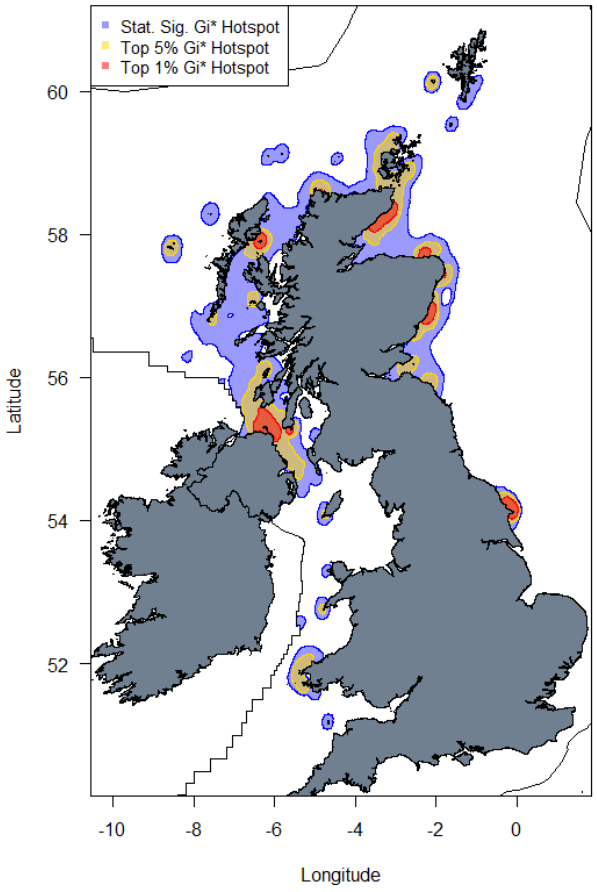
Stat. Sig. Gi* Hotspot
Top 5% Gi* Hotspot
Top 1% Gi* Hotspot
Latitude
60
58
56
54
52
-10
-8
-6
-4
-2
0
Longitude

d)

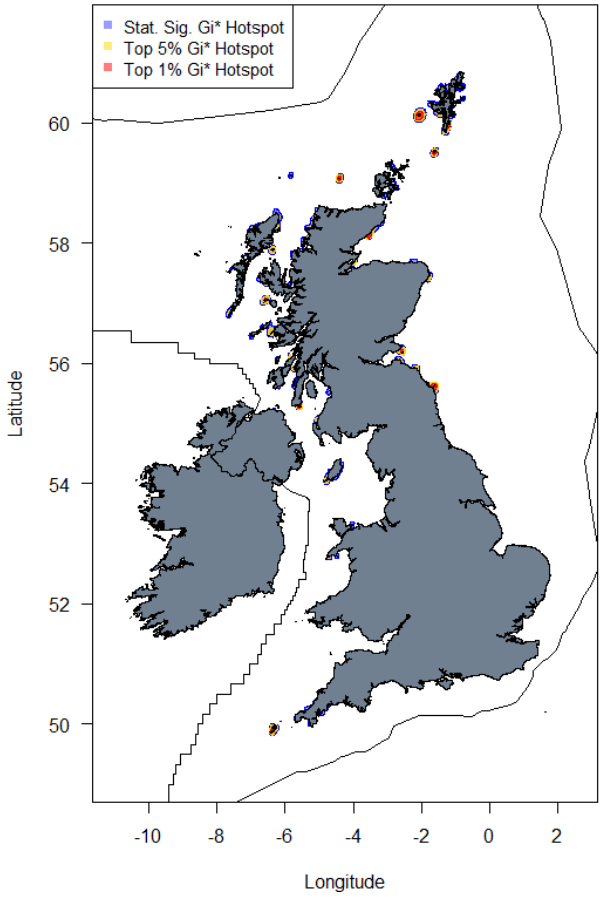
Stat. Sig. Gi* Hotspot
Top 5% Gi* Hotspot
Top 1% Gi* Hotspot
Latitude
60
58
56
54
52
50
-10
-8
-6
-4
-2
0
2
Longitude

A9. Representativeness of tracking data

To estimate the representativeness of our tracking data we adopted the approach introduced by Lascelles et al. (2016) to identify seabird Important Bird Areas (IBAs). The approach examines how estimated core area distribution (50% UD) changes as sample size (number of tracks) increases. For each tracked colony individual foraging trips were assigned a unique identifier and randomly selected iteratively for a sequence of different sample sizes (analysis done at the trip-level; the Lascelles et al. (2016) approach includes a screening for potential pseudo-replication). Sample sizes chosen ranged from 1 to the maximum number of birds tracked at a given colony. For each sample size, a 50% UD was calculated from the sampled data using the average ARS scale to define the smoothing parameter used when constructing UDs. The proportion of unsampled data that fell within this 50% UD was then recorded as an inclusion value. Subsequently, a nonlinear regression was used to estimate the sample size needed for tracking data from a selected colony to be considered representative. The maximum inclusion value achieved by a given colony was then calculated as a percentage of the estimated asymptote value to provide a measure of the representativeness of tracking data.

Lascelles et al. (2016) used a cut-off value of 70% representativeness when deciding whether tracking data was representative enough for further analysis. In most cases tracking data exceeded this 70% threshold value and, as expected, larger sample sizes gave more representative results (Fig. A6). Colonies that did not exceed this 70% threshold were still included in the habitat modelling carried out by Wakefield et al. (2017) as they still provide valuable information on species habitat preferences by sampling different regions. However, model selection was weighted towards colonies in which more birds were tracked and hence data more representative.

As well as uncertainty in the raw tracking data itself there also remains some uncertainty in model results. To address this Wakefield et al. (2017) quantified spatial variation in model uncertainty using parametric resampling in order the calculate coefficient of variation (CV) of model estimates. Due to temporal and spatial auto-correlation present in tracking data model CVs should be treated as relative rather than absolute. Overlaying identified hotspots with maps of model CV shows that hotspots are generally situated in areas in which the CV is low, indicating greater certainty in distribution estimates in such areas (Fig. A7).

Fig. A6. Plots showing the representativeness of tracking data at each colony against the number of birds tracked using the procedure of Lascelles et al. (2016) for (a) kittiwakes, (b) guillemots, (c) razorbills and (d) shags. Size of data points is proportional to $\log^{10}$ colony size, while tabs indicate the identity of each colony (denoted as a three letter code, see Table A1). Colony tabs colour coded, dark blue = Scotland, red = Wales, green = Ireland, orange = Scilly Isles, light blue = Yorkshire, gold = Northumberland.

a) black-legged kittiwakes

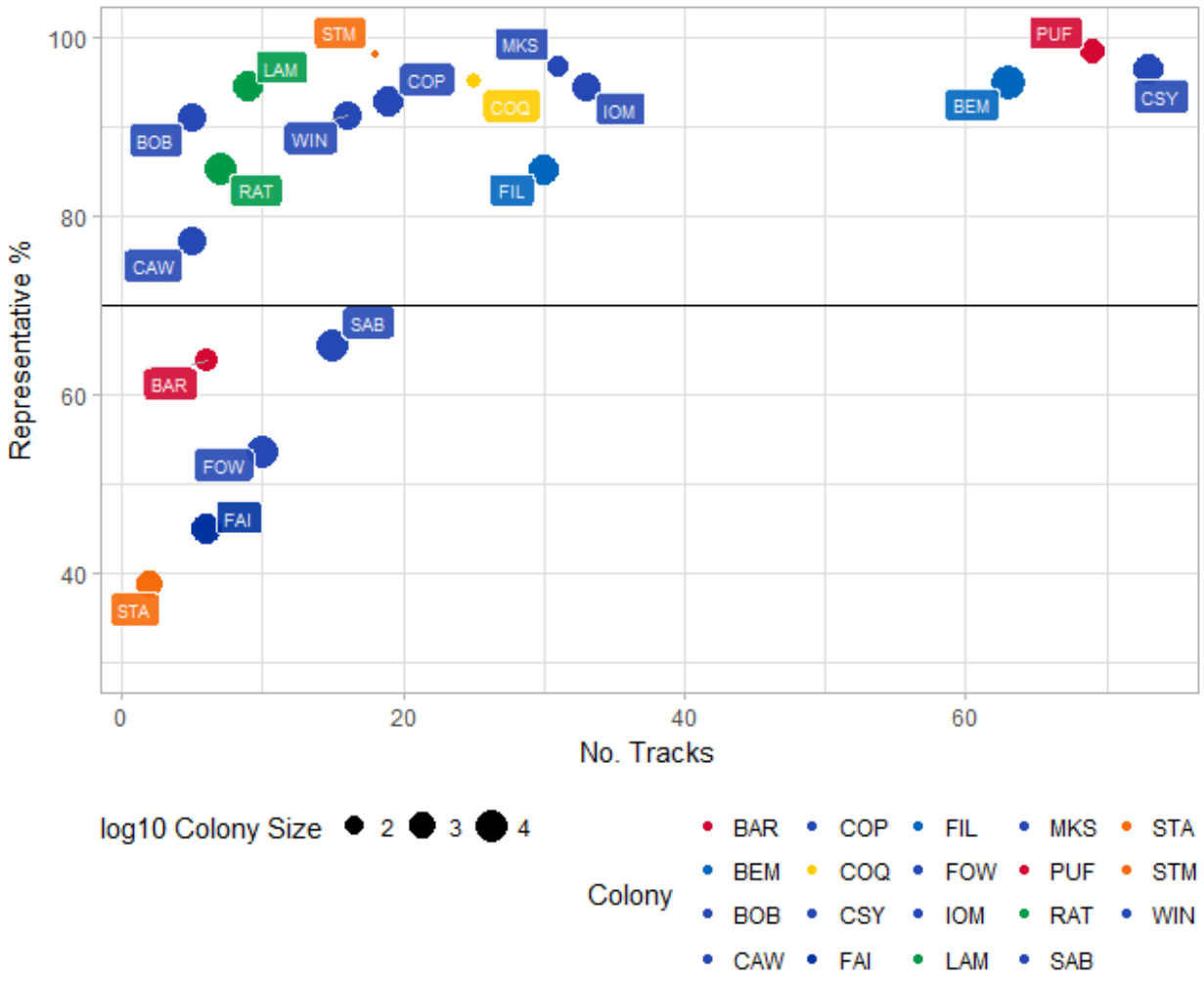

b) common guillemots

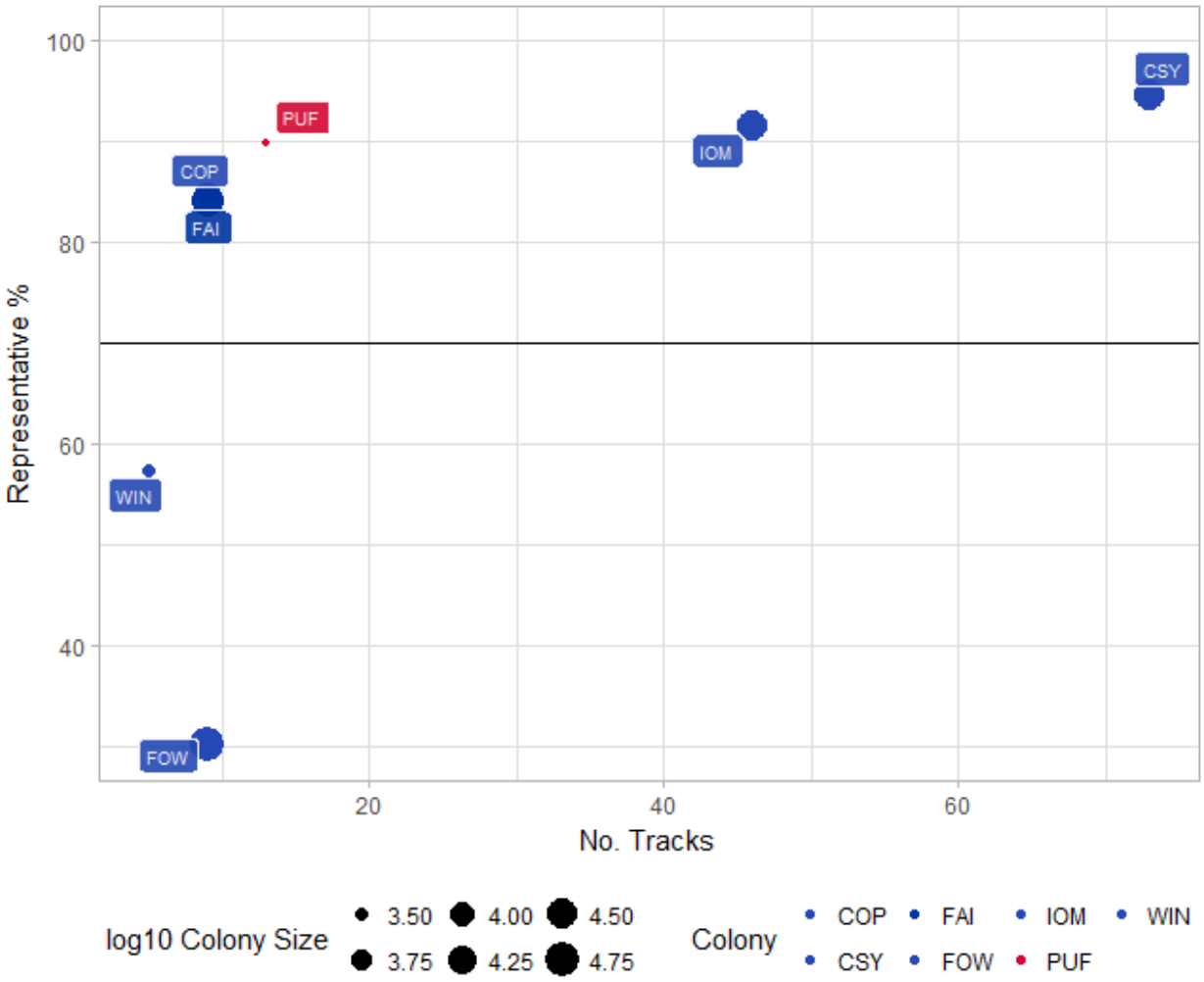

c) razorbills

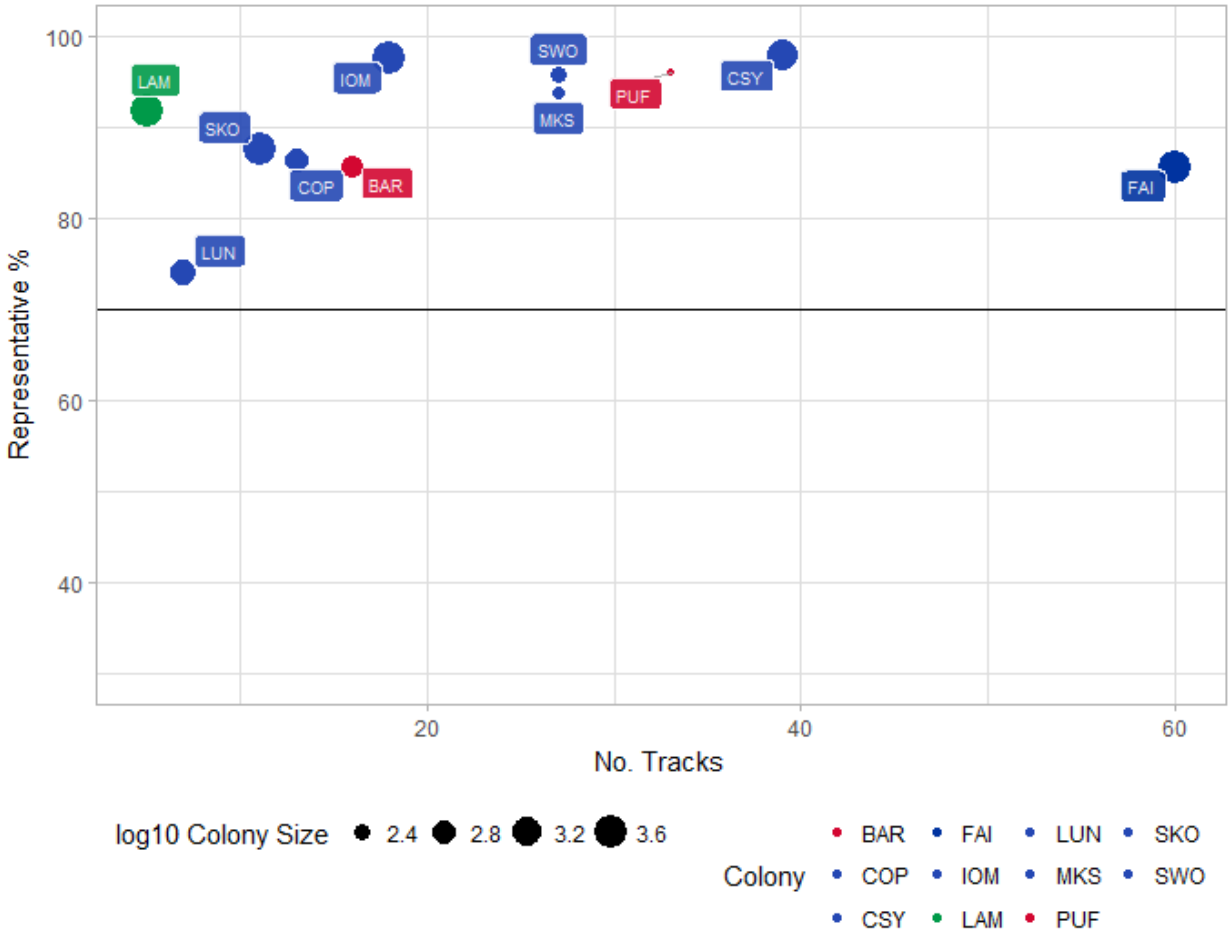

d) European shags

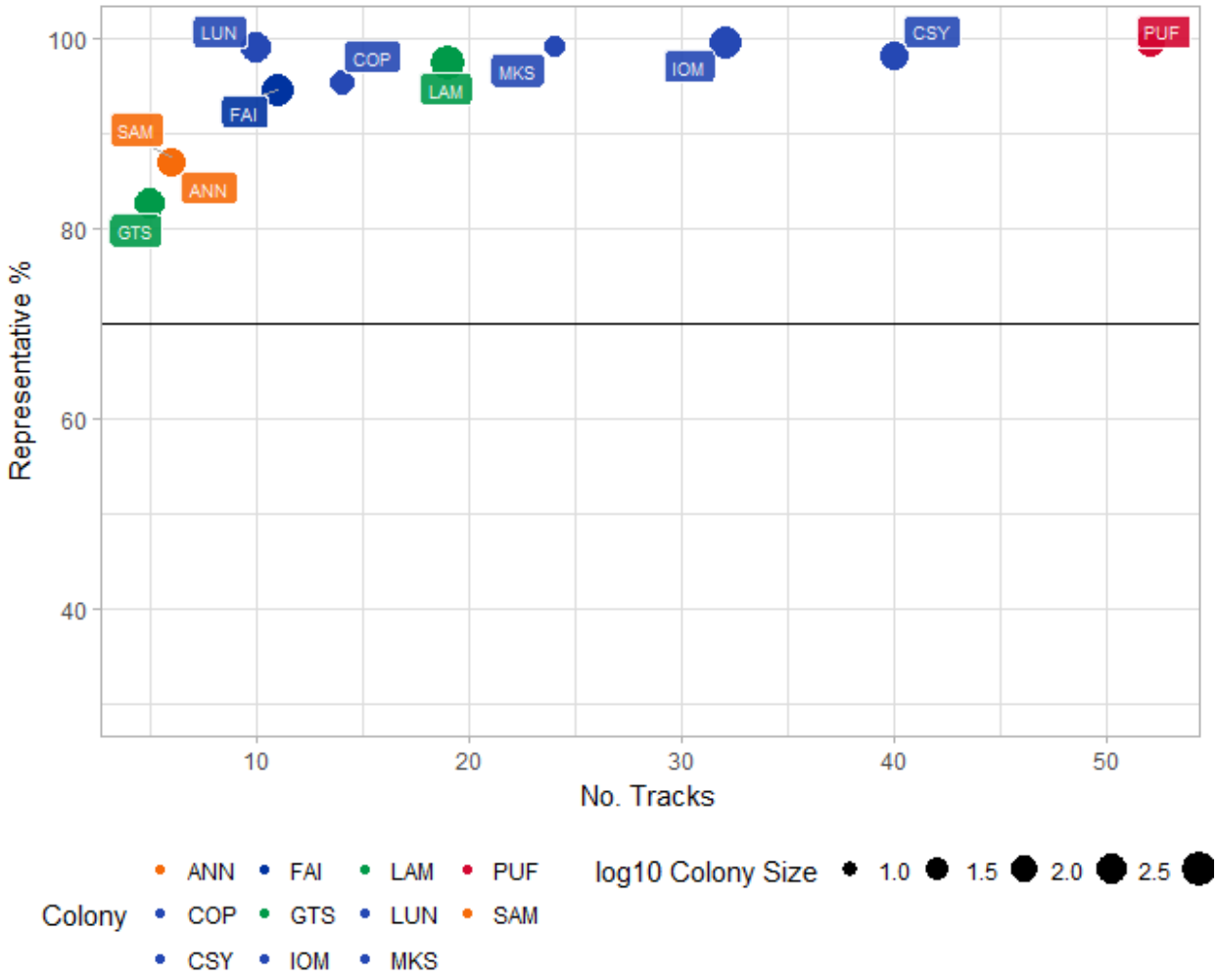

Fig. A7. Left panels) Maps showing the CV of model estimates at the UK-scale together with UK-level hotspots identified for each species. Note that the UK-level hotspots for shags are difficult to see at this scale because they are relatively localised. Right panels) Boxplots showing the distribution of CV values from cells within different UK-level hotspots compared to CV values across the whole extent of the analysis field for each species.

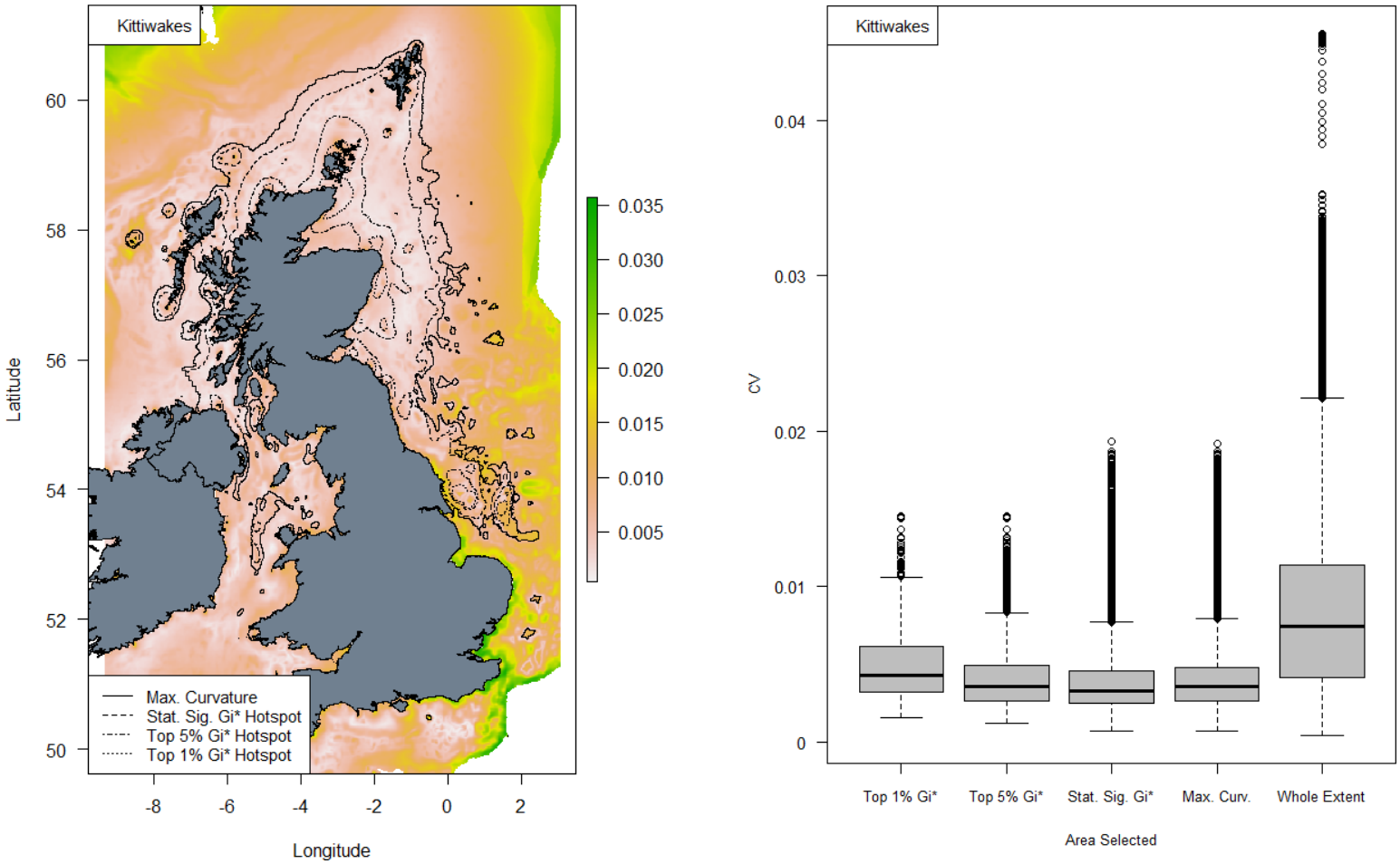

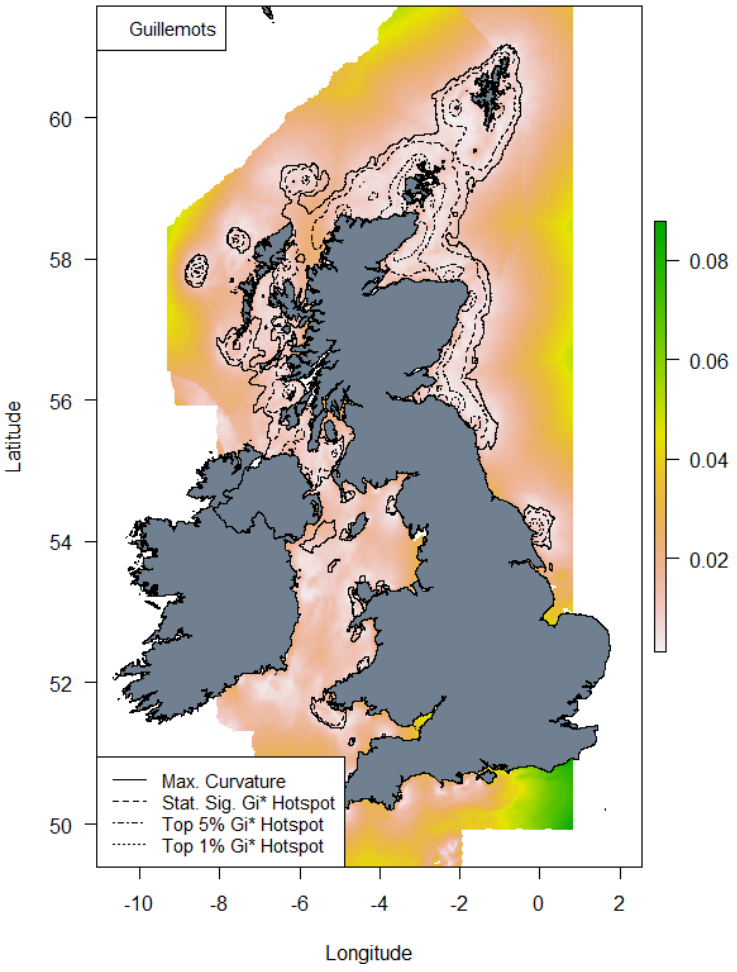
Guillemots
Max. Curvature
Stat. Sig. Gi* Hotspot
Top 5% Gi* Hotspot
Top 1% Gi* Hotspot
Latitude
Longitude
60
58
56
54
52
50
-10
-8
-6
-4
-2
0
2
0.08
0.06
0.04
0.02

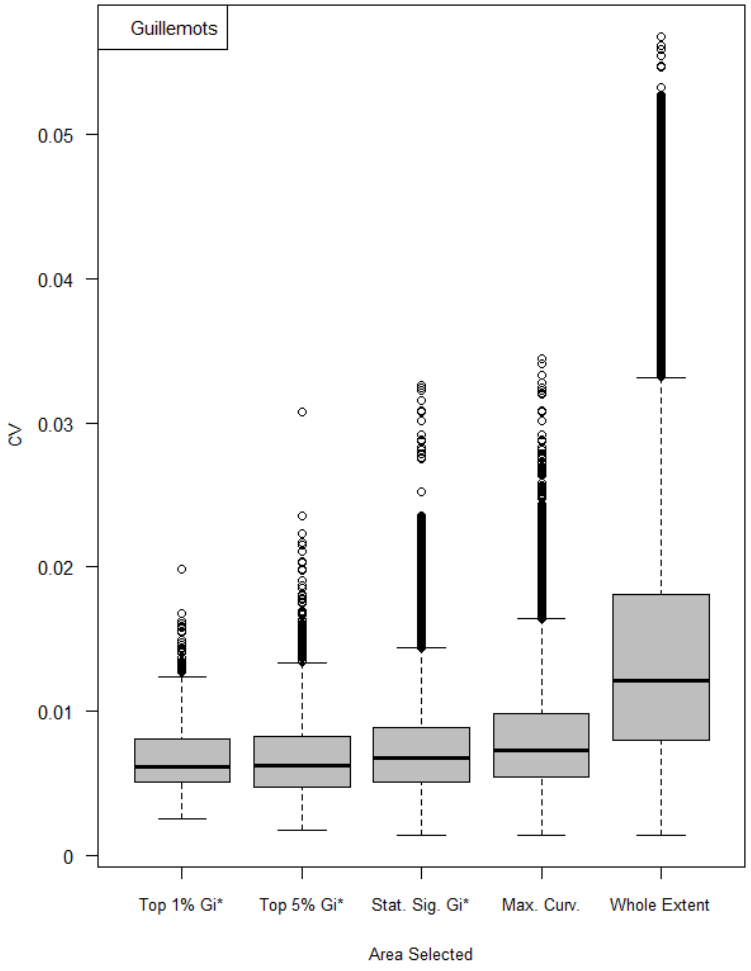
Guillemots
CV
0.05
0.04
0.03
0.02
0.01
0
Top 1% Gi*
Top 5% Gi*
Stat. Sig. Gi*
Max. Curv.
Whole Extent
Area Selected

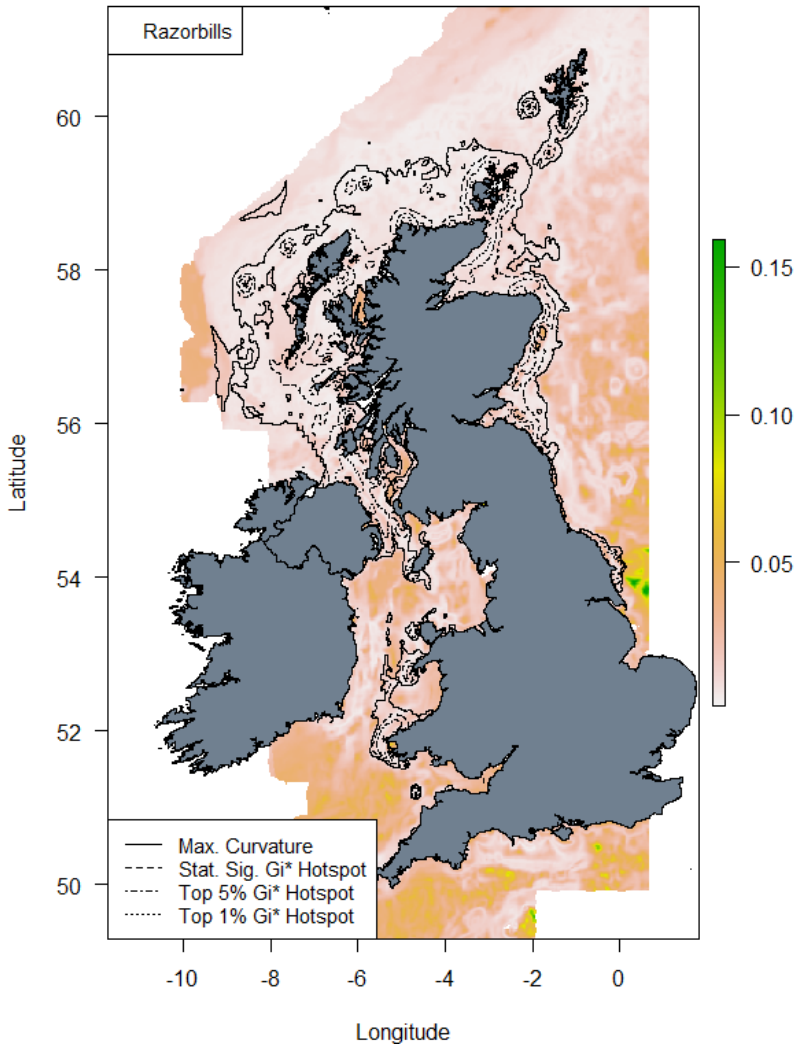
Razorbills
Latitude
Longitude
60
58
56
54
52
50
-10
-8
-6
-4
-2
0
0.15
0.10
0.05
Max. Curvature
Stat. Sig. Gi* Hotspot
Top 5% Gi* Hotspot
Top 1% Gi* Hotspot

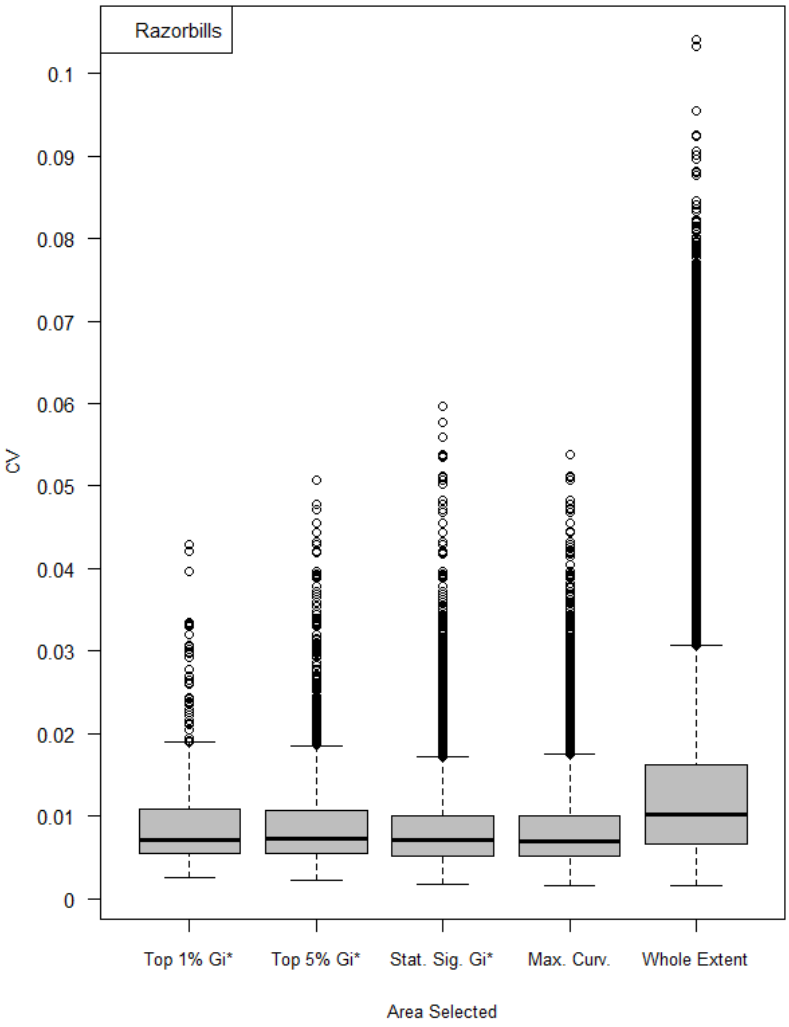
Razorbills
CV
0.1
0.09
0.08
0.07
0.06
0.05
0.04
0.03
0.02
0.01
0
Top 1% Gi*
Top 5% Gi*
Stat. Sig. Gi*
Max. Curv.
Whole Extent
Area Selected

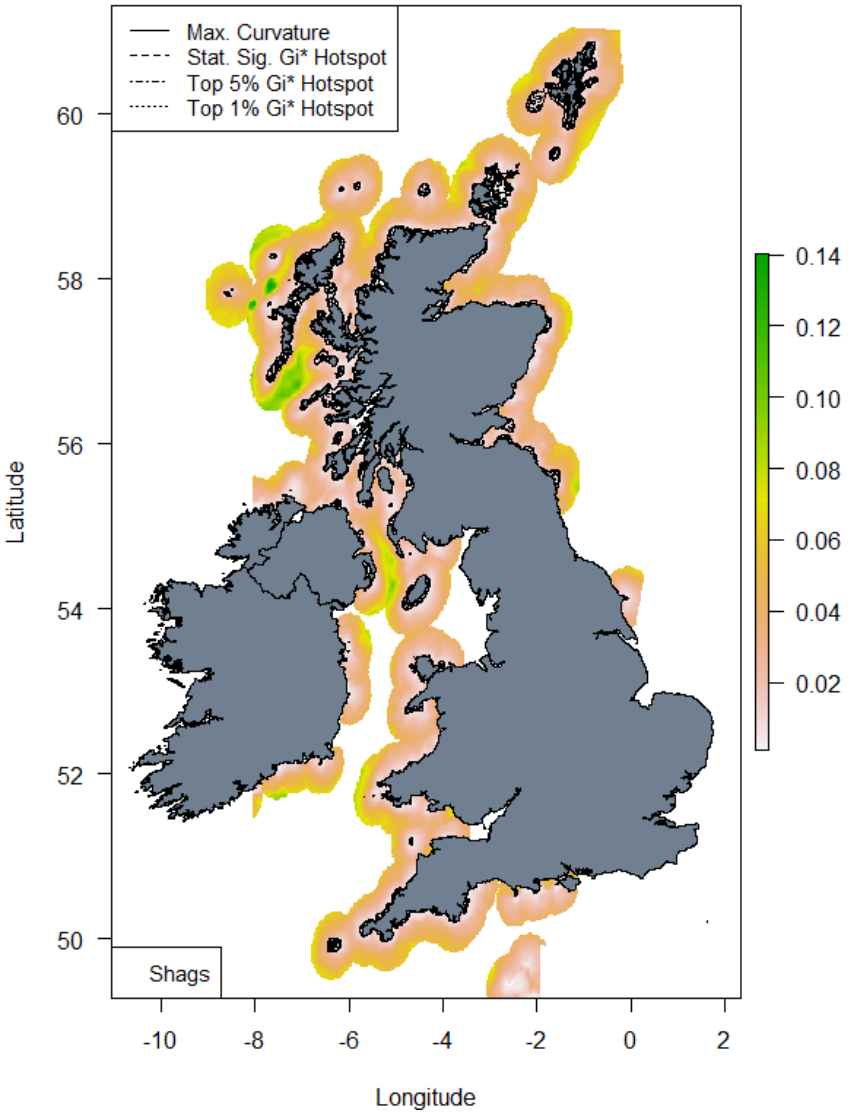
Max. Curvature
Stat. Sig. Gi* Hotspot
Top 5% Gi* Hotspot
Top 1% Gi* Hotspot
Shags
Latitude
Longitude
60
58
56
54
52
50
-10
-8
-6
-4
-2
0
2
0.14
0.12
0.10
0.08
0.06
0.04
0.02

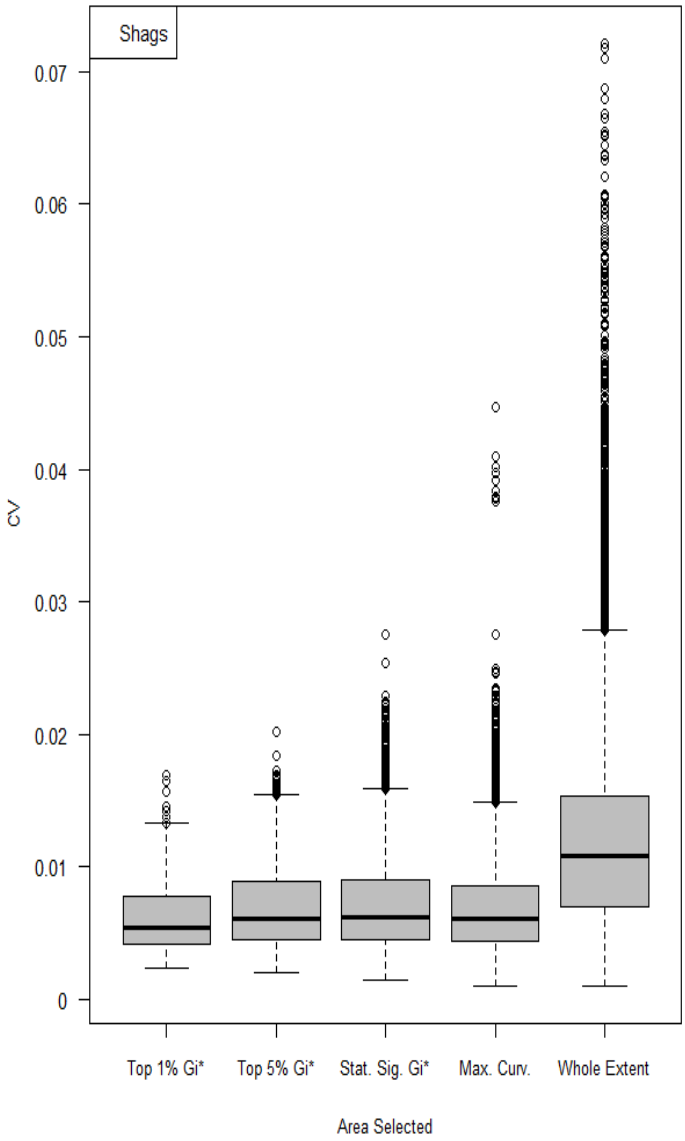
Shags
CV
0.07
0.06
0.05
0.04
0.03
0.02
0.01
0
Top 1% Gi*
Top 5% Gi*
Stat. Sig. Gi*
Max. Curv.
Whole Extent
Area Selected

A10. Model uncertainty in hotspot analysis

The maps of CV in modelled predictions show how uncertainty in the fitted model (standard errors around fitted coefficients) can influence density estimates. To examine what effect such uncertainty had upon hotspot mapping we used the same parametric resampling approach that was used to generate CV maps to explore uncertainty in hotspot modelling. Each hotspot technique (Getis-Ord analysis and maximum curvature was run 100 times for 100 different density surfaces generated from modelled predictions. To assess the uncertainty in hotspot locations we defined hotspots in two different ways. In the strictest case, a cell was only classified as being a hotspot if that cell was identified as a hotspot in all 100 simulations. In the conservative case, a cell was classified as a hotspot if that cell was identified as a hotspot in at least one of the 100 simulations. Due to time constraints this analysis was only conducted in kittiwakes. Kittiwakes were chosen as they covered the largest areas in our study

Across all hotspot methods the difference in size between the strictest method for delineating hotspots and the most conservative was small. Identified hotspots showed a high-degree of overlap and the difference in the area covered was < 5% in all cases.

Fig. A8. Uncertainty in hotspot location due to modelling uncertainty. The plots show hotspots identified using 100 simulated density surfaces predicted using the modelled outputs from Wakefield et al. (2017). In the strictest method of delineating a hotspot cells were classified as a hotspot if they were identified as a hotspot in all 100 simulations. In the conservative method, cells were classified as a hotspot if they were identified as a hotspot in at least one simulation. Hotspot areas showed high overlap across simulations and the difference in the area covered by hotspots using the strictest versus the conservative method was small. a) Hotspots calculated using the top 1% Getis-Ord scores; difference in size of strict versus conservative hotspot = 5%. b) Hotspots calculated using the top 5% Getis-Ord scores; difference in size of strict versus conservative hotspot = 3%. c) Hotspots calculated using statistically significant Getis-Ord scores; difference in size of strict versus conservative hotspot = 2%. d) Hotspots calculated using maximum curvature; difference in size of strict versus conservative hotspot = 1.5%.

a)

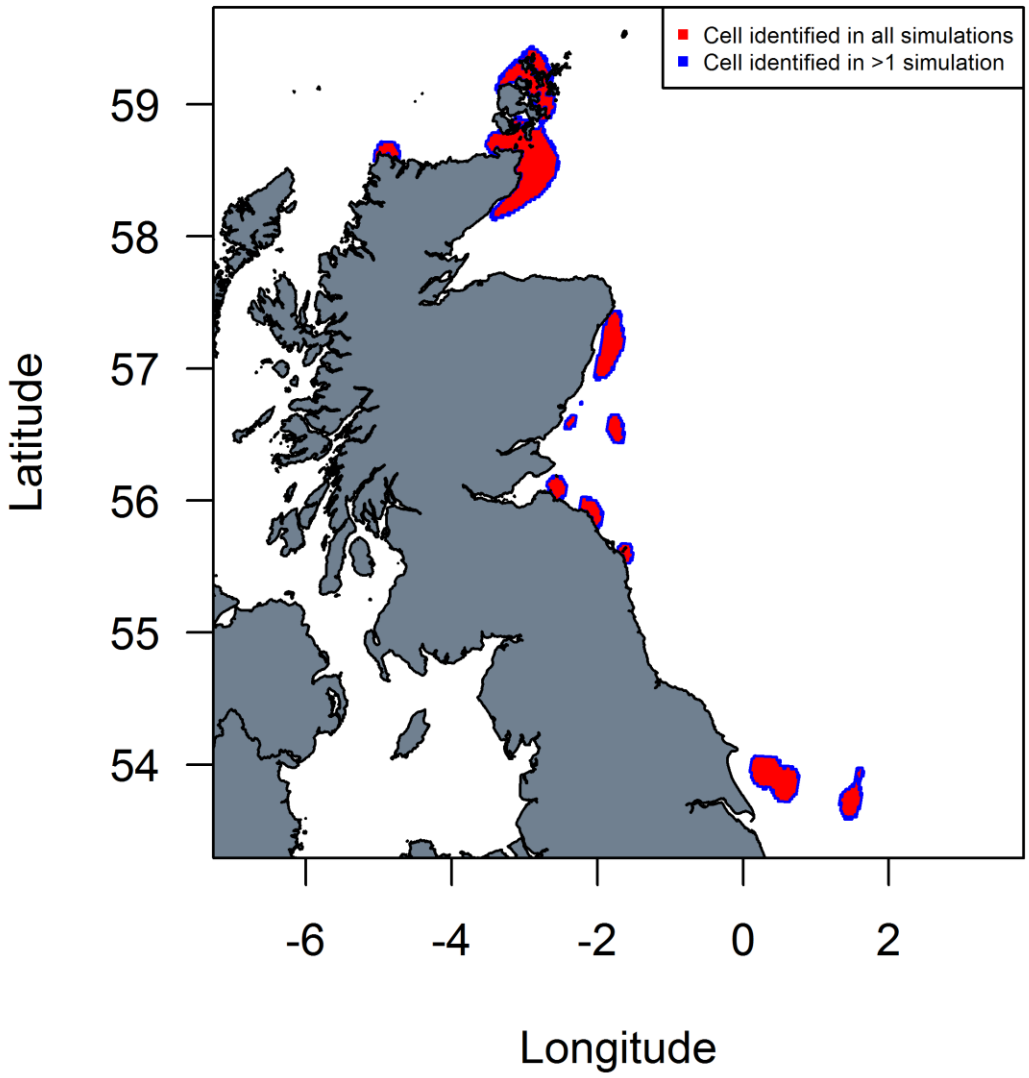
Cell identified in all simulations
Cell identified in >1 simulation
59
58
57
56
55
54
Latitude
-6
-4
-2
0
2
Longitude

b)

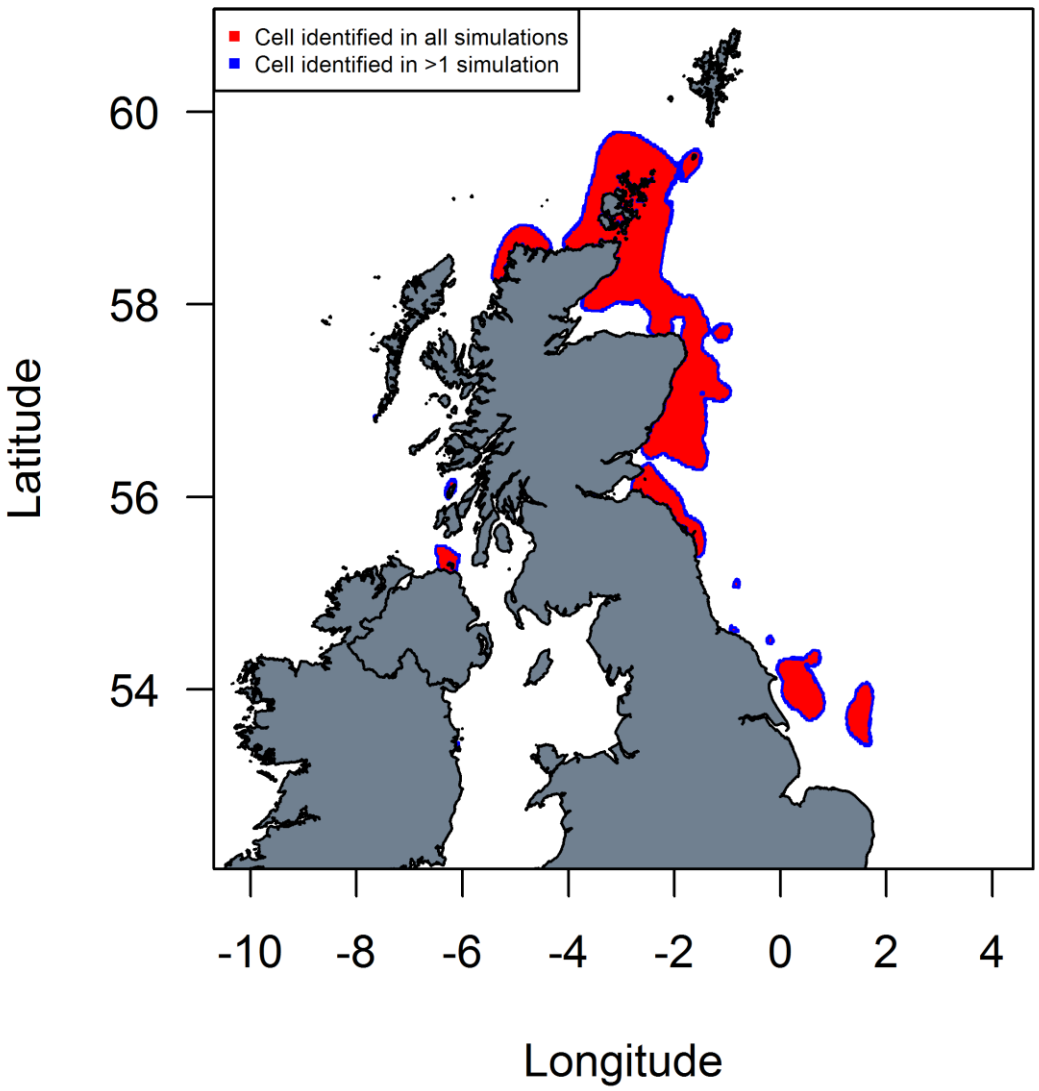
Cell identified in all simulations
Cell identified in >1 simulation
60
58
56
54
Latitude
-10
-8
-6
-4
-2
0
2
4
Longitude

c)

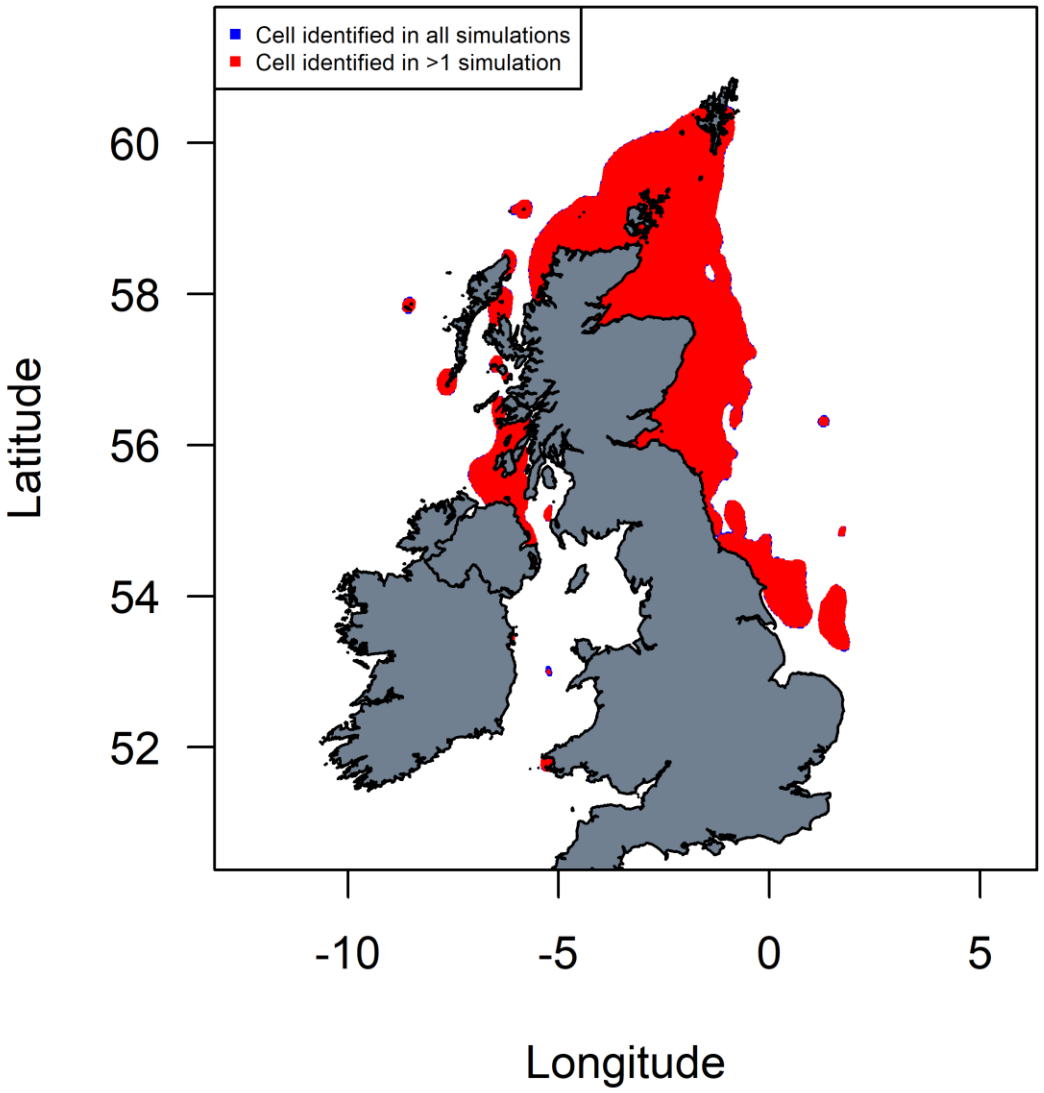
Cell identified in all simulations
Cell identified in >1 simulation
Latitude
60
58
56
54
52
-10
-5
0
5
Longitude

d)

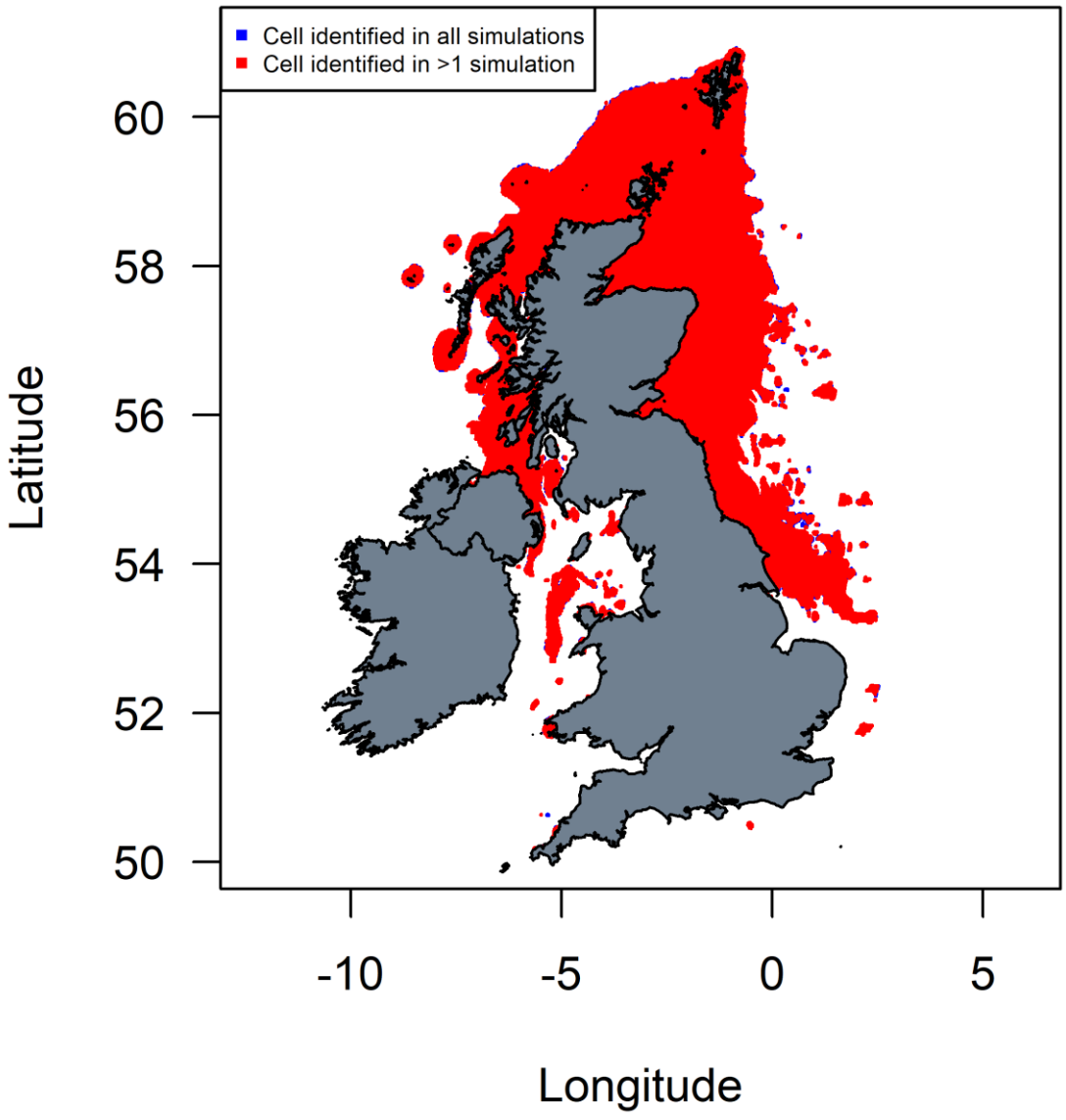
Cell identified in all simulations
Cell identified in >1 simulation
60
58
56
54
52
50
Latitude
-10
-5
0
5
Longitude

Appendix References

Battaile, B. C., Nordstrom, C. A., Liebsch, N. & Trites, A. W. 2015. Foraging a new trail with northern fur seals (Callorhinus ursinus): Lactating seals from islands with contrasting population dynamics have different foraging strategies, and forage at scales previously unrecognized by GPS interpolated dive data. *Marine Mammal Science*, 31, 1494-1520.

Bhattacharyya, A. 1943. On a measure of divergence between two statistical populations defined by their probability distributions. *Bull. Calcutta Math Soc*. 35, 99–110.

Byrne, M. E. & Chamberlain, M. J. 2012. Using first-passage time to link behaviour and habitat in foraging paths of a terrestrial predator, the racoon. *Animal Behaviour*, 84, 593-601.

Calenge, C. 2006. The package "adehabitat" for the R software: a tool for the analysis of space and habitat use by animals. *Ecological modelling*, 197, 516-519.

Fauchald, P. & Tveraa, T. 2003. Using first-passage time in the analysis of area-restricted search and habitat selection. *Ecology*, 84, 282-288

Hadfield, J. D. 2010. MCMC methods for multi-response generalized linear mixed models: the MCMCglmm R package. *Journal of Statistical Software*, 33, 1-22.

Hamer, K. C., E. M. Humphreys, M. C. Magalhaes, Stefan Garthe, J. Hennicke, G. Peters, D. Grémillet, H. Skov, & S. Wanless. 2009. Fine-scale foraging behaviour of a medium-ranging marine predator. *Journal of Animal Ecology*, 78, 880-889.

Lascelles, B.G., Taylor, P.R., Miller, M.G.R., Dias, M.P., Oppel, S., Torres, L., Hedd, A., Le Corre, M., Phillips, R.A., Shaffer, S.A. & Weimerskirch, H. 2016. Applying global criteria to tracking data to define important areas for marine conservation. *Diversity and Distributions*, 22, 422-431.

Le Corre, M., Dussault, C. & Côté, S. D. 2014. Detecting changes in the annual movements of terrestrial migratory species: using the first-passage time to document the spring migration of caribou. *Movement ecology*, 2, 19.

Matthiopoulos, J., Hebblewhite, M., Aarts, G. & Fieberg, J. 2011. Generalized functional responses for species distributions. *Ecology*, 92, 583-589.

Wakefield, E.D., Owen, E., Baer, J., Carroll, M.J., Daunt, F., Dodd, S.G., Green, J.A., Guilford, T., Mavor, R.A., Miller, P.I. & Newell, M.A. 2017. Breeding density, fine-scale tracking, and large-scale modeling reveal the regional distribution of four seabird species. *Ecological Applications*, 27, 2074-2091.